Isw2 and Ino80 Complexes Regulate the Ribosomal DNA Locus and DNA Break Repair Choice

Samuel R. Cutler

A dissertation
submitted in partial fulfillment of the
requirements for the degree of

Doctor of Philosophy

University of Washington

2019

Reading Committee:

Toshio Tsukiyama, Chair
M.K. Raghuraman
Gerald Smith

Program Authorized to Offer Degree:

Molecular and Cellular Biology

University of Washington

ABSTRACT

Isw2 and Ino80 Complexes Regulate
the Ribosomal DNA Locus and DNA Break Repair Choice

Samuel R. Cutler

Chair of the Supervisory Committee:
Toshio Tsukiyama
Member, Division of Basic Sciences, Fred Hutchinson Cancer Research Center
Affiliate Associate Professor, Department of Biochemistry

To achieve the high degree of compaction required to fit the eukaryotic genome into a nucleus, DNA has evolved to be organized in a structure referred to as chromatin. Chromatin involves the tight interaction of DNA with histone octamers known as nucleosomes. Because this association between DNA and nucleosomes inhibits DNA-dependent processes, chromatin structure is carefully regulated to facilitate transcription of RNAs from the DNA template, repair of DNA damage, and replication of the genome. ATP-dependent chromatin remodeling factors use the energy of ATP hydrolysis to modify specific features of chromatin structure. In this dissertation, I focus on elucidating biological functions of the *Saccharomyces cerevisiae* remodeling factors Isw2 and Ino80. I show that these complexes are targeted to the yeast ribosomal DNA locus, where they modify local chromatin structure and regulate replication initiation from this genomic locus and changes of the size of the highly repetitive rDNA array. In addition, I show evidence supporting possible roles for Isw2 and Ino80 in regulating the balance between two mechanisms of repair of DNA double strand breaks. In sum, my work establishes novel functions for these chromatin remodeling factors at a uniquely repetitive and important part of the eukaryotic genome and in a process that is crucial for genome stability.

Table of Contents

List of Figures ii

List of Tables iii

Acknowledgements iv

Dedication v

Chapter 1: Introduction 1

- Chromatin Structure 1
- Chromatin Structure – Post-Translational Modifications 3
- Chromatin Structure – Nucleosome Positioning and Histone Variants 5
- ATP-Dependent Chromatin Remodeling Factors 8
- Budding Yeast Isw2 and Ino80 11
- The Ribosomal DNA Locus 13
- The Cellular Response to DNA Damage and Replication Stress 15
- Description of Dissertation 16

Chapter 2: Chromatin Remodeling Factors Isw2 and Ino80 Regulate Chromatin, Replication, and Copy Number at the Saccharomyces cerevisiae Ribosomal DNA Locus 23

- Summary 23
- Introduction 24
- Results 27
- Discussion 38
- Materials and Methods 45

Chapter 3: A Possible Role for Isw2 and Ino80 in DNA Double Strand Break Repair Choice 61

- Summary 61
- Introduction 62
- Results 64
- Discussion 72
- Materials and Methods 75

Chapter 4: Conclusions and Perspectives 86

- Roles for Isw2 and Ino80 at the ribosomal DNA locus 87
- Roles for Isw2 and Ino80 in dictating DSB repair pathway choice 90

References 94

Vita 105

List of Figures

Figure 1.1: Nucleosome positioning at genes and origins or replication..... 18
Figure 1.2: Nucleosome positioning and nucleosome occupancy..... 19
Figure 1.3: Major structural features of the ATPase subunits of the four ATP-dependent chromatin remodeling factor families..... 20
Figure 1.4: The subunit composition of the *Saccharomyces cerevisiae* Isw2 and Ino80 ATP-dependent chromatin remodeling factors..... 21
Figure 1.5: The ribosomal DNA locus..... 22
Figure 2.1: The Isw2 and Ino80 chromatin remodeling complexes are targeted to the rDNA locus..... 51
Figure 2.2: Nucleosome occupancy, but not transcription, is affected at the 35S rDNA in *isw2Δ* and *nhp10Δ* mutants..... 52
Figure 2.3: Isw2 and Ino80 affect nucleosome positioning in the rDNA IGS..... 53
Figure 2.4: Nucleosome positioning changes at a canonical Isw2 target..... 54
Figure 2.5: Nucleosome positioning at the rDNA..... 55
Figure 2.6: Isw2 and Ino80 facilitate efficient firing of rDNA origin of replication..... 56
Figure 2.7: Strains used in this study have approximately 150 rDNA repeats..... 57
Figure 2.8: Isw2 and Ino80 affect the rate of rDNA copy number change..... 58
Figure 3.1: *isw2Δ nhp10Δ* cells do not arrest in G2/M or activate the Rad53 checkpoint in response to a DSB that cannot be repaired by homologous recombination..... 79
Figure 3.2: Following DSBs that cannot be repaired by homologous recombination, *isw2Δ nhp10Δ* cells have dramatically increased viability relative to WT..... 80
Figure 3.3: HO cutting happens in isw2Δnhp10Δ cells, but with somewhat altered efficiency and/or kinetics..... 81
Figure 3.4: All adapted isw2 nhp10 colonies show evidence of a cut and mutated HO target site..... 82
Figure 3.5: *isw2Δ nhp10Δ* cells in HR-incompetent background have persistent G1 bias..... 83

List of Tables

Table 2.1: Chapter 2 Yeast Strains. 59
Table 3.1: Chapter 3 yeast strains. 84
Table 3.2: Summary of sequenced HO cut site mutations in WT and *isw2Δ nhp10Δ* adapters. 85

Acknowledgements

I thank my advisor, Toshio Tsukiyama, for being an exceptional mentor. From my first days as a rotation student to preparing my paper manuscript through the preparation of my dissertation, Toshi has been supportive, kind, and insightful. He cultivates a collegial and productive atmosphere in lab, and I've learned so much from him about doing high quality science at the bench, thinking critically, and crafting a good scientific story. I also want to thank the many members of the Tsukiyama lab, past and present, who have contributed to this work, starting with Jack Vincent, Tracey Au, and Laura Lee, whose earlier work in this lab as graduate students formed the foundation for my own research. I am particularly appreciative of the diligent mentorship I received from Laura, who helped me get settled in the lab as a grad student and then graciously transitioned the rDNA project to my hands. I also thank the many other postdocs, grad students, and technicians who have made my time in the Tsukiyama lab productive, intellectually enriching, and fun, especially: Jairo Rodriguez, Jeffrey McKnight, Eric Alcid, Bryony Lynch, Joe Boerma, Keean Braceros, Bill Fu, Rachel Dell, Sarah Swygert, Christine Cucinotta, and Marla Spain.

I want to thank members of advisory committee – Sue Biggins, David MacPherson, M.K. Raghuraman, Gerry Smith, and Toshi Taniguchi – for providing excellent scientific feedback and generous mentorship. I especially thank Raghu and Gerry, who, along with Toshi, served on my dissertation reading committee, and whose contributions significantly strengthened this document.

I thank two labs in particular. The members of the Brewer/Raghuraman lab added a great deal to my work through feedback given when I presented at their group meeting, helpful discussions at meetings (including the rDNA symposium at UW), and direct consultation about experimental design and interpretation. Bonny, Raghu, Joe Sanchez, and Liz Kwan were all especially helpful. I also thank the members of Gerry Smith's lab, in particular Randy Hyppa and Andrew Taylor, whose expertise and commiseration were essential to getting my CHEF gels running smoothly.

Dedication

I dedicate this dissertation to my parents, Susan and Jason. This document wouldn't exist without you both, in two major ways. The first is all the support and love and encouragement you have given me over 3+ decades, from my earliest days as a child to your regular visits to Seattle since I moved here. And the second is, through some combination of nature and nurture, I am an equal mixture of both of you, in ways that have specifically brought me to the completion of this PhD. Dad, from you I've gotten a pure love of science – scientific knowledge, the scientific method, the broad lineage of scientific inquiry. Mom, from you I've gotten a sense of awe about the beauty and complexity of the natural world, a feeling of awe that has motivated my dedication to science since a very young age, and specifically biology since high school. I'm enormously grateful to you both for all you've done as my parents, my teachers, and my friends.

I also dedicate this dissertation to my amazing partner, Jo. You have been there from the beginning, from my year of rotations to settling in Toshi's lab, from preparing for my General Exam to completing my General Exam, from changing projects to publishing my *Genetics* paper, from traveling for conferences to defending my dissertation. Through it all, you have been a source of steadfast support and love. Together, we have relaxed at home, explored Seattle, and adventured around the Northwest, Canada, Costa Rica, and more, on sea and on land, in cities and mountains. I couldn't ask for a better partner, and I'm so grateful for your presence in my life.

Chapter 1

Introduction

Chromatin Structure

If all the DNA in a single human cell was stretched out and laid end-to-end, it would be approximately 2 meters long. Those 2 m are contained in a nucleus that is approximately 10 microns in diameter. Thus, containing the human genome in its nucleus requires approximately 100,000-fold compaction. The orderly and reproducible packaging of this negatively charged DNA around positively charged histone proteins is described by the term chromatin, and the most basic unit of chromatin is the nucleosome. The nucleosome core particle comprises 147 base pairs of DNA wrapped in 1.65 turns around an octamer of histone proteins, two each of histone H2A, H2B, H3, and H4 (LUGER *et al.* 1997). Nucleosomes are separated from one another by sequences of "linker DNA", a configuration described as resembling "beads on a string", with histone octamer "beads" connected on "strings" of DNA. Early observations of this basic structure came from electron micrograph images (OLINS and OLINS 1974). Beyond this level of organization, there is some evidence that chromatin forms higher-order structures such as a 30 nm fiber and 120 nm chromonema (RYDBERG *et al.* 1998; ADKINS *et al.* 2004; WOODCOCK and GHOSH 2010; BICKMORE and VAN STEENSEL 2013). However, accumulating evidence suggests that these forms of DNA may be unique to *in vitro* experiments, and that this scale of chromatin organization *in vivo* may be considerably less regimented, characterized by disordered 5-24 nm chains of chromatin (OU *et al.* 2017).

At the level of the entire genome, chromatin can be broadly separated into heterochromatin and euchromatin. Heterochromatin was originally identified as being strongly stained by basic dyes, and the definition has since been refined to include qualities of being physically compacted and transcriptionally silent (WOODCOCK and GHOSH 2010). Physically, heterochromatin tends to contain structures such as telomeres and to associate with the nuclear periphery (MARSHALL 2002; SCHOEFTNER and BLASCO 2009). Heterochromatin can be further divided into two sub-types. Constitutive heterochromatin is almost always compacted, tends to have a generally low density of genes, and is typically replicated later in S-phase. Facultative heterochromatin is sometimes compact and transcriptionally silent but can reversibly become more open and transcriptionally active in response to specific environmental or developmental cues. Euchromatin shares many attributes of the open form of facultative heterochromatin, as it is light-staining, de-compacted, transcriptionally active, and associated more with the interior of the nucleus (WOODCOCK and GHOSH 2010).

Focusing on an intermediate genomic scale, accumulating evidence supports the existence of topologically associated domains (TADs), regions of the genome that, in humans, span approximately hundreds of kilobases (kbs) of DNA and tend to physically associate within themselves, to the exclusion of other parts of the genome (LIEBERMAN-AIDEN *et al.* 2009; DIXON *et al.* 2012; SEXTON *et al.* 2012). One possible explanation for the formation of individual TADs is the loop-extrusion model, which proposes that nuclear factors drive the formation of loops of DNA until reaching boundary factors that mark the edges of the loops. The resulting loops are discernible as TADs (SANBORN *et al.* 2015; FUDENBERG *et al.* 2016). In yeast, chromosome-interacting domains (CIDs) have been found

that are conceptually similar to TADs, but considerably smaller, typically spanning one to four genes and approximately 0.5 to less than 10 kb of DNA (HSIEH *et al.* 2015; SWYGERT *et al.* 2019). At the scale of hundreds of kilobases to megabases, spanning multiple TADs, chromosome packaging can be described by a "fractal globule" model, according to which regions are more likely to physically associate with themselves than other regions, and chromatin is not totally randomly distributed within the nucleus (LIEBERMAN-AIDEN *et al.* 2009; MIRNY 2011).

Chromatin Structure – Post-Translational Modifications

Chromatin structure facilitates the large-scale compaction of DNA into the eukaryotic nucleus. However, nucleosomes obstruct access of DNA-binding proteins to DNA and impede the progress of DNA and RNA polymerases. Because the cell must transcribe the underlying the genome's DNA into RNA, replicate the DNA to facilitate cell division, and repair damaged DNA, two broad mechanisms have evolved to regulate these processes by the modification of chromatin structure: regulation of the post-translational modification of histone proteins, and regulation of the positioning, occupancy, and histone composition of nucleosomes. Histone proteins can be post-translationally modified in a variety of ways, including by methylation, acetylation, phosphorylation, ubiquitylation, ADP-ribosylation, and glycosylation (BERGER 2002; BOWMAN and POIRIER 2015). Specific residues of each histone can be modified in specific ways, and the flexible tails of histones H3 and H4 that extend out from the nucleosome core particle are particularly rich in residues that are commonly modified (KOUZARIDES 2007). These histone **p**ost-**t**ranslational **m**odifications (PTMs) exert a significant influence on DNA-dependent processes, and they

have been the subject of intense study dating back to the discovery that histone acetylation inhibited the ability of histones to block transcription (ALLFREY *et al.* 1964).

There are two broad, not mutually exclusive explanations of how histone PTMs are able to exert this influence. The first is that chemical modification of histone proteins might alter the affinity between negatively charged DNA and basic nucleosomes, thus modulating the tightness of association between the two and, by extension, the accessibility of the DNA to DNA-binding proteins (GRANT 2001). The second explanation arose out of the recognition of the diversity of specific combinations of histone modifications associated with certain genomic loci, developmental stages, and cell types. This understanding led to the proposal of a "histone code", which states that certain combinations of histone modification exert specific effects on chromatin structure and DNA-dependent processes (STRAHL and ALLIS 2000). For example, in *Drosophila melanogaster*, it has been found that actively transcribed genes tend to be hyper-acetylated on histones H3 and H4 and methylated on lysines 4 and 79 on H3, while inactive genes are more associated with the absence of those marks (SCHUBELER *et al.* 2004). In human cells, actively transcribed genes tend to be associated with a single methyl group added to H3K27, H3K9, H3K20, H3K79, and H2BK5, while three methyl groups added to some of those same histone residues – H3K27, H3K9, and H3K79 – can be associated with inactive genes (BARSKI *et al.* 2007).

To regulate the careful balance of histone PTMs throughout the genome, cells employ a variety of enzymes that add and remove the modifications. One of the earliest such enzymes to be characterized was a homolog of the yeast Gcn5 protein identified in *Tetrahymena*. In both species, the protein acts as a promoter of transcription. By demonstrating the **h**istone **a**cetyl **t**ransferase (HAT) activity of Gcn5, this study linked the

modification of chromatin structure to the regulation of DNA dependent processes such as, in this case, transcription (BROWNELL *et al.* 1996). Since then, many enzymes have been shown to add and remove the histone PTMs discussed above (STRAHL and ALLIS 2000; BERGER 2002; LAWRENCE *et al.* 2016).

Chromatin Structure – Nucleosome Positioning and Histone Variants

In addition to PTMs of histones, the positioning, occupancy, and histone composition of nucleosomes contribute to the regulation of DNA-dependent processes. A critical feature of chromatin structure is a stereotypical pattern of nucleosome positioning around genes. Upstream of a gene's **t**ranscription **s**tart **s**ite (TSS) there is a **n**ucleosome-**d**epleted **r**egion (NDR, sometimes also referred to as a **n**ucleosome-**f**ree **r**egion, or NFR), a stretch of DNA that lacks nucleosomes. The lack of nucleosomes facilitates access to the DNA of DNA-binding proteins that facilitate the initiation of transcription. Located at the 5' end of the gene, this TSS-adjacent "5' NDR" is flanked by well-positioned nucleosomes, called the -1 and +1 nucleosomes. Proceeding downstream in the gene, there is a gradient of progressively less well-positioned nucleosomes, culminating in a 3' NDR that contains the gene's **t**ranscription **t**ermination **s**ite (TTS) (YUAN *et al.* 2005; MAVRICH *et al.* 2008; JIANG and PUGH 2009) [Figure 1.1A].

Because a nucleosome is a discrete object that can occupy only one position at a time on a length of DNA, nucleosome "positioning" and "occupancy" have meanings at two levels: that of an individual nucleosome in a single molecule of chromatin, and that of a population of nucleosomes considered as an ensemble. For a nucleosome to be "well-positioned" requires that in a population of cells, a nucleosome is located in the same

region of DNA a very high proportion of those cells. In contrast, a "poorly positioned" nucleosome may occupy a wide range of positions in that same population of cells [Figure 1.2A]. A similar probabilistic methodology applies to the idea of nucleosome occupancy. In a population of cells, a region such as an NDR that has *low* nucleosome occupancy is very unlikely to contain a nucleosome, while in that same population of cells, a region with *high* nucleosome occupancy will be very likely to contain a nucleosome (STRUHL and SEGAL 2013) [Figure 1.2B].

The positioning of NDR-flanking nucleosomes can have important consequences for DNA-dependent processes. An early clue about this phenomenon came from the finding that DNA encoding globin genes was more readily digested by deoxyribonuclease (DNase) in nuclei obtained from chicken erythrocytes, where the globin genes are active, than in nuclei from fibroblast or brain cells, where those genes are inactive (WEINTRAUB and GROUDINE 1976). This experiment provided evidence of a link between chromatin structure and gene expression. The yeast *PHO5* gene, encoding an acid phosphatase, is another canonical example of this principle. When environmental phosphate is abundant and cellular demand for Pho5 is low, a specific pattern of nucleosome positioning in the gene's promoter prevents transcription of *PHO5*; when phosphate is low and Pho5 demand high, the nucleosomal organization changes in such a way to permit active transcription (REINKE and HORZ 2003; MARTINEZ-CAMPA *et al.* 2004).

In addition to genes, origins of replication are also significantly influenced by chromatin structure. In budding yeast, origins of replication, called ARSs (**A**utonomously **R**eplicating **S**equences) all share certain DNA sequence characteristics. The most critical component of the ARS is the ACS, or **A**RS **C**onsensus **S**equence, an 11 bp motif that is the

binding target for ORC (**O**rigin **R**ecognition **C**omplex) (BREWER and FANGMAN 1987; BELL and STILLMAN 1992; MARAHRENS and STILLMAN 1992). Binding of ORC to the ACS is the essential first step in the eventual firing of the origin (FRAGKOS *et al.* 2015). Early *in vitro* experiments demonstrated that positioning a nucleosome directly over an ACS, a region that is normally depleted of nucleosomes, blocked firing from that origin (SIMPSON 1990). A mere absence of nucleosomes covering the ACS is not the only chromatin requirement for proper origin functioning, however, as properly positioned nucleosomes flanking the ARS are necessary for origin firing (LIPFORD and BELL 2001). Indeed, much like gene promoters, functional yeast origins are flanked by a stereotypical pattern of nucleosomes, with the ARS located in an NDR flanked by well-positioned nucleosomes, and progressively less well-positioned nucleosomes radiating out in both directions (EATON *et al.* 2010)[Figure 1.1B].

In addition to the canonical histone proteins – H2A, H2B, H3, and H4 – there are many variant histones that are substituted for canonical histones throughout the cell cycle, and whose inclusion in nucleosomes alters the physical and functional properties of chromatin (VENKATESH and WORKMAN 2015; TALBERT and HENIKOFF 2017). For example, replacement of H3 with a centromeric variant, called CENP-A in vertebrates and Cse4 in *Saccharomyces cerevisiae*, is a critical requirement for the formation of proper centromeric chromatin (MCKINLEY and CHEESEMAN 2016). The H2A variant H2A.Z is associated with the promoter regions of euchromatic genes. In some contexts, patterns of transcription do not correlate well with the presence or absence of H2A.Z, though some evidence suggests this histone may associate with the promoters of repressed genes to facilitate their rapid activation when needed (RAISNER *et al.* 2005; ZHANG *et al.* 2005; TALBERT and HENIKOFF 2017). In metazoans, histone H3.3 is found in gene bodies and promoters as well as

enhancer elements, with critical roles in metazoans in both development and maintenance of embryonic stem cells (MITO *et al.* 2005; ELSAESSER *et al.* 2010; GOLDBERG *et al.* 2010; FILIPESCU *et al.* 2013).

Much like specific classes of enzymes have been found to regulate the addition and removal of histone PTMs, specific enzymes have been found to regulate the positioning, occupancy, and histone composition of nucleosomes. The complexes responsible for regulating these attributes of chromatin structure are known as ATP-dependent chromatin remodeling factors.

ATP-Dependent Chromatin Remodeling Factors

ATP-dependent chromatin remodeling factors use the energy of ATP hydrolysis to translocate DNA to slide or eject nucleosomes and to exchange histone variants within nucleosomes (SAHA *et al.* 2002; WHITEHOUSE *et al.* 2003; CLAPIER *et al.* 2017).There are four broad families of remodeling factors which are distinguished by their structurally similar catalytic ATPase subunits: SWI/SNF (mating-type **swi**tching defective/**s**ucrose **n**on **f**ermenting), ISWI (**i**mitation **SWI**), CHD (**c**hromodomain, **h**elicase, **D**NA binding), and INO80 (**ino**sitol-requiring). Each remodeling factor complex family is defined by its ATPase-containing subunit, all of which share two RecA-like lobes separated from one another by a linker region, but otherwise have unique features (CLAPIER and CAIRNS 2009)[Figure 1.3]. In addition to having one of these four ATPase subunits, all remodeling factor complexes are characterized by a greater affinity for nucleosomes than for naked DNA, as well as additional subunits that regulate the activity of the ATPase and subunits that regulate binding to target chromatin (CLAPIER and CAIRNS 2009; CLAPIER *et al.* 2017).

The SWI/SNF complex, the first chromatin remodeling factor to be characterized, was originally identified in independent genetic screens in yeast. What was originally called the *SWI2* gene was identified as being necessary for the proper transcription of the HO endonuclease, which is in turn necessary for mating type-**swi**tching (STERN *et al.* 1984; BREEDEN and NASMYTH 1987). The same gene, but identified as *SNF2*, was found to be necessary for the fermentation of sucrose (**s**ucrose **n**on-**f**ermenting)(NEIGEBORN and CARLSON 1984). Further evidence supported a broad role for the SWI/SNF complex in activating many targets throughout the genome (PETERSON and HERSKOWITZ 1992; WINSTON and CARLSON 1992; CLAPIER and CAIRNS 2009). Mechanistically, the SWI/SNF complex slides nucleosomes: it re-positions nucleosomes in *cis*, along the same strand of DNA, without disrupting the fundamental organization of the histone octamer (WHITEHOUSE *et al.* 1999; KASSABOV *et al.* 2002). This sliding activity is important in transcriptional regulation, as one of the two yeast SWI/SNF family members, RSC, positions nucleosomes around the promoter of the *CHA1* gene to facilitate its transcriptional repression (MOREIRA and HOLMBERG 1999). RSC has also been found to eject nucleosomes (LORCH *et al.* 2011). Compared to nucleosome sliding, this ejection function requires stronger coupling of the ATPase activity of catalytic subunit Sth1 to DNA translocation (CLAPIER *et al.* 2016).

The chromatin remodeling activity of what would eventually be identified as ISWI was first discovered in the form of the ATP-dependent disruption of nucleosome structure around the *hsp70* gene promoter in *D. melanogaster* (TSUKIYAMA *et al.* 1994). This activity was biochemically purified and identified as the remodeling factor NURF (TSUKIYAMA and WU 1995). This family of remodeling factors was called ISWI (**Imi**tation **S**witch), reflecting its ATPase subunit's having similar, but still distinct, structural and biochemical properties

as that of SWI/SNF. ISWI family members are responsible for the establishment of arrays of regularly-spaced nucleosomes (ITO *et al.* 1997; VARGA-WEISZ *et al.* 1997). This function is the result of coupling ATP-dependent sliding of nucleosomes with the ability to sense the distance between nucleosomes (HAMICHE *et al.* 1999; LANGST *et al.* 1999; YANG *et al.* 2006). Yeast Isw2 positions nucleosomes into thermodynamically unfavorable positions at the 5' and 3' ends of genes, repressing transcription of a variety of coding and anti-sense transcripts (GOLDMARK *et al.* 2000; FAZZIO *et al.* 2001; WHITEHOUSE and TSUKIYAMA 2006; WHITEHOUSE *et al.* 2007).

The Chd family of remodelers is defined by an ATPase subunit that contains a pair of chromodomains that bind methylated histones (CLAPIER and CAIRNS 2009; CLAPIER *et al.* 2017). Yeast Chd1 often acts in parallel with ISWI family remodelers, principally to create regularly-spaced nucleosomal arrays and to prevent the aberrant exchange of histone variants in the coding regions of actively transcribed genes (TRAN *et al.* 2000; GKIKOPOULOS *et al.* 2011). Metazoan CHD family members, in addition to performing this spacing function, can also exchange histone variants (MURAWSKA and BREHM 2011). For example, in Drosophila, CHD1 is required for the incorporation of histone variant H3.3 into the chromatin of sperm cells, which is in turn necessary for proper mitosis in the fertilized zygote (KONEV *et al.* 2007).

The Ino80 family of chromatin remodelers was first discovered in yeast, where the *INO80* gene product was shown to have sequence similarities to *SNF2* and to be necessary for growth in medium lacking **Ino**sitol (EBBERT *et al.* 1999). This complex has been shown to slide nucleosomes, create regularly-spaced nucleosomal arrays, and regulate gene transcription (JIN *et al.* 2005; CAI *et al.* 2007; UDUGAMA *et al.* 2011). The other member of

this remodeler family is Swr1, whose principal activity is to exchange canonical histone H2A with the variant H2A.Z (KOBOR *et al.* 2004; MIZUGUCHI *et al.* 2004; RANJAN *et al.* 2015). This incorporation of H2A.Z-H2B dimers is balanced by Ino80's ability to replace H2A.Z-H2B with canonical H2A-H2B dimers, as loss of Ino80 results in aberrant accumulation of H2A.Z throughout the genome, particularly outside of H2A.Z's normal localization in gene bodies (PAPAMICHOS-CHRONAKIS *et al.* 2011). Both Ino80 and Swr1 are recruited to sites of DNA damage through the accumulation at break sites of phosphorylated H2A.X (MORRISON *et al.* 2004; VAN ATTIKUM *et al.* 2004). Both remodelers contribute to the proper recruitment of DNA damage factors to the sites of damage, promoting resection – the generation of single-stranded DNA – and eventual resolution of the damage (PAPAMICHOS-CHRONAKIS *et al.* 2006; VAN ATTIKUM *et al.* 2007).

Budding Yeast Isw2 and Ino80

The budding yeast *S. cerevisiae* has three members of the ISWI family of remodeling factors: Isw1a, Isw1b, and Isw2 (BAO and SHEN 2007; CLAPIER and CAIRNS 2009). The Isw2 complex exists in either a two-subunit form containing the catalytic Isw2 ATPase and Itc1 or in a four-subunit form containing Isw2, Itc1, Dls1, and Dpb4 (TSUKIYAMA *et al.* 1999; IIDA and ARAKI 2004)[Figure 1.4A]. Isw2 represses the transcription of specific genes, including early meiotic genes, by sliding nucleosomes into 5' **n**ucleosome **f**ree **r**egions (NFRs, also referred to as **n**ucleosome **d**epleted **r**egions, or NDRs) (GOLDMARK *et al.* 2000; FAZZIO *et al.* 2001; FAZZIO and TSUKIYAMA 2003). Isw2 influences the positioning of nucleosomes at over 1,000 loci in the yeast genome, including 5' and 3' ends of RNA Pol II-transcribed genes and RNA Pol III-transcribed tRNA genes (WHITEHOUSE *et al.* 2007). The transcription factor

Ume6 is involved in targeting Isw2 to many genes (TSUKIYAMA *et al.* 1994; YADON *et al.* 2013). Bdp1, a subunit of TFIIIB, a basal transcription factor for RNA Polymerase III, is necessary for targeting of Isw2 to tRNA genes. This site-specific targeting is necessary for the establishment by Isw2 of specific local chromatin structure and spatially periodic integration of Ty elements upstream of tRNA genes (BACHMAN *et al.* 2005; GELBART *et al.* 2005).

The *S. cerevisiae* Ino80 complex contains fifteen subunits. Based on their structural organization, some of these subunits have been organized into discrete modules, notably the Arp8 module, containing Arp8, Arp4, Actin, Taf14 and Ies4; the Nhp10 module, containing Nhp10, Ies1, Ies3, and Ies5; and the Arp5 module, containing Arp 5 and Ies6 (TOSI *et al.* 2013) [Figure 1.4B]. As described above, yeast Ino80 substitutes canonical H2A-H2B dimers for Swr1-deposited H2A.Z-H2B dimers and has roles in regulating transcription (EBBERT *et al.* 1999; SHEN *et al.* 2000; PAPAMICHOS-CHRONAKIS *et al.* 2011), progression of replication forks, and the DNA damage response (MORRISON *et al.* 2004; PAPAMICHOS-CHRONAKIS and PETERSON 2008).

Isw2 and Ino80 have parallel functions in promoting the replication of late-replicating parts of the yeast genome in the presence of the replication stress-inducing agent methyl methanesulfonate (MMS) (VINCENT *et al.* 2008). Double mutants lacking full function of both remodelers, such as *isw2Δ nhp10Δ* cells, have delayed S-phase progression in the presence of MMS. This defect is due at least in part to a failure to properly attenuate the S-phase checkpoint response, preventing the cell from fully replicating its genome in a timely manner (VINCENT *et al.* 2008; AU *et al.* 2011; LEE *et al.* 2015). This activity has not been mechanistically connected to any well-characterized checkpoint or DNA damage

response pathways, though the involvement may be mediated in part through direct interaction between either remodeling factor and the single-stranded DNA-binding protein RPA (AU *et al.* 2011; LEE *et al.* 2015). Thus, though lacking Isw2 and Ino80 clearly causes a defect in S phase checkpoint attenuation, the core mechanism by which this happens remains unclear.

The Ribosomal DNA Locus

Due to the enormous cellular demand for proteins, cells have an enormous demand for ribosomes, and thus, for ribosomal components. Reflecting this need, a typical rapidly growing cell of the budding yeast *Saccharomyces cerevisiae* contains an estimated 200,000 ribosomes, and the ribosomal RNA (rRNA) in those ribosomes accounts for approximately 80% of all cellular RNA (WARNER 1999). To produce sufficient rRNA, eukaryotic genomes have evolved to contain many copies of the genes that encode rRNAs, ranging across organisms from around a hundred copies to thousands of copies per genome. Tandem, head-to-tail arrays of these rRNA genes serve as a major structural component of the nucleolus, a distinct nuclear structure dedicated to the transcription and processing of rRNAs (GRUMMT and PIKAARD 2003). In different organisms, tandem arrays of rRNA genes can occur on a single chromosome or across multiple chromosomes (AGRAWAL and GANLEY 2018). The specific structure of the arrays, also referred to as the rDNA (ribosomal DNA) locus, also varies across eukaryotes, but is defined by a basic arrangement. One gene, transcribed as a single unit, encodes three of the four rRNAs. In humans, this single unit is referred to as the 45S rRNA. It contains three rRNAs that form the ribosome, the 18S, 5.8S, and 28S, as well as transcribed spacer units that are removed from the 45S RNA via a series

of cleavage and processing steps, to eventually yield the 3 distinct, mature rRNAs (Figure 1.4A). The fourth rRNA, the 5S, is located next to the 45S-equivalent gene in some organisms, such as in the budding yeast *Saccharomyces cerevisiae*, and is located in a totally different genomic location in other organisms, as is the case in mammals (GRUMMT and PIKAARD 2003; SCHNEIDER 2012).

Chromatin structure is an important regulator of rDNA biology. From yeast to humans, rDNA repeats tend to exist in one of 2 distinct states: actively transcribed and significantly depleted of nucleosomes, or transcriptionally silent and highly occupied with nucleosomes (CONCONI *et al.* 1989; DAMMANN *et al.* 1993; FRENCH *et al.* 2003; MERZ *et al.* 2008)[Figure 1.5B]. According to one model, this transcriptional paradigm facilitates genome stability by allowing for robust production of rRNAs while also maintaining a pool of un-transcribed repeats to allow for repair in the event of DNA damage (IDE *et al.* 2010). This model does not fully account for the number of un-transcribed repeats in each normal rDNA array, as there are far more such repeats than would be needed solely to serve as templates for repair. Thus, the reason for this large excess of un-transcribed repeats remains unknown. In humans, the transcriptional status of individual rDNA repeats is regulated in part through local chromatin structure by the **N**ucle**o**lar **R**emodeling **C**omplex (NoRC), comprised of TIP5 and the SNF2h, the human orthologue of yeast Isw2. NoRC represses rRNA transcription by sliding nucleosomes around the 45S promoter (STROHNER *et al.* 2001) and by recruitment of histone de-acetylase and histone methyltransferase activity (SANTORO *et al.* 2002; ZHOU *et al.* 2002). In yeast, the histone de-acetylases Sir2 and Rpd3 regulate the overall accessibility of rDNA chromatin, transcription, and changes in the

number of rDNA repeats in the tandem array (FRITZE *et al.* 1997; SMITH and BOEKE 1997; SANDMEIER *et al.* 2002; KOBAYASHI and GANLEY 2005).

The Cellular Response to DNA Damage and Replication Stress

Damage to genomic DNA or stress that prevents replication of DNA triggers a cellular checkpoint response that delays cell cycle progression, preventing cellular division until the underlying damage or stress can be resolved. At any stage of the cell cycle, a checkpoint response can be stimulated by DNA damage, and during S phase, such a response can also be caused by replication stress such as depletion of dNTP pools or compromised function of DNA polymerases (SYMINGTON and GAUTIER 2011; ZOU 2013). In *S. cerevisiae*, a critical and common early step in all versions of this process is the activation of the kinase Mec1, the yeast homolog of the human ATR (**a**taxia **t**elangiectasia and **R**ad3-related) kinase (ZOU and ELLEDGE 2003; ZOU 2013). At stalled replication forks, the S-phase checkpoint is activated by the recruitment of the 9-1-1 complex (Rad17, Ddc1, Mec3) followed by recruitment and phosphorylation of Rad53 (SUN *et al.* 1998; MELO *et al.* 2001; MAJKA *et al.* 2006). Budding yeast have two parallel pathways that can activate the G2/M checkpoint, of which one requires both Rad53 and the kinase Dun1, and the other requires Pds1 (GARDNER *et al.* 1999). In addition to timely activation of a checkpoint response, deactivation of the checkpoint is also vital for long-term cellular viability. Without the Rad53 phosphatases *PPH3* and *PTC2*, Rad53 cannot be un-phosphorylated, even after resolution of the initial cause of checkpoint activation. In such cells, the checkpoint remains active and replication forks fail to restart, resulting in cell death [Szyjka 2008].

Two of the major mechanisms of repair of DNA double strand breaks are **h**omologous **r**ecombination (HR) and **n**on-**h**omologous **e**nd **j**oining (NHEJ). Repair by HR involves the formation of single-stranded DNA surrounding the break site, a process known as resection, followed by the interaction of these resected ends with homology donors that allows for the accurate repair of the lesion (AYLON *et al.* 2004; CHAPMAN *et al.* 2012; CECCALDI *et al.* 2016). NHEJ does not require resection of the broken DNA ends; instead, the Yku70 and Yku80 proteins bind to the broken ends and promote their direction ligation to one another, in a process that restores the integrity of the DNA fiber but can often mutate the DNA sequence (CLERICI *et al.* 2008; CHANG *et al.* 2017). The cell cycle stage in which the damage occurs strongly influences whether a DSB is repaired by HR or NHEJ. Damage sustained in S or G2 will typically be repaired by HR, when an already-replicated sister chromatid is more likely to be available to serve as a homology donor. In contrast, damage sustained in G1 is more likely to be repaired by NHEJ, as at this cell cycle stage in a haploid yeast cell, a homology donor may not exist (AYLON *et al.* 2004; IRA *et al.* 2004; JAZAYERI *et al.* 2006; SYMINGTON and GAUTIER 2011).

Description of Dissertation

The goal of this dissertation is to reveal mechanisms of the regulation of chromatin structure and how this affects important biological processes. The research described takes advantage of the budding yeast *Saccharomyces cerevisiae*, a single-celled eukaryote that is genetically tractable and amenable to robust molecular analysis but still maintains a high degree of conservation with higher eukaryotes, including in its chromatin structure and regulation. I have focused my work primarily on the ATP-dependent chromatin remodeling

factors Isw2 and Ino80, continuing a progression of work examining the biology of these complexes in tandem.

In Chapter 2, I focus on the roles played by Isw2 and Ino80 at the ribosomal DNA (rDNA) locus. This research began with the observation that both complexes are targeted to the rDNA. I showed that Isw2 and Ino80 together modify local chromatin structure by positioning nucleosomes in the rDNA inter-genic spacer and by altering the proportion of actively transcribed, nucleosome depleted rDNA repeats to transcriptionally silent, nucleosome occupied repeats. In addition, I found evidence that Isw2 and Ino80 promote efficient firing of the ribosomal origin of replication and robust increase of rDNA copy number.

Chapter 3 describes work that initially sought to explore roles for Isw2 and Ino80 in the G2/M checkpoint response. Earlier work had found that these factors function in parallel to attenuate the S-phase checkpoint response (VINCENT *et al.* 2008; AU *et al.* 2011; LEE *et al.* 2015). Following these studies, we wondered if the same might be true of the G2/M checkpoint. To address this question, I employed a system to create an inducible DSB that could not be repaired by homologous recombination. In characterizing unexpected phenotypes of our remodeling factor mutant in this background, I uncovered possible parallel roles for Isw2 and Ino80 in promoting the normal preference for HR over NHEJ.

In Chapter 4, I review the major conclusions of this dissertation and discuss possible mechanisms to explain my findings. I also draw a connection between Chapters 2 and 3, proposing a possible link between these two bodies of data that would explain an un-answered mechanistic question about Isw2 and Ino80 involvement in rDNA copy number change. Finally, I propose ways to follow up on the conclusions presented.

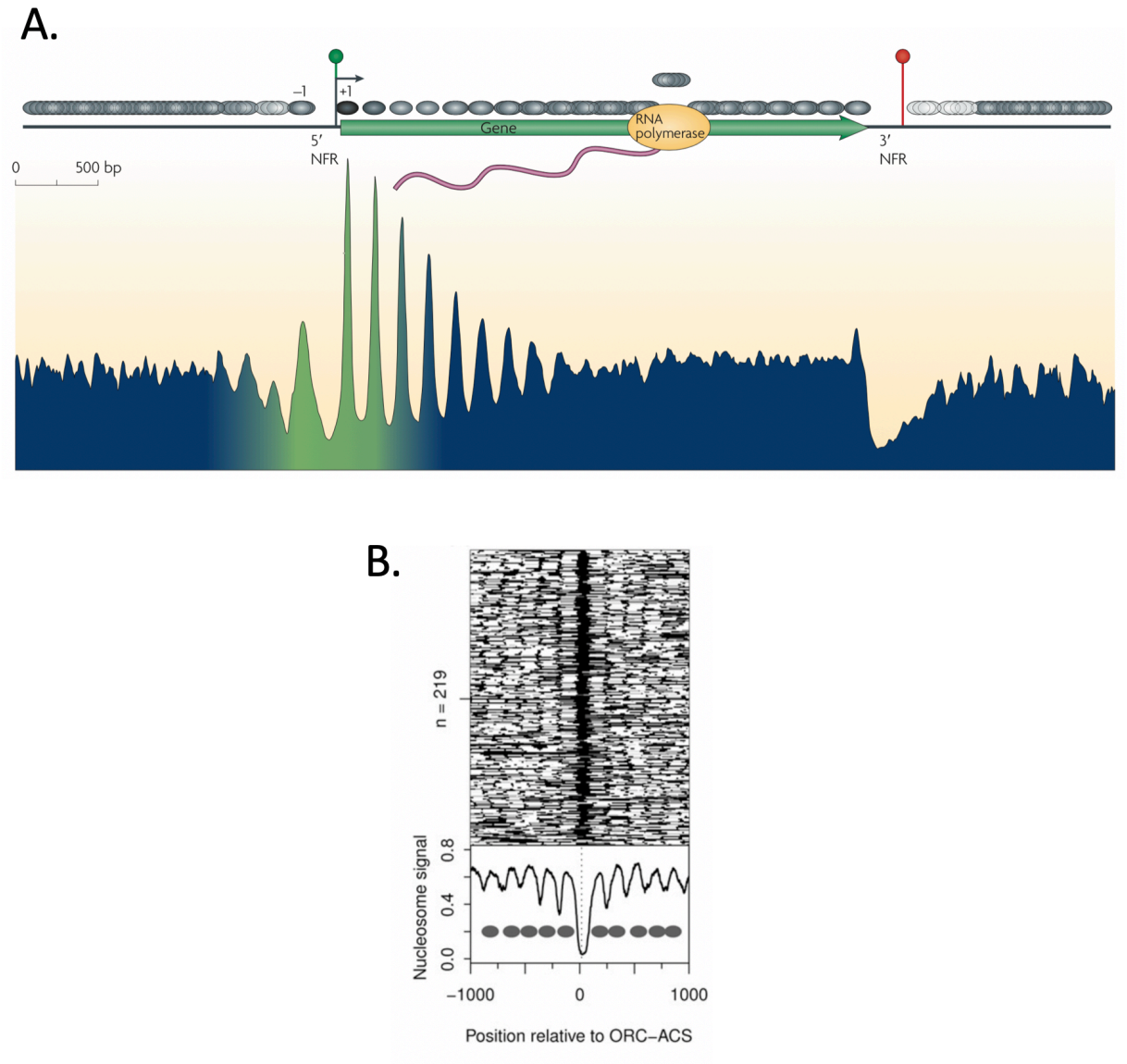

Figure 1.1: Nucleosome positioning at genes and origins or replication.

A) Schematic of an idealized gene illustrating conventions of nucleosome positioning. Nucleosomes are represented by grey ovals. In the lower panel, signal height indicates how well-positioned each nucleosome is, and color indicates different histone variants and PTMs. The best-positioned nucleosomes flank the 5' **n**ucleosome **f**ree **r**egion (NFR), and this region also is most likely to have nucleosomes containing H2A.Z and modified with H3K4 methylation. Figure from Jiang and Pugh, *Nat Rev Genet* (2009) B) Data from micrococcal nuclease (MNase) digestion followed by deep sequencing (MNase-seq), aligned to the ACSs of 219 ORC-bound ARSs. Upper panel shows tracks from each ARS; lower panel shows an averaged metaplot for all ARSs. Figure from Eaton *et al*, *Genes Dev* (2010).

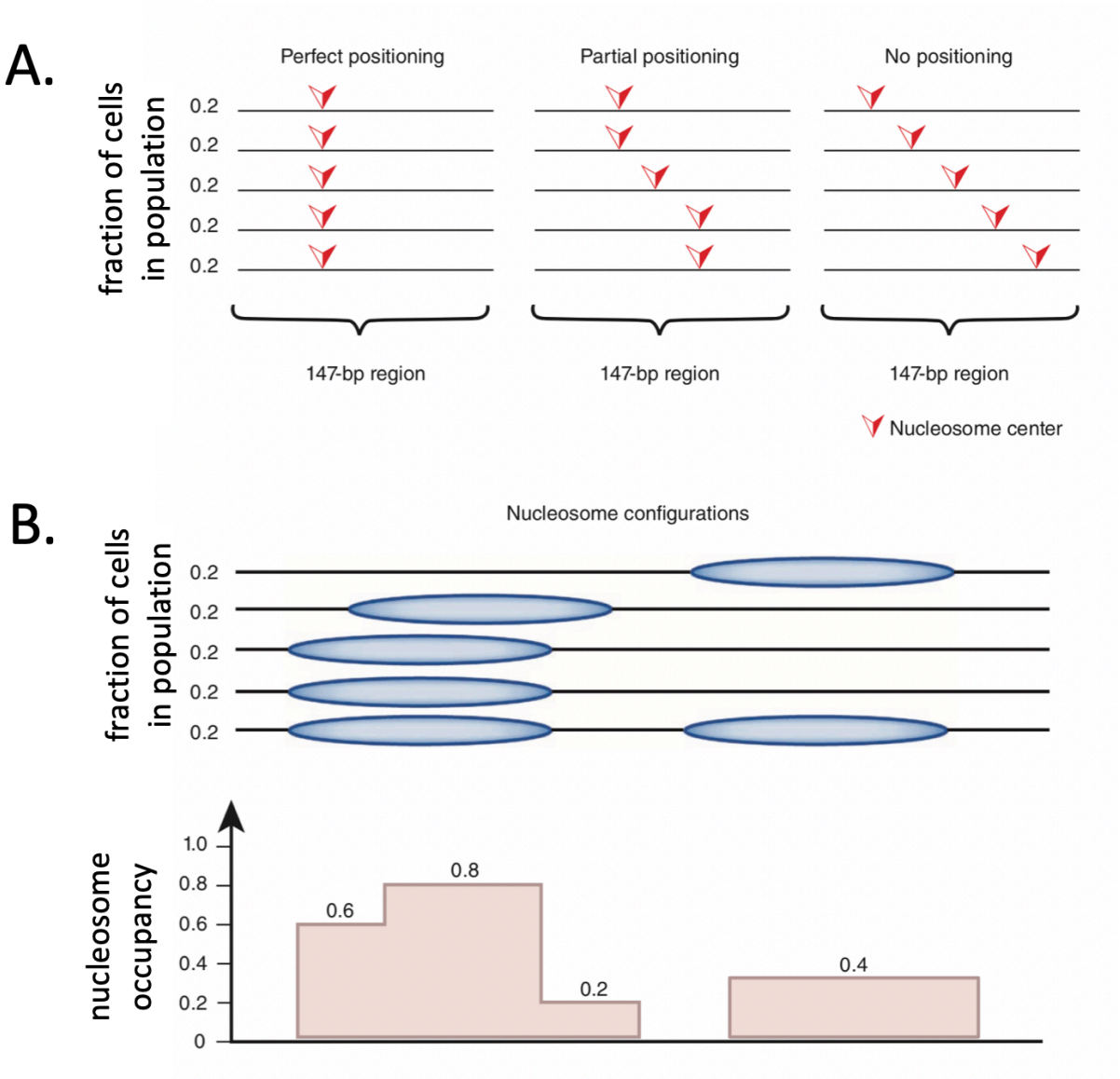

Figure 1.2: Nucleosome positioning and nucleosome occupancy.

A) A nucleosome is "well-positioned" if most such nucleosomes in a population have their dyad (center of 147 bp of nucleosome-protected DNA) at the same base pair. A nucleosome is "partially positioned" if some but not all such nucleosomes in a population have their dyad in the same approximate range of base pairs. A nucleosome is "weakly positioned" if there is little consistency in dyad location across nucleosomes in the population. B) The "nucleosome occupancy" at any base pair is the likelihood that that base pair is covered by a nucleosome in a population. Top panel: cartoons of individual fragments of chromatin. Bottom panel: plots of nucleosome occupancy assuming a population of cells as summarized above. Figure from Struhl and Segal, *Nat Struct Mol Bio* (2013).

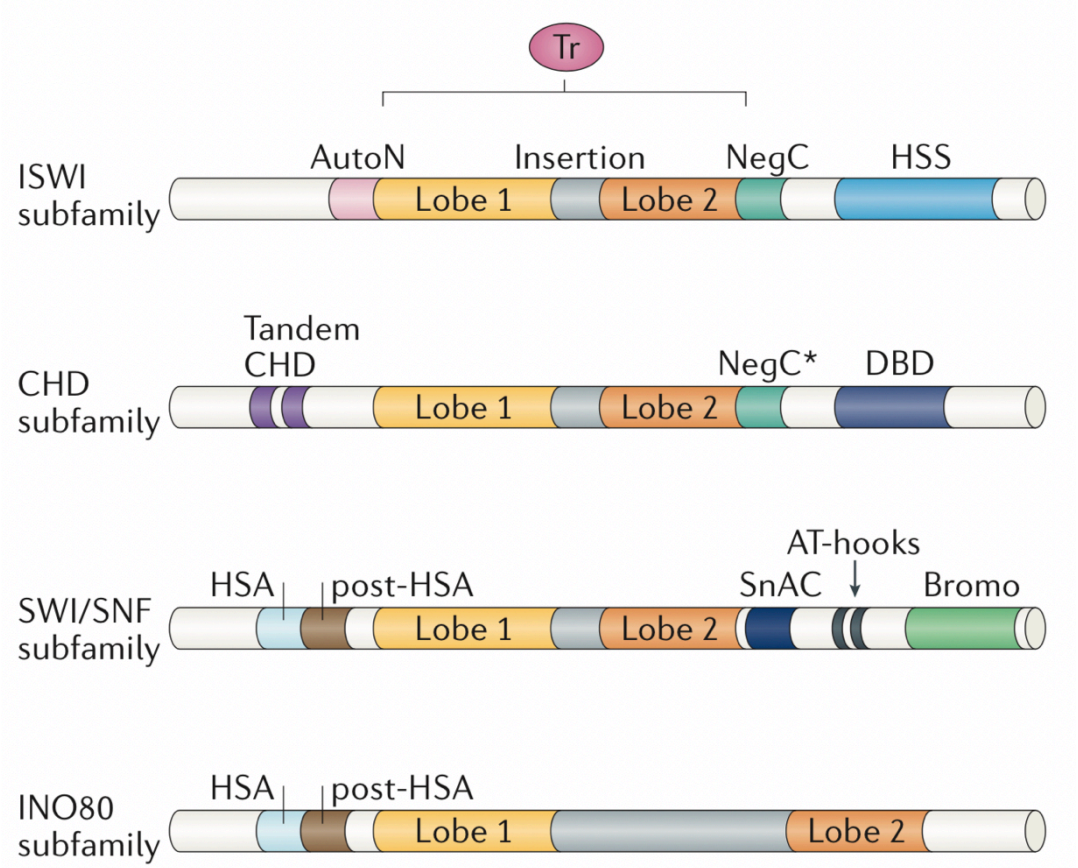

Figure 1.3: Major structural features of the ATPase subunits of the four ATP-dependent chromatin remodeling factor families.

All ATPases have an ATPase-translocase domain, characterized by two RecA-like lobes, labelled as "Lobe 1" and "Lobe 2" in each schematic. Other structural features, as well as the length and activity of the linker region between the RecA-like lobes, distinguish the four families. Abbreviations of motif elements: Tr = **tr**anslocase; AutoN = **auto**-inhibitory **N**-terminal; NegC = **neg**ative regulator of **c**oupling; HSS = **H**AND-**S**ANT-**S**LIDE; CHD = **ch**romo**d**omain; DBD = **D**NA-**b**inding **d**omain; HSA = **h**elicase/**S**ANT-**a**ssociated domain; SnAC = **Sn**f2 **A**TP-**c**oupling; Bromo = **bromo**domain. Figure from Clapier *et al*, *Nat Rev Mol Cell Biol* (2017).

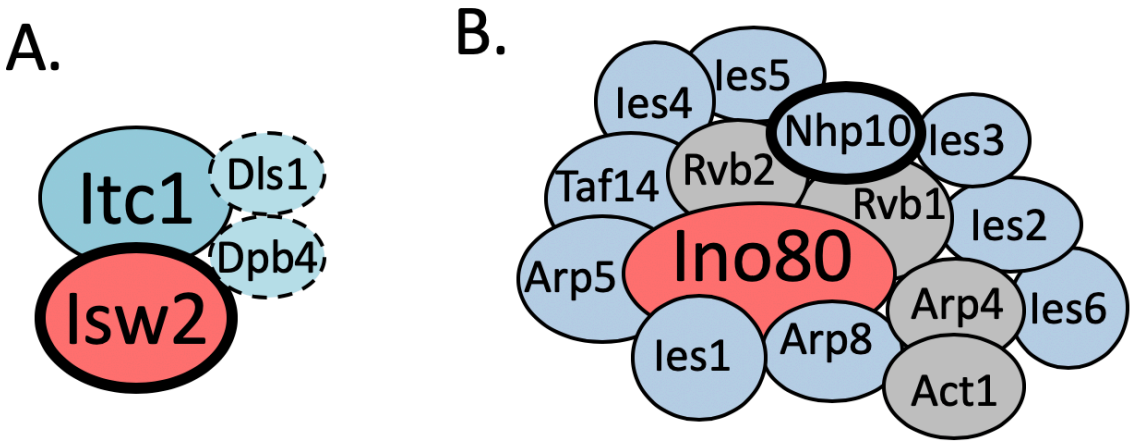

Figure 1.4: The subunit composition of the *Saccharomyces cerevisiae* Isw2 and Ino80 ATP-dependent chromatin remodeling factors.

A) Isw2 exists as a 2-subunit complex (with Itc1) or a 4-subunit complex (with Itc1, Dls1, and Dpb4 – the latter 2 indicated with dashed border). B) The Ino80 complex contains 15 subunits. The Rvb1, Rvb2, Arp4, and Act1 subunits have known functions outside of the Ino80 complex, and are indicated in grey; all other subunits function only within the Ino80 complex. In both A and B, the ATPase subunit of the complex is indicated with red, and the subunit of primary focus in this work (Isw2 and Nhp10) is indicated with a thicker border.

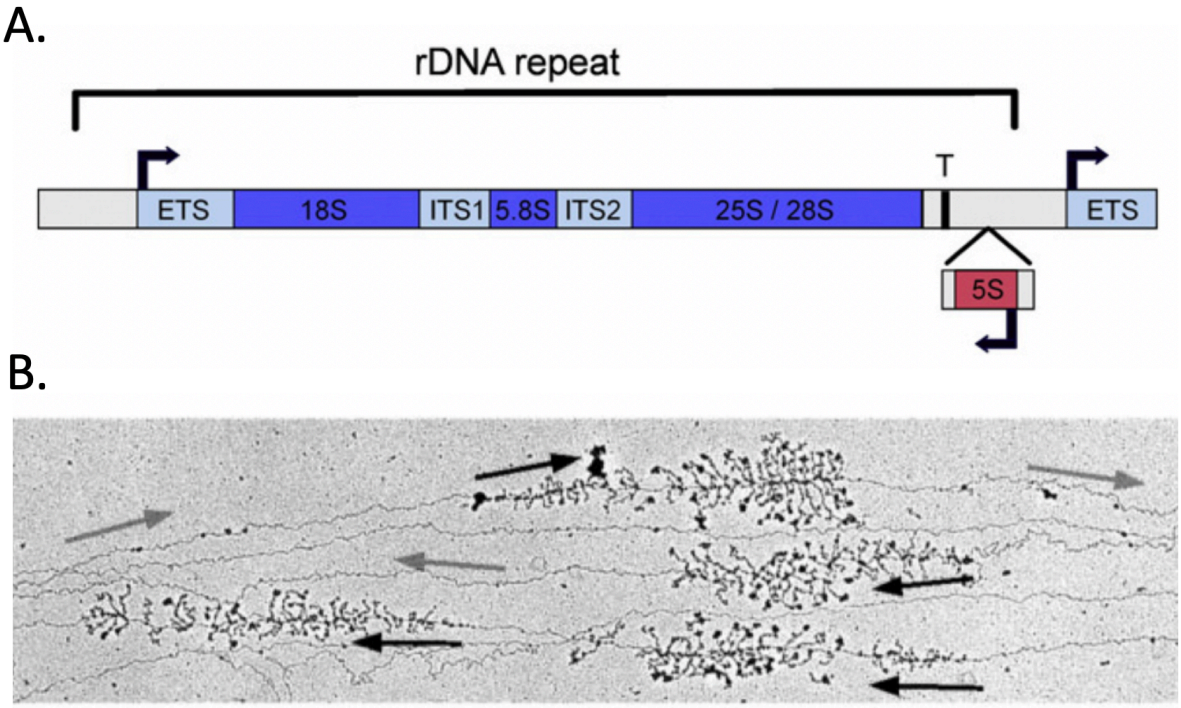

Figure 1.5: The ribosomal DNA locus.

A) Core features of the rDNA repeat across eukaryotic life. There is a major transcript (the 45S in humans, 35S in yeast) that contains **e**xternal and **i**nternal **t**ranscribed **s**pacers (ETS and ITS units) that are removed from the primary transcript to produce mature 18S, 5.8S, and 25S/28S rRNAs that are core parts of ribosomes. The 5S rRNA is present adjacent to the 35S/45S transcript in some organisms, such as yeast, and is located in a different genomic location in other organisms, such as humans. The beginning of the next repeat in the tandem array is visible to the right. Figure from Schneider, *Gene* (2012) B) Electron micrograph showing the on/off transcriptional paradigm of the rDNA locus in *Saccharomyces cerevisiae*. Actively transcribed repeats are densely loaded with polymerase, while inactive repeats are essentially totally devoid of polymerase. Figure from French *et al*, *Mol Cell Bio* (2003).

Chapter 2

Chromatin remodeling factors Isw2 and Ino80 regulate chromatin, replication, and copy number of the *Saccharomyces cerevisiae* ribosomal DNA locus

Modified from published manuscript:
Cutler, S., Lee, L.J., and Tsukiyama, T.

Summary

In the budding yeast *Saccharomyces cerevisiae*, ribosomal RNA genes are encoded in a highly repetitive tandem array referred to as the ribosomal DNA (rDNA) locus. The yeast rDNA is the site of a diverse set of DNA-dependent processes, including transcription of ribosomal RNAs by RNA Polymerases I and III, transcription of non-coding RNAs by RNA Polymerase II, DNA replication initiation, replication fork blocking, and recombination-mediated regulation of rDNA repeat copy number. All of this takes place in the context of chromatin, but little is known about the roles played by ATP-dependent chromatin remodeling factors at the yeast rDNA. In this work, I report that the Isw2 and Ino80 chromatin remodeling factors are targeted to this highly repetitive locus. I characterize for the first time their function in modifying local chromatin structure, finding that loss of these factors decreases the fraction of actively transcribed 35S ribosomal RNA genes and the positioning of nucleosomes flanking the ribosomal origin of replication. In addition, I report that Isw2 and Ino80 promote efficient firing of the ribosomal origin of replication and facilitate the regulated increase of rDNA repeat copy number. This work significantly

expands our understanding of the importance of ATP-dependent chromatin remodeling for rDNA biology.

Introduction

In exponentially growing cells, the enormous cellular demand for ribosomes is reflected in the proportion of resources dedicated to their production. For example, the production of ribosomal RNAs (rRNAs) accounts for an estimated 60% of all transcriptional activity in cycling yeast cells (WARNER 1999). Because single genomic copies of rRNA genes would not support such large volumes of transcriptional output, eukaryotic genomes have evolved to include highly repetitive clusters of rRNA genes, termed the ribosomal DNA (rDNA) locus. In a typical cell of the budding yeast *Saccharomyces cerevisiae*, the rDNA locus comprises approximately 150-200 tandem repeats [Figure 2.1A]. Each repeat contains a 35S ribosomal RNA (rRNA) gene, transcribed by RNA Polymerase I (Pol I), and an **i**nter-**g**enic **s**pacer (IGS). This spacer is split into IGS1 and IGS2 regions, also known as the **n**on-**t**ranscribed **s**pacer 1 and 2 (NTS1 and NTS2), by the 5S rRNA gene, which is transcribed by RNA Polymerase III (Pol III). Due to its large size and repetitive nature, the rDNA locus has unique regulatory needs, and the IGS1 and IGS2 regions contain genetic elements that are critical to addressing these needs.

If the rDNA locus lacked an origin of replication (autonomously replicating sequence, or ARS), replicating the rDNA array would require replication forks to traverse nearly a megabase of DNA from either end of the array. To avoid this problem, the IGS1 contains a ribosomal ARS (rARS). As a consequence, the approximately 150 ARSs in a typical rDNA array account for nearly one third of all genomic origins of replication.

Because replication factors are limiting during each S-phase (MANTIERO *et al.* 2011), firing of too many rARSs would take vital replicative resources away from other parts of the genome, raising the risk of delayed or incomplete replication. As a result, only around 20% of rARSs will fire in any given round of cell division (WALMSLEY *et al.* 1984; BREWER and FANGMAN 1988). If too few rARSs fire, replication of the rDNA array may be delayed or incomplete (YOSHIDA *et al.* 2014). Thus, properly striking this balance by regulating origin efficiency at the rDNA has critical consequences for global genome stability. Another balance must be carefully achieved in maintaining the proper size of the rDNA array. The array must be large enough to support sufficient transcription of rRNAs, but small enough to be efficiently replicated without demanding too large a proportion of the limited pool of replication factors (MANTIERO *et al.* 2011). Thus, a mechanism exists to change the size of the array by adding or removing copies of the rDNA repeat as needed, and the IGS1 region contains two genetic elements that are critical for this process: a bi-directional RNA Pol II promoter, E-pro, and a replication fork block (RFB).

All DNA-dependent processes occurring at the rDNA happen in the context of chromatin structure. The Sir2 and Rpd3 histone deacetylases (HDACs) have well-established roles in regulating rDNA chromatin structure, origin activity, and copy number maintenance (FRITZE *et al.* 1997; SANDMEIER *et al.* 2002; KOBAYASHI and GANLEY 2005; YOSHIDA *et al.* 2014). In addition, the rDNA locus is regulated by ATP-dependent chromatin remodeling factors, which use the energy of ATP hydrolysis to modify the position and histone composition of nucleosomes. In humans, the nucleolar remodeling complex (NoRC) positions nucleosomes and recruits histone methyltransferase and histone deacetylase activity to promote rDNA silencing (SANTORO *et al.* 2002; LI *et al.* 2006). In budding yeast,

the SWI/SNF (ZHANG *et al.* 2013), Isw1, Isw2, and Chd1 (JONES *et al.* 2007) complexes have been implicated in regulating transcription of rRNAs. However, it has not been shown how remodeling factors modify chromatin structure at the yeast rDNA or affect any DNA-dependent processes at this locus beyond rRNA transcription.

In this work, I show that the Isw2 and Ino80 ATP-dependent chromatin remodeling factors regulate chromatin structure at the rDNA. The Isw2 complex is known to slide nucleosomes over gene promoters (FAZZIO and TSUKIYAMA 2003), an activity that generally represses transcription, both for coding genes (GOLDMARK *et al.* 2000; FAZZIO *et al.* 2001) and antisense transcripts (WHITEHOUSE *et al.* 2007). The Ino80 complex slides and evicts nucleosomes and removes the histone variant, H2A.Z (TSUKUDA *et al.* 2005; PAPAMICHOS-CHRONAKIS *et al.* 2011; UDUGAMA *et al.* 2011; ZHOU *et al.* 2018). Ino80 is also involved in regulating the checkpoint response following DNA damage, DNA damage repair, and DNA replication (MORRISON *et al.* 2004; MORRISON *et al.* 2007; SHIMADA *et al.* 2008). Isw2 and Ino80 function together to promote replication of late-replicating regions of the genome in the presence of replication stress and to attenuate the S-phase checkpoint response (VINCENT *et al.* 2008; AU *et al.* 2011; LEE *et al.* 2015). Here, I show that both Isw2 and Ino80 are targeted to the ribosomal DNA locus. Further, I report for the first time that these remodeling factors affect local chromatin structure, as loss of the factors increases nucleosome occupancy in the 35S gene and alters the positioning of nucleosomes flanking the rARS. I find that loss of Isw2 and Ino80 reduces the proportion of active rDNA repeats without affecting overall transcription of rRNAs, but that Isw2 and Ino80 positively contribute both to the efficiency of the rARS and to the rate of rDNA repeat copy number increase. In sum, this study expands our understanding of how ATP-dependent chromatin

remodeling factors affect both chromatin structure and essential biological processes at the ribosomal DNA locus.

Results

The Isw2 and Ino80 chromatin remodeling complexes are targeted to the ribosomal DNA locus

All of the DNA-dependent processes that take place at the rDNA locus occur in the context of chromatin. Although HDACs such as Rpd3 and Sir2 have well-characterized functions in regulating chromatin structure, transcription, and copy number maintenance at the *S. cerevisiae* rDNA (FRITZE *et al.* 1997; SMITH and BOEKE 1997; SANDMEIER *et al.* 2002; KOBAYASHI and GANLEY 2005), comparatively little is known about the roles played by ATP-dependent chromatin remodeling factors at this vital genomic locus. To address this question, I performed chromatin immuno-precipitation followed by deep sequencing (ChIP-seq) to map where the Isw2 and Ino80 chromatin remodeling factors are targeted at the rDNA. By this method, I found that Isw2, the catalytic subunit of that complex, and Nhp10, a protein that only functions as a subunit of the Ino80 complex (MORRISON *et al.* 2004), were both targeted to the rDNA [Figure 2.1B]. The ChIP-seq signal for Isw2 was slightly above the genome-average throughout the 35S gene body. The pattern of targeting in the IGS included small peaks flanking the 5S gene and the region containing E-pro and the RFB, but the most prominent signal was a striking, bimodal peak on top of and to one side of the rARS. Nhp10 was also present throughout the 35S gene body and showed a small peak around the 5S gene. The ChIP-seq patterns of both factors at the rDNA were consistent with peaks elsewhere in the genome with regard to both shape and magnitude: Isw2 tended to have fairly defined peaks that rise well above the genome average, located

in intergenic regions, and Nhp10 peaks were generally less prominent relative to the genome average and more diffusely spread throughout a transcription unit [Figure 2.1C]. Out of 830 peaks identified genome-wide by the MACS peaks-calling algorithm in this Nhp10 ChIP-seq data set, this rDNA peak had the third-lowest p-value (p = 4.81E-73). Given these distinct targeting patterns, I hypothesized that these ATP-dependent chromatin remodeling factors might have previously unknown functions at this highly repetitive, unique genomic locus.

Isw2 and Ino80 affect nucleosome occupancy over the 35S rRNA gene

In light of the established functions of the Isw2 and Ino80 complexes, I first asked whether these chromatin remodeling factors affect nucleosome occupancy within the rDNA locus. Individual rDNA repeats exist in one of two discrete states, being either highly occupied with nucleosomes and transcriptionally inactive, or heavily depleted of nucleosomes and highly transcriptionally active (CONCONI *et al.* 1989; FRENCH *et al.* 2003; MERZ *et al.* 2008). I assessed how nucleosome occupancy at the rDNA is affected by these two chromatin remodeling factors with ChIP-seq of histone H3 in wild-type, *isw2Δ*, *nhp10Δ*, and *isw2Δ nhp10Δ* strains. This analysis revealed that nucleosome occupancy throughout the 35S gene body is appreciably increased in the *isw2Δ nhp10Δ* double mutant compared to wild-type and single deletion strains [Figure 2.2A]. Notably, this is the part of the rDNA in which the ChIP-seq signals of both chromatin remodeling factors most strongly overlap, suggesting the possibility that these factors may work together in this region.

Because individual rDNA repeats exist in one of two discrete chromatin states, I hypothesized that the increased nucleosome occupancy in *isw2Δ nhp10Δ* cells reflected a

reduced ratio of active to inactive rDNA repeats. To test this, I used psoralen cross-linking, a well-established method to determine the ratio of active to inactive rDNA repeats (CONCONI *et al.* 1989; DAMMANN *et al.* 1993). Occupancy of chromatin by nucleosomes blocks incorporation of psoralen. Therefore, actively transcribed, nucleosome-depleted rDNA repeats become more heavily cross-linked with psoralen, and thus migrate more slowly in an agarose gel, than inactive, nucleosome-occupied repeats. After digestion with appropriate restriction enzymes, Southern blotting, and hybridization with a probe targeting a region of the 35S gene unit, two discrete bands representing active and inactive repeats can be resolved (CONCONI *et al.* 1989; DAMMANN *et al.* 1993). This method showed that, as expected, a very large proportion of repeats are active in an asynchronously growing strain with only 20 copies of the rDNA (FRENCH *et al.* 2003), and a very small proportion of repeats are active in a wild-type strain at stationary phase. I found that *isw2Δ nhp10Δ* cells have a significantly reduced proportion of active repeats compared to wild-type, *isw2Δ*, or *nhp10Δ* cells [Figure 2.2B, $p < 0.05$], consistent with the observed increase in H3 occupancy in double mutant cells. Based on these results, I concluded that the Isw2 and Ino80 chromatin remodeling factors increase the fraction of active rDNA repeats.

Transcription of 35S ribosomal RNA is not affected by loss of Isw2 or Nhp10

Based on the reduced proportion of nucleosome-depleted rDNA repeats in the *isw2Δ nhp10Δ* mutant, I hypothesized that these cells would also show reduced levels of 35S rRNA transcription. The 35S is transcribed as a single long transcript before being cleaved and folded in a series of processing steps to yield mature 18S, 5.8S, and 25S RNAs (WOOLFORD and BASERGA 2013). Because mature rRNAs are components of ribosomes and thus highly stable and abundant, nascent RNA needs to be measured to assess the net production of

rRNAs. The External Transcribed Spacer 1 (ETS1) and Internal Transcribed Spacer 1 (ITS1) sections of the 35S gene are transcribed but removed at early stages of rRNA processing. Levels of these RNA sequences thus reflect levels of nascent rRNA and are used to measure the rate of 35S transcription (BYWATER *et al.* 2012; LARIBEE *et al.* 2015). Adopting this approach, I performed reverse-transcription quantitative PCR (RT-qPCR) targeting parts of the ETS1 and ITS1 regions of the 35S pre-rRNA [Figure 2.2A]. As expected, I found significantly reduced levels of both ETS1 and ITS1 in cells lacking the RNA Pol I subunit, *RPA49* ($p = 0.0021$ and $p = 0.037$, respectively); *rpa49Δ* strains are known to have a reduced rate of RNA Pol I transcription (BECKOUET *et al.* 2008; LARIBEE *et al.* 2015). In contrast, I did not see evidence of a significant difference in rates of 35S transcription in *isw2Δ nhp10Δ* compared to wild-type [Figure 2.2C] ($p = 0.19$ and $p = 1.00$). To confirm this result by an independent method, I performed ChIP-seq analysis of the Pol I subunit RPA190, and observed virtually identical profiles in *isw2Δ nhp10Δ* and wild-type strains, with regard to both shape and overall levels [Figure 2.2D]. Based on these results, I concluded that *isw2Δ nhp10Δ* cells exhibit no significant defects in 35S transcription despite the differences in nucleosome occupancy and the proportion of nucleosome-occupied rDNA repeats in these mutants.

Isw2 and Ino80 affect nucleosome positioning in the rDNA inter-genic spacer

In addition to nucleosome occupancy, nucleosome positioning is known to be affected by both of these chromatin remodeling factors (FAZZIO and TSUKIYAMA 2003; UDUGAMA *et al.* 2011). ChIP-seq of histone H3 is suitable for measuring nucleosome occupancy, but because it relies on sonication-based fragmentation of chromatin, it lacks

sufficient resolution to accurately reveal nucleosome positioning. Therefore, I assessed nucleosome positioning at the rDNA by micrococcal nuclease (MNase) digestion followed by deep sequencing (MNase-seq). During the preparation of MNase-digested DNA, I gel purified mononucleosome-sized fragments of ~150 bp and then interpreted each size-selected, paired-end read as coming from a nucleosome-protected fragment of DNA. From each paired-end read, the nucleosomal dyad center was inferred and plotted [Figure 2.3A]. By this method, nucleosome positions appeared strongly shifted at known Isw2 targets in *isw2Δ* and *isw2Δ nhp10Δ* mutants [Figure 2.4]. In contrast, no gross differences in nucleosome positions were observed throughout the 35S gene body [Figure 2.5] or in the rDNA inter-genic spacer region [Figure 2.3A]. However, sequencing data must be interpreted carefully within the highly repetitive rDNA, as such data represent an average of the signal at all ~150 rDNA repeats in all cells sampled, and nucleosomes in only a fraction of those repeats may change positions in any given cell.

To refine our analysis, I compared MNase-seq profiles for the tested strains using ribbon plots in which the primary line shows the average signal at each base pair across multiple biological replicates, and the ribbon represents the standard error of the mean for those replicates [Figure 2.3B]. This method revealed highly reproducible, strain-specific differences in nucleosome positioning at the rDNA for two pairs of nucleosomes. One pair is in between the 35S promoter and the rARS, with each nucleosome substantially overlapping one of the two sub-peaks of the highly prominent Isw2 peak [Figure 2.3B, left panel, identified as nucleosomes 1 and 2]. The other pair of affected nucleosomes is in the region between the rARS and the 5S gene, overlapping half of the short, broad Isw2 peak encompassing the 5S gene [Figure 2.3B, right panel, nucleosomes 3 and 4]. Each of these

four MNase-seq dyad peaks has two or three sub-species of nucleosome positions. I interpret each of these distinct sub-species as representing one of two or three distinct positions occupied by that nucleosome in different individual rDNA repeats in the array. Each of the four genotypes tested had a characteristic pattern of the relative heights of these two sub-species, which I propose reflects different proportions of rDNA arrays containing nucleosomes at each possible position. The overall trend among these mutants is that in *isw2Δ nhp10Δ* cells, any given rDNA repeat is more likely to have nucleosomes positioned such that they are encroaching on the rARS [Figures 2.3B and 2.3C]. In contrast, in both *nhp10Δ* and wild-type cells, these same nucleosomes are more likely to be positioned farther away from the rARS, and in *isw2Δ* cells these nucleosomes have profiles somewhere in between wild-type and the double mutant.

It has been shown that the strength of MNase digestion can affect nucleosome mapping results, especially for nucleosomes that are highly MNase sensitive (WEINER *et al.* 2010). Because the differences in MNase-seq signal at the rDNA locus were more subtle than what is typically observed at single-copy loci, I sought to ensure that these differences are not due to differential MNase sensitivity of these nucleosomes. To this end, I compared the MNase-seq profiles for these nucleosomes in wild-type and *isw2Δ nhp10Δ* strains using three different concentrations of MNase (Figure 2.3D, Figure 2.5B). The overall shapes of the MNase-seq profiles varied depending on the MNase concentrations used. However, at any specific degree of digestion, the relative heights of nucleosomal sub-species for wild-type versus *isw2Δ nhp10Δ* cells matched the patterns described above. These results confirmed that the observed differences in nucleosome positions in mutants were not due to differential MNase sensitivity of these nucleosomes.

Isw2 and Ino80 facilitate efficient firing of rDNA origin of replication

The prominent Isw2 peak around the rARS coupled with the shrinkage of the rARS-containing nucleosome-depleted region (NDR) in chromatin remodeling factor mutants led us to ask whether origin activity is affected by these factors. To address this question, I performed two-dimensional (2D) gel electrophoresis probing activity of the rARS (BREWER and FANGMAN 1987). The Y arc of the 2D gel is comprised of restriction fragments in the process of being passively replicated, and the bubble arc of restriction fragments in which an origin of replication has actively fired. Therefore, the ratio of bubble to Y arc signals from asynchronously growing cells reflects the ratio of actively to passively replicated restriction fragments, and thus of origin efficiency [Figure 2.6A]. By this method, the ratio of bubble arc to Y arc signal, and thus rARS origin efficiency, was greatest in the wild-type and *isw2Δ* cells. In contrast, origin efficiency was moderately reduced in *nhp10Δ* cells, by approximately 10%, and even more reduced, by nearly 30%, in *isw2Δ nhp10Δ* double mutants [Figure 2.6B, $p = 0.04$]. This reduction in origin efficiency in the double mutant is approximately half the magnitude of the reported increase in rARS efficiency in cells lacking *SIR2* (PASERO *et al.* 2002), the best-characterized chromatin regulator of rARS activity. To test whether Isw2 and Nhp10 also affect rARS firing under a sub-optimal growth condition, I performed 2D gels of wild type and double mutant cells at 23°. Consistent with our model, robust reduction in origin efficiency was also detectable in the double mutant under this condition [Figure 2.6C].

To use another method to corroborate this finding, I employed ChIP-seq of MCM4, a subunit of the mini-chromosome-maintenance (MCM) helicase complex, a critical

component of the replication machinery. I arrested WT and *isw2Δ nhp10Δ* cells in G1 with alpha-factor, then released into fresh medium without alpha-factor, sampling chromatin at 20' and 50' post-release. Both WT and *isw2Δ nhp10Δ* have clear peaks of MCM at the rARS at the G1 time point, reflecting the assembly of the pre-replication complex [Figure 2.6D]. However, at this time point, the MCM peak is much smaller in the double mutant than in WT. At the 20' time point, the WT peak has shrunken considerably, and a distinct peak has formed at the RFB, likely indicative of robust pausing of many replication bubbles. In contrast, the double mutant's MCM peak has not shrunk by as much relative to G1, with little peak visible at the RFB. Finally, by the 50' time point, essentially no MCM signal is visible in the IGS in the WT, while in the double mutant, a small peak lingers at the rARS and, for the first time, a small peak is visible at the RFB. These data are consistent with a smaller proportion of rDNA repeats in *isw2Δ nhp10Δ* cells containing actively-firing rARSs, as well as potentially having slightly different kinetics of rARS activity, at least in a system of release from G1 arrest. Collectively, these results indicate that the Isw2 and Ino80 chromatin remodeling factors promote the efficient firing of the ribosomal origin of replication.

Isw2 and Ino80 affect the rate of rDNA copy number increase

Each yeast strain maintains a particular number of rDNA repeats, typically ~150-200 repeats. The lower limit on the number of repeats is imposed both by the demand for transcription of rRNAs (WARNER 1999) and by the benefit to genome stability of having enough rDNA repeats such that not all repeats are transcribed simultaneously (IDE *et al.* 2010). An upper limit on the number of repeats comes from balancing the above needs

against the burden of replicating a lengthy rDNA array in a context of limiting replication factors (SALIM *et al.* 2017). All of the strains used in the previously described experiments maintain approximately the same steady-state rDNA copy number of ~150 copies [Figure 2.7], indicating that loss of Isw2 and Nhp10 does not affect the steady-state size of the rDNA array. This, however, does not necessarily mean these remodeling factors play no roles in rDNA copy number change, because cells with optimally sized rDNA arrays are unlikely to visibly alter the sizes of those arrays during exponential growth without any perturbation. To determine whether Isw2 and Ino80 affect the process of regulated rDNA copy number change, I employed an established experimental system for this purpose. This approach uses a strain background in which endogenous *FOB1* has been deleted and the rDNA array reduced to 20 repeats. In the absence of Fob1, there is no pausing at the RFB, stabilizing rDNA copy number. These cells can survive with 20 copies of the rDNA, but because this is a sub-optimal number of repeats, introduction of Fob1 via a plasmid causes a rapid increase in the number of rDNA repeats via homologous recombination until the rDNA array reaches a more-optimal size of approximately 150 copies (KOBAYASHI and GANLEY 2005). The rate of rDNA copy number change can vary between strains, as cells of the W303 background increase copy number more rapidly than BY4741 derivatives (M.K. Raghuraman and Bonny Brewer, personal communication).

Starting with a *fob1Δ* strain with 20 copies of the rDNA, *ISW2*, *NHP10*, or both genes were deleted. *FOB1* was then re-introduced on a plasmid, and the cells were cultured continuously under selection for almost 200 generations. Samples were taken at multiple time points, synchronized such that time points were taken for all tested strains at the same number of generations after re-introduction of Fob1, thus controlling for any small

differences in growth rate between the strains. The copy number of rDNA repeats was monitored by CHEF gel electrophoresis of intact chromosomal DNA followed by Southern blot analysis using a probe against Chromosome XII. This experiment thus reveals the regulated process of rDNA copy number increase by the cell, distinct from the small, likely stochastic fluctuations around the optimal copy number for any given strain.

Although all four strains began to increase their rDNA copy number immediately following introduction of plasmid-borne Fob1, each of the strains behaved differently [Figure 2.8A, B]. In wild-type and *isw2Δ* cells, and to a slightly lesser degree in *nhp10Δ* cells, there was a strong jump in copy number at around 35 generations after Fob1 re-introduction, the earliest time point I was able to sample. In contrast, *isw2Δ nhp10Δ* cells exhibited only a very small increase in copy number at 35 generations. After nearly 200 generations in the presence of Fob1, both the wild-type and *isw2Δ* strains had recovered essentially wild-type rDNA copy number of around 150 copies, and *nhp10Δ* was close to this number. In contrast, *isw2Δ nhp10Δ* had barely reached 100 copies by this time point. Based on this data, I conclude that Isw2 and Ino80 facilitate the regulated increase of rDNA copy number in the rDNA array, and that their loss reduces the rate at which rDNA copy number can be increased in a population of cells.

Given the established role for Ino80 in the DNA damage response (VAN ATTIKUM *et al.* 2004; PAPAMICHOS-CHRONAKIS *et al.* 2006; VAN ATTIKUM *et al.* 2007), I wondered whether the reduced rate of rDNA copy number increase in the *isw2Δ nhp10Δ* cells was unique to the rDNA locus or the result of a more general defect in recombination. To address this question, I measured the recombination efficiency of remodeling factor mutants at a locus outside of the rDNA. To this end, I linearized plasmid pRS406, containing a wild-type *URA3*

gene, by restriction digesting with StuI, an enzyme that cuts in the middle of the *URA3* gene. This linearized plasmid was then integrated into WT, *isw2Δ*, *nhp10Δ*, and *isw2Δ nhp10Δ* strains with the *ura3-1* allele, producing a gene duplication of a *ura3-1* adjacent to *URA3*. These strains were cultured first in the absence of uracil, to maximize the proportion of URA3+ cells, and then switched to growth without selection in YPD for approximately ten generations. During this time, the *URA3* allele would recombine with the mutant *ura3-1* allele at some low frequency, leading to a single mutant allele, and thus rendering the cell able to survive in the presence of 5-FOA. Cells were then plated on 5-FOA medium and the number of 5-FOA-resistant colonies was counted. From this count, the number of recombination events was calculated (LURIA and DELBRUCK 1943; LEA and COULSON 1949), and this value was normalized to the total number of cell divisions in each culture to yield the rate of recombination events per cell division.

For all tested strains, this rate was found to be approximately $5x10^{-6}$ [Figure 2.8C]. This is a reasonable number, as it is approximately tenfold lower than the frequency of mitotic recombination for a similar side-by-side duplication of the *HIS4* gene in *Saccharomyces cerevisiae*, found to be approximately $5x10^{-5}$ per cell (JACKSON and FINK 1981). Based on this assay, none of the tested strains significantly differed in their rates of recombination. I therefore concluded that the reduced rate of rDNA copy number increase observed in *isw2Δ nhp10Δ* cells resulted not from a general defect in recombination, but rather from the loss of a unique function of these chromatin remodeling factors in promoting rDNA copy number change.

Discussion

The ribosomal DNA locus is the evolutionarily conserved site of many different DNA-dependent processes, all of which must be carefully balanced. Sufficient rRNA must be transcribed to support ribosome biogenesis, but without interfering with faithful replication of the rDNA (WARNER 1999). The rDNA array must be fully replicated, while still allowing for the replication of other parts of the genome (YOSHIDA *et al.* 2014). The size of the rDNA array must be carefully maintained through recombination, yet the array must be protected from unintended recombination despite its highly repetitive nature. Many studies have detailed these complex processes, but relatively little is known about how ATP-dependent chromatin remodeling factors dynamically regulate chromatin structure at the *S. cerevisiae* rDNA locus to allow for these processes to occur. The SWI/SNF complex localizes to the rDNA and that deletion of its Snf6 subunit reduces 35S rRNA transcription (ZHANG *et al.* 2013). In addition, it was shown that Isw2, Isw1, and Chd1 are present at the rDNA, and that their simultaneous deletion reduces 35S rRNA transcriptional termination (JONES *et al.* 2007). However, the nature of chromatin regulation by these remodeling factors at the rDNA locus remains unknown, as does their involvement in processes beyond transcription of rRNA. In this study, I show that in addition to Isw2, the Ino80 ATP-dependent chromatin remodeling factor is targeted to the yeast rDNA. I show for the first time that these factors modify local chromatin structure at the levels of nucleosome occupancy, the ratio of nucleosome-occupied to nucleosome-depleted rDNA repeats, and nucleosome positioning. In addition, I find that these chromatin remodeling factors affect two critical activities that take place at the rDNA, replication initiation from the ribosomal ARS, and rDNA array amplification.

Our data indicate that Isw2 and Ino80 do not affect overall levels of 35S rRNA transcription, a result that initially surprised us. According to one part of the accepted model, nucleosome occupancy through the 35S gene body dictates 35S transcription, as rDNA repeats that are heavily occupied with nucleosomes are transcriptionally silent, while repeats that are depleted of nucleosomes are transcriptionally active (MERZ *et al.* 2008). Thus, based on the increased nucleosome occupancy and reduced proportion of psoralen-accessible rDNA repeats observed in *isw2Δ nhp10Δ* cells, I expected that 35S rRNA transcription would be correspondingly decreased. The lack of an effect on transcription may be explained by the robustness of 35S transcriptional regulation: When one element of this system is disrupted, another element is adjusted to maintain the desired level of transcription. For example, in a *S. cerevisiae* strain in which the rDNA array has been reduced from a normal size of ~150 copies down to ~40 copies, loading of RNA Pol I on any given active repeat is increased, such that there is no net decrease in 35S transcriptional output (FRENCH *et al.* 2003). Similarly, in mammalian cells, inducing silencing of some rDNA repeats by depletion of **u**pstream **b**inding **f**actor (UBF) leads to a compensatory increase in transcription per active repeat (SANIJ *et al.* 2008). I therefore speculate that the robust homeostatic regulation of rRNA transcription overcomes changes in nucleosome occupancy in *isw2Δ nhp10Δ* cells, reacting to a reduced proportion of active repeats by increasing RNA Pol I transcription in each active unit. This would produce no net alteration in rRNA production compared to wild-type cells.

A critical transcriptional regulator at the mammalian rDNA is the Nucleolar Remodeling Complex (NoRC), which contains SNF2h, the mammalian orthologue of yeast Isw2. Among other activities that influence rRNA transcription, this complex shifts the

nucleosome at the promoter of the 45S rRNA gene, the mammalian orthologue of the yeast 35S, into a transcriptionally repressive position (LI *et al.* 2006). Notably, I see nearly identical nucleosome positioning profiles at the comparable nucleosome in *isw2Δ* and *isw2Δ nhp10Δ* cells compared to wild-type cells [Figure 2.5C]. This finding, in conjunction with our observing no differences in rRNA transcription in these deletion strains, distinguishes the Isw2-mediated regulation of the yeast rDNA from the NoRC-mediated regulation of the mammalian rDNA.

While I find that loss of Isw2 and Ino80 does not affect net rRNA transcription, I do find that their loss reduces the activity of the rARS. There are multiple reports that chromatin structure around replication origins significantly affects DNA replication. Blocking an ARS with a nucleosome reduces the efficiency of that ARS (SIMPSON 1990), and proper positioning of nucleosomes adjacent to an ARS is important for replication initiation (LIPFORD and BELL 2001). Compared to naked DNA, chromatinized DNA influences where the **o**rigin **r**ecognition **c**omplex (ORC) binds duringorigin licensing, suggesting that chromatin structure regulates which origins fire during S-phase (KURAT *et al.* 2017). Consistent with these findings, ATP-dependent chromatin remodeling factors contribute to regulating replication initiation. For example, the SWI/SNF complex is targeted to a subset of origins in HeLa cells (EUSKIRCHEN *et al.* 2011) and facilitates replication initiation at one out of four natural ARSs tested in a mini-chromosome maintenance assay in *S. cerevisiae* (FLANAGAN and PETERSON 1999). By applying an *in vitro* replication assay to nucleosomal templates remodeled by different chromatin remodeling factors, a recent study found that most factors permitted origin licensing, but that Isw2 and Chd1 prevented it (AZMI *et al.* 2017). As far as we know, however, there have been no reports of how chromatin

remodeling factors change chromatin structure to affect activity of replication origins at their native loci. Our work therefore established the first example in which chromatin remodeling factors affect both chromatin structure and replication initiation at a specific origin of replication at its natural genomic locus *in vivo*.

I report that loss of *ISW2* and *NHP10*, individually and together, reduced the efficiency of the rARS during logarithmic growth conditions in rich medium. I found that *isw2Δ nhp10Δ* cells have the most robust differences in nucleosome positioning compared to wild-type cells, with a clear trend of an enrichment for nucleosomes in positions that encroach on the rARS. These same cells have the most reduced efficiency at this ARS compared to wild-type. This effect is opposite that of Isw2 at Pol II-transcribed genes. At such genes, when *ISW2* is deleted, NDRs at the end of the gene targeted by Isw2 tend to widen, and nearby coding and non-coding transcription increases, suggesting that this remodeling factor typically functions to narrow these NDRs and repress transcription (WHITEHOUSE *et al.* 2007). Our data suggest that the NDR containing the rARS overall becomes narrower and origin efficiency goes down in *isw2Δ nhp10Δ* cells, suggesting a normal function of these factors in keeping this NDR wide and thus permissive to replication initiation. Given that both Isw2 and Nhp10 are present at the rARS and alter positions of nucleosomes around rARS, it is plausible that they play direct roles in rARS activity. In addition, reduced rARS efficiency in our mutants may also be partially due to the altered ratio of transcriptionally active to inactive rDNA repeats. It has been shown that rARSs are more likely to fire when they are adjacent to actively transcribed 35S genes (MULLER *et al.* 2000). The proportion of actively transcribed repeats is reduced in *isw2Δ nhp10Δ* cells, and thus a reduced proportion of rARSs in the array are adjacent to actively

transcribed repeats, possibly contributing to the reduced origin efficiency I observe in these mutants. I also note that despite this significant reduction in rARS efficiency, *isw2Δ nhp10Δ* cells do not have an obvious growth defect in rich medium at 30°. As described earlier, *sir2Δ* strains have an even greater magnitude change in rARS activity and are similarly healthy under such conditions. These results collectively suggest the robustness of replication control mechanisms at the rDNA locus under un-stressed conditions.

In addition to regulating rARS activity, a cell must carefully calibrate the size of the rDNA array. This highly repetitive locus must be large enough to allow for the transcription of sufficient ribosomal RNA to satisfy a cell's demand for ribosomes. In a typical yeast cell, approximately 75 copies of the rDNA are actively transcribed to satisfy this demand (WARNER 1999). However, those 75 copies of the rDNA repeat must be insufficient under some circumstances, as a typical yeast rDNA array contains around 150 copies of the rDNA repeat. These additional copies are believed to be necessary to maximize genome stability. Active ribosomal RNA genes are transcribed at extremely high levels, with densely loaded transcriptional machinery. This presents an obstacle to the repair of damage to the underlying DNA, and persistent, un-repaired damage to the rDNA array delays complete replication of the genome and progression through S-phase (IDE *et al.* 2010). Thus, to maximize genome stability, the rDNA array must be large enough to support sufficient rRNA transcription without requiring all repeats to be actively transcribed. This requirement imposes a lower limit on the optimal size of the rDNA array. Similarly, the array cannot exceed a certain size. If the rDNA grows too large, its complete replication would require an excessively large proportion of the finite pool of replisome components available during each S-phase, depriving other parts of the genome of those replication

factors (YOSHIDA *et al.* 2014). In addition, having a smaller rDNA array improves growth during persistent replication stress, perhaps by making more of the limiting replication factors available to other parts of the genome (SALIM *et al.* 2017). Thus, the number of repeats in the rDNA locus must be actively managed by the cell to facilitate optimal transcriptional output and maximize genome stability.

During unperturbed growth, changes in rDNA copy number are subtle and take place in only a small fraction of cells within the population, making it difficult to detect these changes or to investigate their underlying mechanisms. As a consequence, most of our knowledge about the mechanism of rDNA copy number change comes from studying the cellular response to a significant perturbation in copy number, a situation in which copy number change is readily detectable. For example, if an rDNA array is artificially truncated, it will steadily increase until it reaches a normal size (KOBAYASHI *et al.* 1998). Conversely, the rDNA array will shrink when the *RPA135* subunit of RNA Pol I is deleted (BREWER *et al.* 1992; KOBAYASHI *et al.* 1998), when the activity of the origin recognition complex is compromised (SANCHEZ *et al.* 2017), or when a number of other replication factors are lost (SALIM *et al.* 2017). Together, these studies demonstrate that maintenance of the size of the rDNA is a vital process that is actively regulated by the cell.

In this study, I describe a nearly two-fold reduction in the rate of copy number increase in *isw2Δ nhp10Δ* cells relative to wild-type cells and moderate reductions in the rate of increase in *isw2Δ* and *nhp10Δ* cells. According to one accepted model, a critical step in the process of rDNA copy number change is the repair of the DNA double strand break (DSB) that takes place at RFB-paused replication forks (KOBAYASHI and GANLEY 2005; JACK *et al.* 2015). Although Ino80 plays roles in DSB repair (PAPAMICHOS-CHRONAKIS *et al.* 2006;

PAPAMICHOS-CHRONAKIS *et al.* 2011; LADEMANN *et al.* 2017), the mutants I used did not exhibit a general recombination defect [Figure 2.8C]. This result argues against the possibility that *isw2Δ* and *nhp10Δ* mutations affect rDNA array expansion indirectly through recombination itself or transcription of factors involved in recombination and demonstrates that Isw2 and Ino80 play special roles at the rDNA locus.

It is possible that the reduced proportion of transcriptionally active rDNA repeats in *isw2Δ nhp10Δ* cells indirectly affects the rate of rDNA expansion. The efficiency of the ARS in the rDNA IGS correlates with the rate of copy number increase in that rDNA array (GANLEY *et al.* 2009). Accordingly, it is possible that the rARS efficiency decreases at least partly due to the reduced ratio of transcriptionally active to inactive repeats in the double mutant (see discussion above), which in turn reduces the frequency of copy number change events, thus accounting for the reduced rate of copy number increase in the double mutant cells. Despite the strong reduction in the rate of rDNA copy number expansion, *isw2Δ nhp10Δ* cells have normal-sized rDNA arrays. I suspect this is likely due to the fact that fluctuation in rDNA copy number during exponential growth is small, making detection of defects in copy number change difficult. However, I cannot exclude the possibility that rDNA copy number maintenance and expansion have currently unknown mechanistic differences. Though the complexities of this highly repetitive locus create challenges in establishing direct, causal mechanisms, this work establishes a novel role for ATP-dependent chromatin remodeling factors in strongly influencing multiple aspects of rDNA biology, including the process of rDNA copy number change.

Materials and Methods

Yeast strains and media

Strains used are listed in Table 2.1. Strains generated using standard gene replacement protocols (GOLDSTEIN and MCCUSKER 1999). Unless otherwise indicated, yeast cells were grown in YEPD medium (2% Bacto Peptone, 1% yeast extract, 2% glucose). All strains were derived from *MAT***a** W303-1a (THOMAS and ROTHSTEIN 1989; ZHAO *et al.* 1998). With the exception of the rDNA copy number mutants used in the copy number change experiments, all strains used have nearly identical rDNA copy number of approximately 150 rDNA repeats [Figure 2.7].

Chromatin immunoprecipitation and micrococcal nuclease digestion followed by deep sequencing

Chromatin immunoprecipitation (ChIP) and micrococcal nuclease (MNase) digestion were performed as described previously (RODRIGUEZ *et al.* 2014). For H3-ChIP experiments, anti-H3 C-terminal antibody (Abcam catalog # ab1791) was used; for all other ChIPs, the targeted protein was epitope-tagged at the C-terminus with FLAG and immuno-precipitated using an anti-FLAG monoclonal antibody (Sigma catalog # F3165). All Isw2 ChIP-seq was performed on a FLAG-tagged, catalytically inactive allele of *ISW2* as previously described (GELBART *et al.* 2005). All libraries were constructed using the Nugen Ovation Ultralow System V2 (catalog # 0344-32) and then single-end (ChIP-seq) or paired-end (MNase-seq) sequenced, with 50 bp read length, on Illumina Hi-Seq 2500. Ribbon plots, bar graphs, and line graphs were generated with the ggplot2 R package

(http://ggplot2.org/). For MACS2 peaks-calling, the following parameters were used: macs2 callpeak -t <filename>.bam -c <filename_sorted>.bam -f BAM -g 1.21e7 -B --nomodel --extsize 147

For all depictions of deep-sequencing data at the rDNA, a single copy of the rDNA locus is shown. Our reference genome contains two copies of the rDNA repeat, and any read mapping to the rDNA is randomly assigned to one of these 2 copies. Thus, sequencing data reflects the average signal across all rDNA repeats in all cells sampled. For ChIP-seq analyses, IP and input DNA from the same chromatin prep were both sequenced. Normalization of IP to input was done using these matched samples, thus controlling for any minor variation in rDNA copy number that might otherwise affect direct comparison between different samples.

Reverse Transcription- and ChIP-quantitative PCR

RNA was isolated using hot acid phenol, then cleaned up with the Qiagen RNEasy Cleanup Kit (catalog # 74204) plus on-column treatment with DNase I (Qiagen catalog # 79254). cDNA was generated from the RNA using Superscript III Reverse Transcriptase (ThermoFisher catalog # 18080093). Quantitative PCR was performed on both cDNA and ChIP DNA using 2x Power SYBR Master Mix (Fisher Scientific catalog # 4367659) run on the ABI QuantStudio5 Real Time PCR System machine.

Psoralen Crosslinking

Assay was performed as previously described (DAMMANN *et al.* 1993; SMITH and BOEKE 1997; SANDMEIER *et al.* 2002). Cells were grown to mid-log phase (OD_{660} = 0.5-0.7), approximately

$3x10^8$ cells were collected, washed twice with ice cold water, and then re-suspended in 1.4 ml cold TE buffer. Cells were transferred to 6-well plates, and 70 µl of psoralen (200 ug/ml in 100% ethanol) was added to the cells. On ice, the plates were irradiated with 365 nm UV for five minutes with a Spectrolinker XL-1500. Psoralen addition followed by UV irradiation was repeated four additional times, for a total of five rounds. Cells were collected, washed in water, spheroplasted with zymoylase 100T, and washed in spheroplast buffer. The pellet was lysed by re-suspension in TE buffer with 0.5% SDS and then treated with Proteinase K overnight at 50°. DNA was extracted with Phenol:Chloroform:Isoamyl alcohol, ethanol precipitated, and then digested for three hours with New England Biolabs (NEB) *Eco*RI-HF. Samples were treated with RNase A at 37° for 30 minutes, ethanol precipitated, quantified, and then run in 1.3% LE agarose gels in 0.5X TBE for 24 hours at 2 V/cm. Gels were irradiated for two minutes per side with 254 nm UV, transferred to a GeneScreen Plus membrane in 10x SSC, and then hybridized with a probe contained within a *Eco*RI restriction fragment in the rDNA ETS1. Membranes were visualized using a Typhoon Phosphor Imager, and images were visualized using ImageJ software.

2D gel electrophoresis

DNA sample preparation was based on the Brewer/Raghuraman lab protocol (http://fangman-brewer.genetics.washington.edu/plug.html). Cells were grown to mid-log phase (OD_{660} = 0.5-0.7), sodium azide added to 0.1% final concentration, and then cultures were washed in water. Cell pellets were re-suspended in 50 mM EDTA, mixed with an equal volume of 1.0% Low-Melt Agarose (BioRad catalog # 161-3111), and pipetted into plug molds. Cells in plugs were spheroplasted with 0.5 mg/ml Zymolyase 20-T, thoroughly

washed, and stored in TE at 4°C. Plugs were digested with *Nhe*I for 5 hours at 37°C, then run in 0.4% agarose gels in TBE at 1 V/cm for 22 hours at room temperature. Gels were stained with ethidium bromide (EtBr), visualized with UV, and the desired size range for each sample was identified in the gel and physically cut out. This piece of gel was then rotated 90° and placed in a new gel tray, and warm 1.1% agarose in TBE was poured around it. This gel was then run at 5 V/cm for 6 hours at 4°C. After running, the gel was visualized, transferred onto a GeneScreen Plus membrane (Perkin Elmer, catalog # NEF986001PK), and hybridized with a probe encompassing the **r**eplication **f**ork **b**lock (RFB).

rDNA copy number change assay

Strains were made from YSI102 (IDE *et al.* 2010), in which the endogenous *FOB1* gene had been deleted, and the number of rDNA repeats reduced to 20 copies. From the 20-rDNA-copy *fob1* parent, *isw2Δ*, *nhp10Δ*, and *isw2Δ nhp10Δ* strains were generated. Separately, the *FOB1* gene was Gibson cloned into the pRS426 plasmid. Either this *FOB1*-pRS426 plasmid or a pRS426 plasmid with no *FOB1* gene was then transformed into each 20-copy strain and plated on yeast complete (BYWATER *et al.*) –URA medium with 2% glucose. Individual transformants were re-streaked on selective medium, presence of the desired plasmid was confirmed by PCR, and then transformants were inoculated into liquid YC –URA + 2% glucose. Cultures were allowed to reach saturation, and then aliquots were collected, washed in cold 50 mM EDTA, and cell pellets frozen in liquid nitrogen and stored at -80°C. From the remaining saturated cultures, all strains were diluted by the same factor, then allowed to grow back to saturation, at which point the next time point would be collected,

up to ~200 generations. Generations were calculated from the base 2 log of the dilution factor applied at each passage (for example, a saturated culture diluted by a factor of 1,024 into the same volume of medium would require 10 generations to return to saturation).

Contour-Clamped Homogeneous Electric Field (CHEF) gel electrophoresis and Southern blotting

Samples for CHEF gels were prepared in agarose based on a previously described method (KWAN *et al.* 2016). Frozen cell pellets were thawed, re-suspended in 100 mM EDTA, then mixed with 0.8% Low-Melt Agarose and 25 mg/ml zymolyase 20T. This mixture was pipetted into plug molds, allowed to solidify at 4°C, then washed with a series of buffers (Solution V: 500 mM EDTA pH 7.5, 10 mM Tris pH 7.5; Solution VI: 5% sarcosyl, 5 mg/ml Proteinase K, 500 mM EDTA pH 7.5; Solution VII: 2 mM Tris pH 7.5, 1 mM EDTA, pH 8.0). Before being run, plugs were incubated for approximately 30 minutes in 0.5x TBE running buffer at 4°C before being placed on gel comb teeth, positioned in gel mold, and then warm 0.8% 0.5x TBE was poured. CHEF gel was run on a CHEF-DR II with a program adapted from Ide *et al* MCB 2007: Block 1 = 2.0 V/cm, pulse time of 1,200 seconds to 1,400 seconds, total run time 72 hours; Block 2 = 6.0 V/cm, pulse time of 25 seconds to 146 seconds, total run time 7.5 hours. After electrophoresis, gels were incubated with 0.5 ug/ml EtBr in running buffer for 30-45 minutes, UV-irradiated with a Stratagene Stratalinker to nick DNA, transferred onto HyBond N+ positively charged membrane (GE, catalog # RPN303B), and hybridized with a probe targeting the RFB.

***URA3* recombination assay**

Strains were generated by integration of plasmid pRS406, containing the *URA3* gene, linearized by digestion with StuI, which cuts this plasmid in one place in the middle of the *URA3* gene. Linearized plasmid was thus integrated into the existing *ura3-1* allele, resulting in a locus with a *URA3* allele next to a *ura3-1* allele. Cells were inoculated into liquid YC-URA medium, and cultures were grown to saturation. Culture concentrations were measured, and a specific number of cells was inoculated into YPD. Cultures were grown for 24 hours, and the concentration was measured and used to calculate the number of cell divisions that had occurred in the culture. Cells were diluted to yield a countable number of colonies, and then plated on both YPD and 5-FOA plates. The number of 5-FOA-resistant colonies per culture was used to calculate the number of recombination events that had occurred in each culture that resulted in loss of the *URA3* gene, leaving only *ura3-1*, and thus rendering the cell and its descendants resistant to 5-FOA (LURIA and DELBRUCK 1943; LEA and COULSON 1949). This number of recombination events was then normalized to the number of cell divisions that had occurred in each culture.

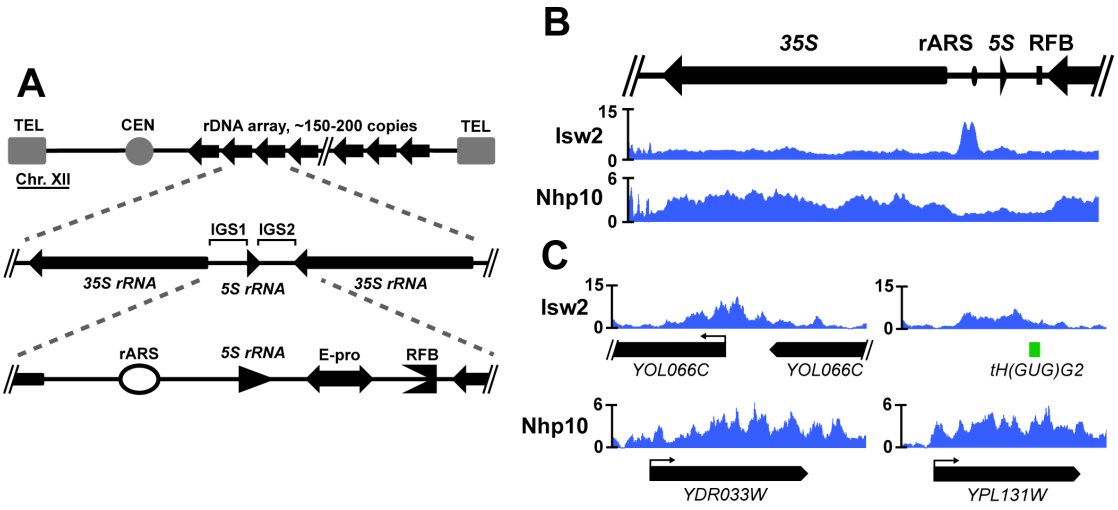

Figure 2.1: The Isw2 and Ino80 chromatin remodeling complexes are targeted to the rDNA locus.

(A) A schematic drawing of the rDNA locus in *S. cerevisiae*. In a typical yeast cell, the rDNA locus, comprised of a tandem array of ~150 copies of the rDNA repeat, accounts for approximately 1.5 Mb of chromosome XII. Each repeat contains a 35S rRNA gene and an inter-genic spacer (IGS) region in between adjacent 35S genes, itself split into IGS1 and IGS2 regions by the 5S rRNA gene. IGS1 contains the ribosomal origin of replication, or autonomously replicating sequence (rARS), and IGS2 contains the bi-directional RNA Polymerase II promoter, E-pro, and a replication fork block (RFB). (B) The Isw2 subunit of the Isw2 complex and the Nhp10 subunit of the Ino80 complex were each FLAG-tagged, chromatin immuno-precipitated, and deep-sequenced (ChIP-seq). (C) Representative ChIP-seq signals of Isw2 and Nhp10 at single copy targets outside of the rDNA.

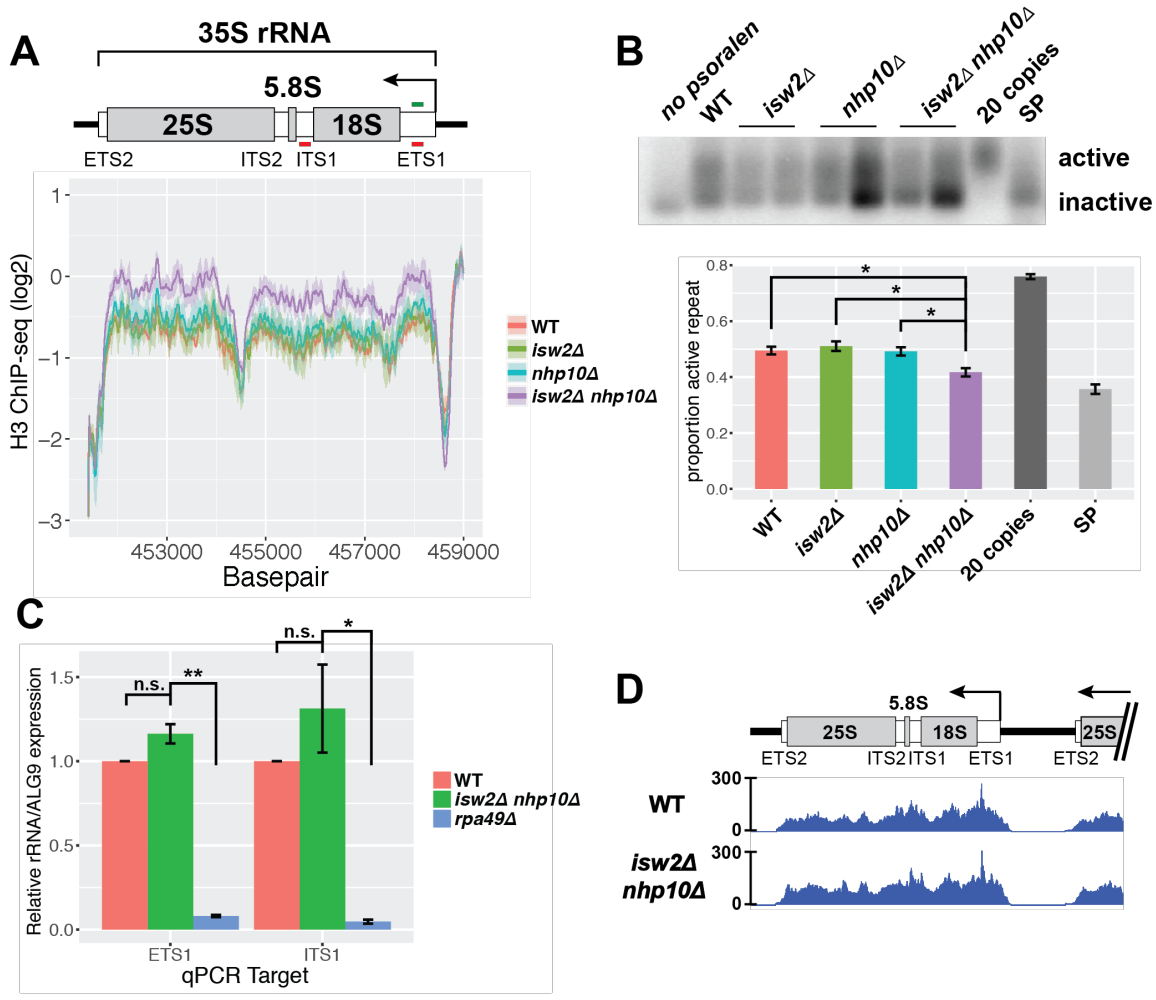

Figure 2.2: Nucleosome occupancy, but not transcription, is affected at the 35S rDNA in *isw2Δ* and *nhp10Δ* mutants.

(A) Histone H3 ChIP-seq at the 35S rRNA gene. Line represents average log2 ChIP-seq signal at each base pair for two independent experiments, and the ribbon represents the standard error of the mean at each base pair. ETS1 and ITS1 qPCR primer sets are indicated with red lines, and ETS1 hybridization probe used in the Southern blot shown in 2B indicated in green. (B) Psoralen cross-linked DNA, digested with *Eco*RI and hybridized with a probe to the ETS1 region. Two independent isolates of each remodeling factor mutant are shown. For quantification, signal strengths of the active and inactive bands were measured with ImageJ software, and the proportion of the total signal present in the "active" band was calculated. Values for each genotype reflect between 3 and 5 biological replicates, and error bars represent SEM. The "20 copies" sample comes from a strain with only 20 copies of the rDNA repeat, and "SP" is the WT strain at stationary phase. (C) RT-qPCR measuring the ETS1 and ITS1 of the 35S pre-rRNA. For each qPCR target, expression for all strains normalized to WT. For (B) and (C), statistical significance determined by pairwise t-tests followed by Bonferroni correction for multiple testing. * - $p < 0.05$, ** - $p < 0.005$. (D) RNA Pol I ChIP-seq (FLAG-tagged RNA Pol I subunit *RPA190*).

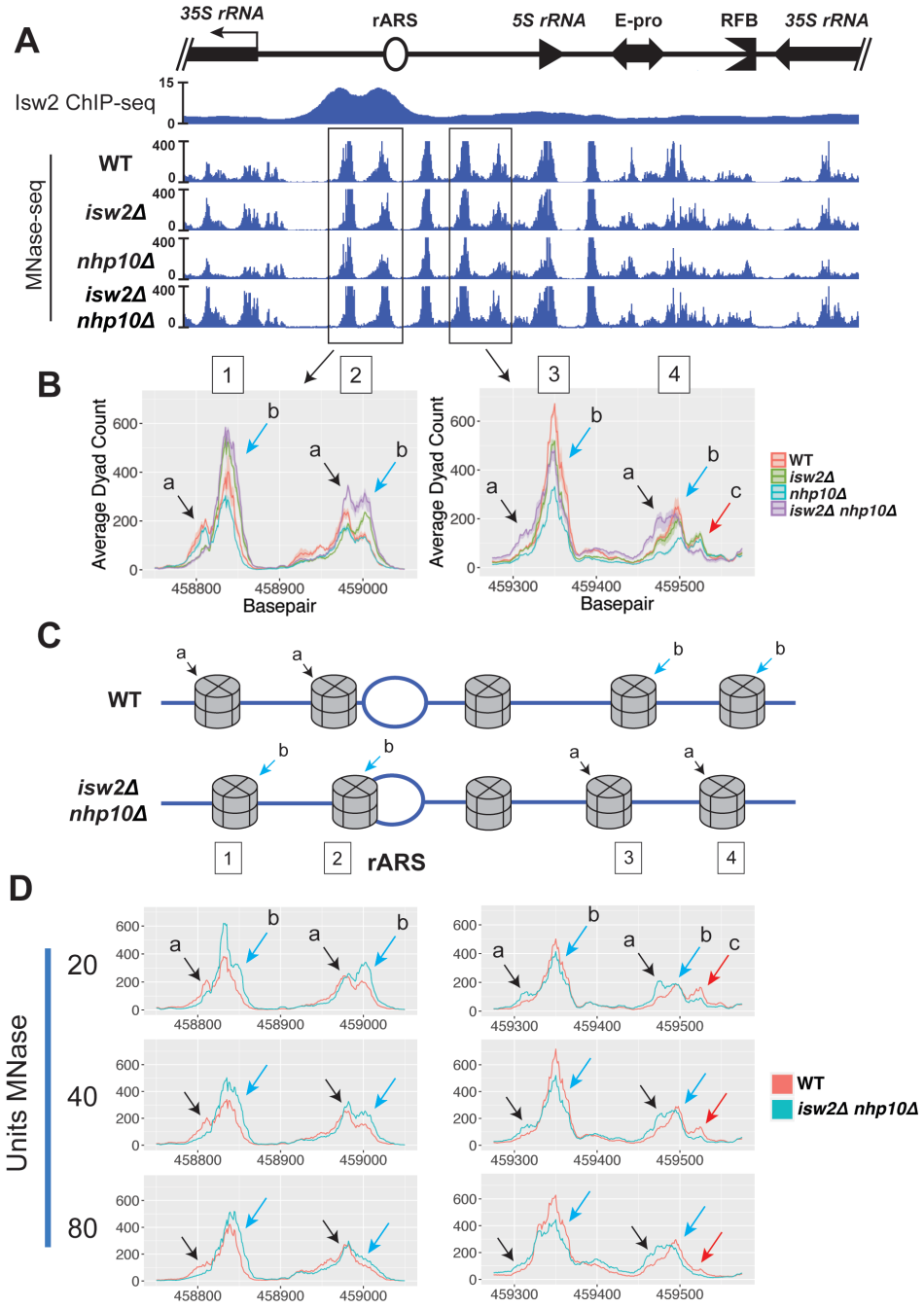

Figure 2.3: Isw2 and Ino80 affect nucleosome positioning in the rDNA IGS.

(A) MNase-seq in the IGS, with Isw2 ChIP-seq data overlaid. Values are dyad counts normalized to the genome-wide average dyad count per base pair. (B) Ribbon plots, as in Figure 2.2A, focused on two pairs of nucleosomes. Different sub-species of nucleosome positions indicated with colored arrows and letters. (C) Cartoon of 5 nucleosomes flanking the rARS, illustrating possible arrangements of nucleosomes reflecting different predominant sub-species of positions for each nucleosome. (D) MNase-seq comparing WT and *isw2Δ nhp10Δ* cells across three different strengths of MNase digestion.

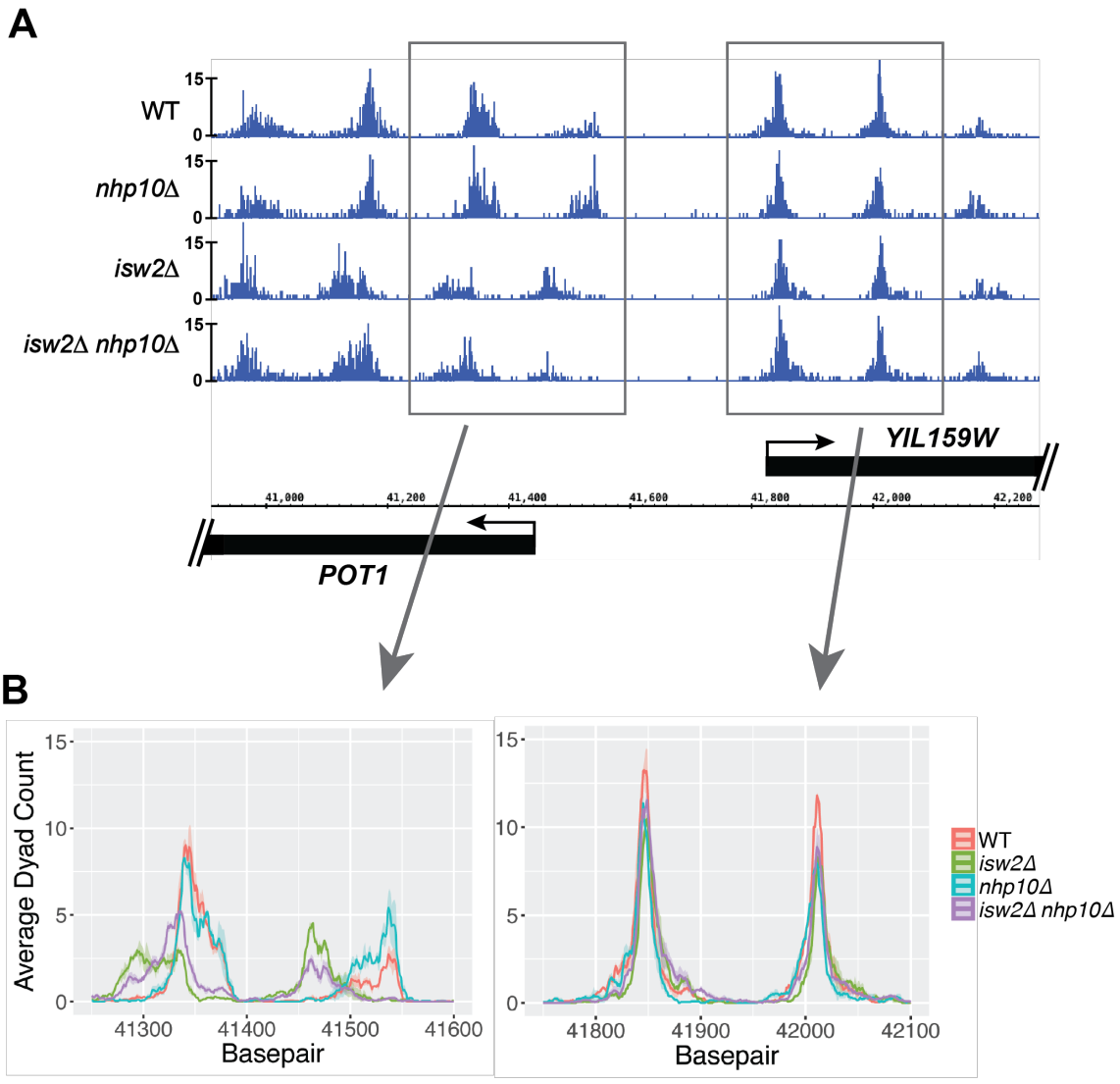

Figure 2.4: Nucleosome positioning changes at a canonical Isw2 target.

(A) MNase-seq data at a well-established Isw2 target, the 5' end of the *POT1* gene. (B) Visualization of the same data shown in A with the ribbon plots used in Figure 2.3B, focusing on two pairs of nucleosomes.

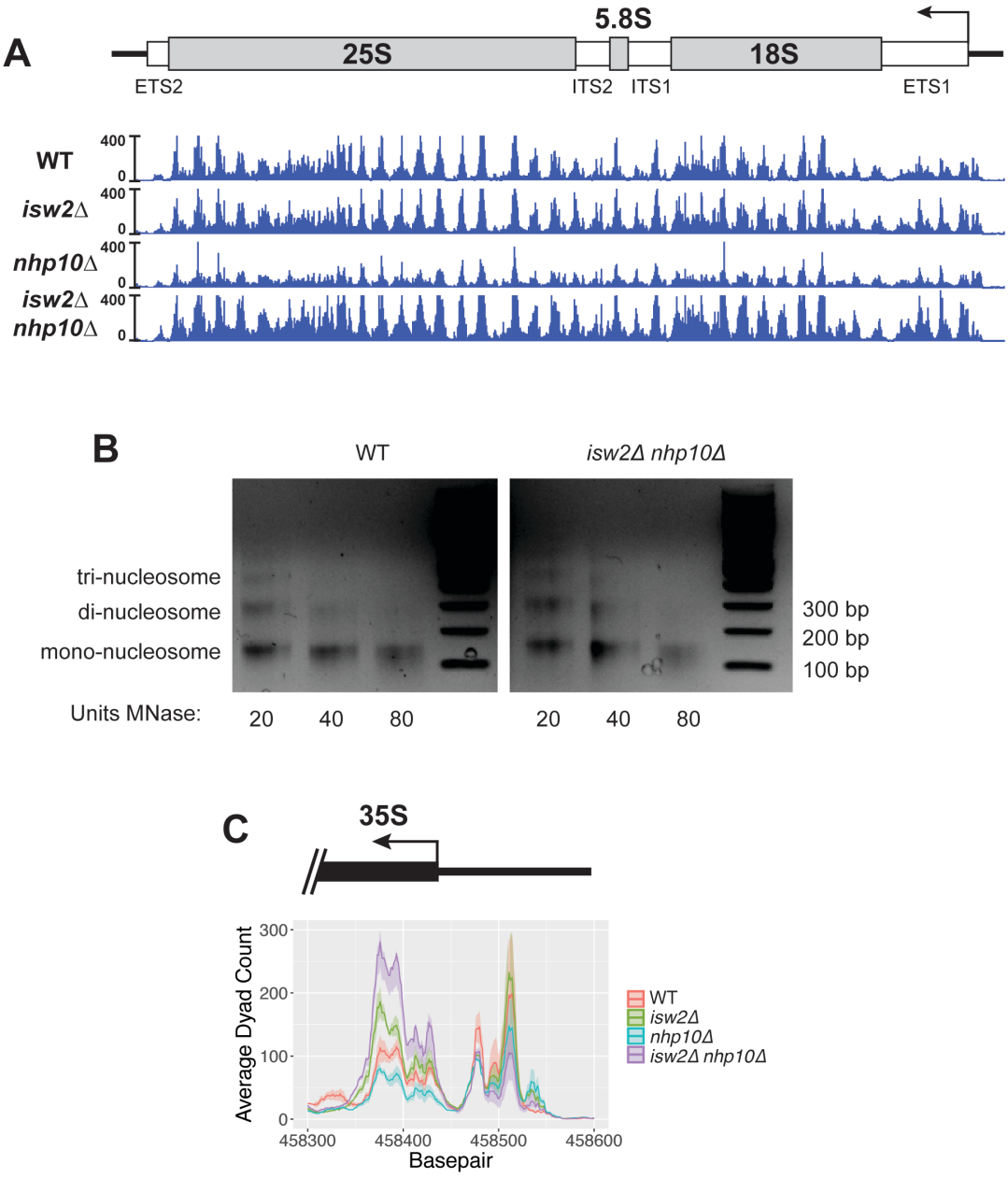

Figure 2.5: Nucleosome positioning at the rDNA.

(A) MNase-seq data analyzed with dyad mapping showing the entire 35S rRNA gene. No stark differences in nucleosome positioning can be seen. (B) Representative gel indicating how nucleosomal ladders appear after digestion with 20, 40, or 80 units of MNase. Note that for all MNase-seq analyses, regardless of level of digestion, the mono-nucleosomal band was gel-purified and was the sole source of material that was deep sequenced. (C) MNase-seq ribbon plot at the 35S promoter region showing no appreciable differences in nucleosome positioning across the strains tested.

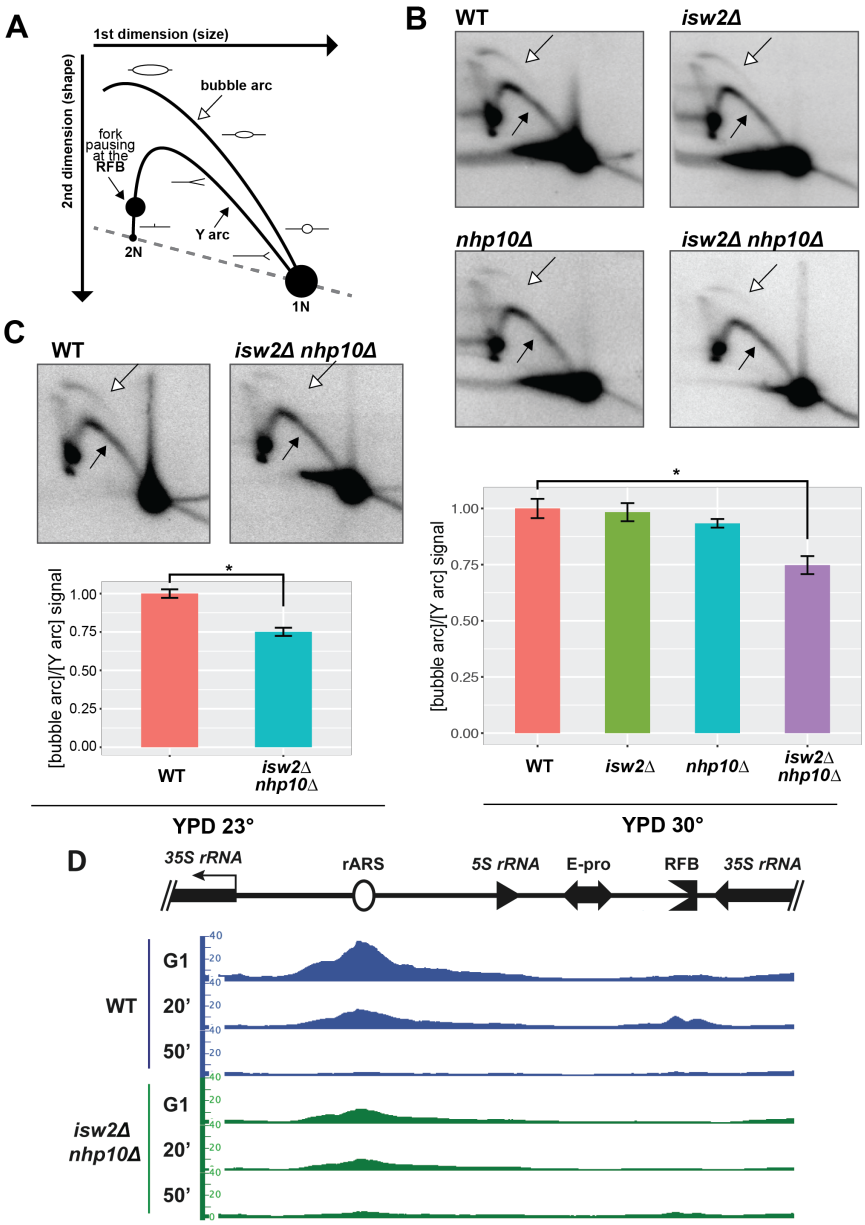

Figure 2.6: Isw2 and Ino80 facilitate efficient firing of rDNA origin of replication.

(A) Schematic of 2D gel with features annotated. (B) Representative 2D gels of *Nhe*I-digested DNA over rARS and RFB, from cells grown in YPD at 30°. Exposures of the blots have been adjusted so that the Y arc is of comparable intensity for each blot. Bubble arc indicated by empty arrow, Y arc indicated by filled arrow. Quantification reflects at least two independent experiments for each genotype. All values normalized to the bubble:Y ratio for WT. Error bars show SEM. Statistical significance determined by pairwise t-tests followed by Bonferroni correction for multiple testing. * - $p < 0.05$. (C) As in B, but from cells grown in YPD at 23°. Statistical significance determined by Welch's t-test. * - $p < 0.05$. D) MCM4 ChIP-seq. Cells were arrested in G1, released into YPD without alpha-factor, and sampled at 20' and 50' post-release.

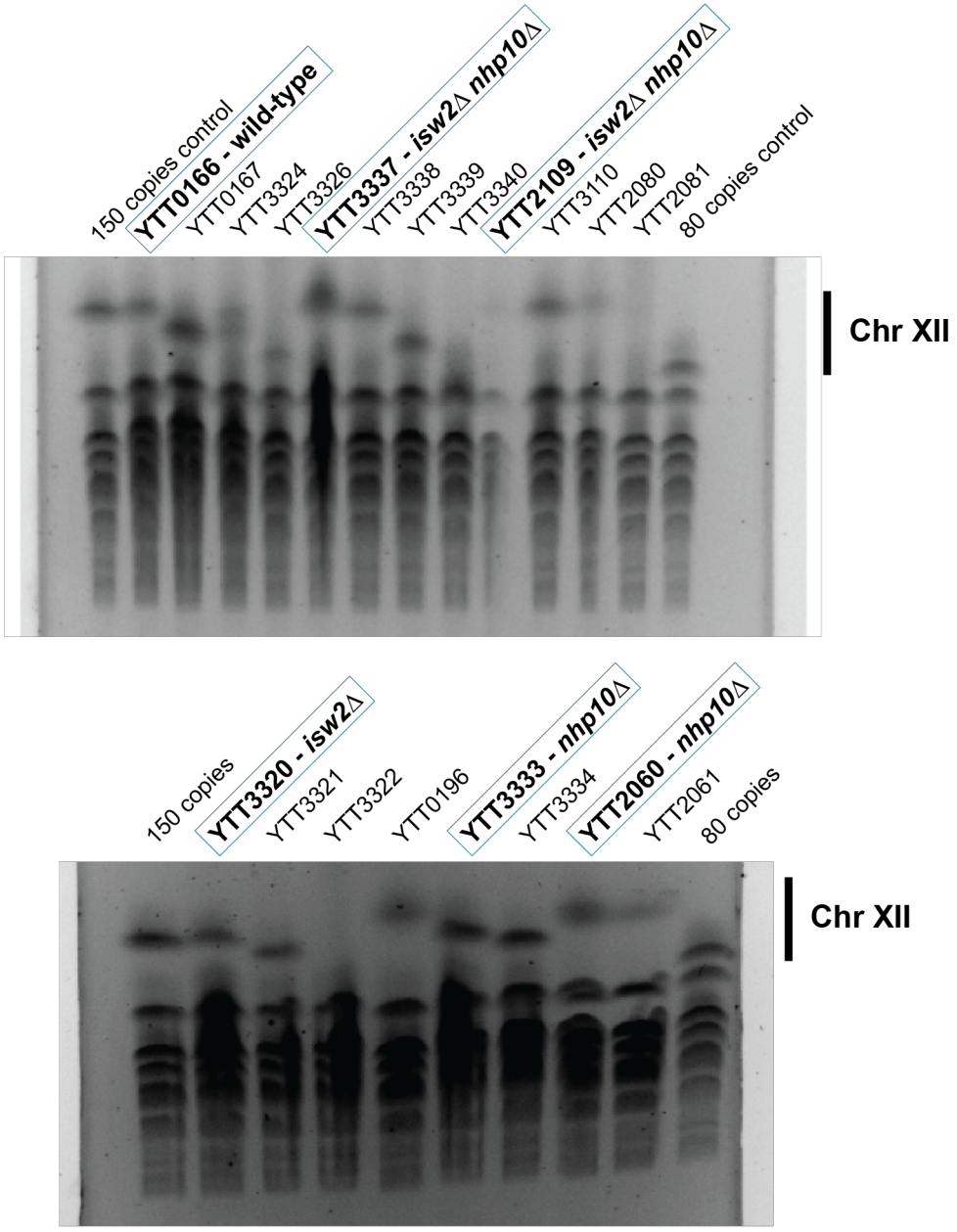

Figure 2.7: Strains used in this study have approximately 150 rDNA repeats.

Two different ethidium bromide-stained CHEF gels in which un-digested DNA was run, allowing for visualization of whole chromosomes. On each gel, control strains containing 150 or 80 rDNA repeats are run on the outside lanes as references. Most bands have migrated the same distance across all strains, indicating those chromosomes are the same size in those strains, with the exception of the rDNA-containing Chr. XII, which is indicated. The major strains used for most of the experiments in this study (excluding the rDNA copy number assays) are highlighted by bold text and a blue border.

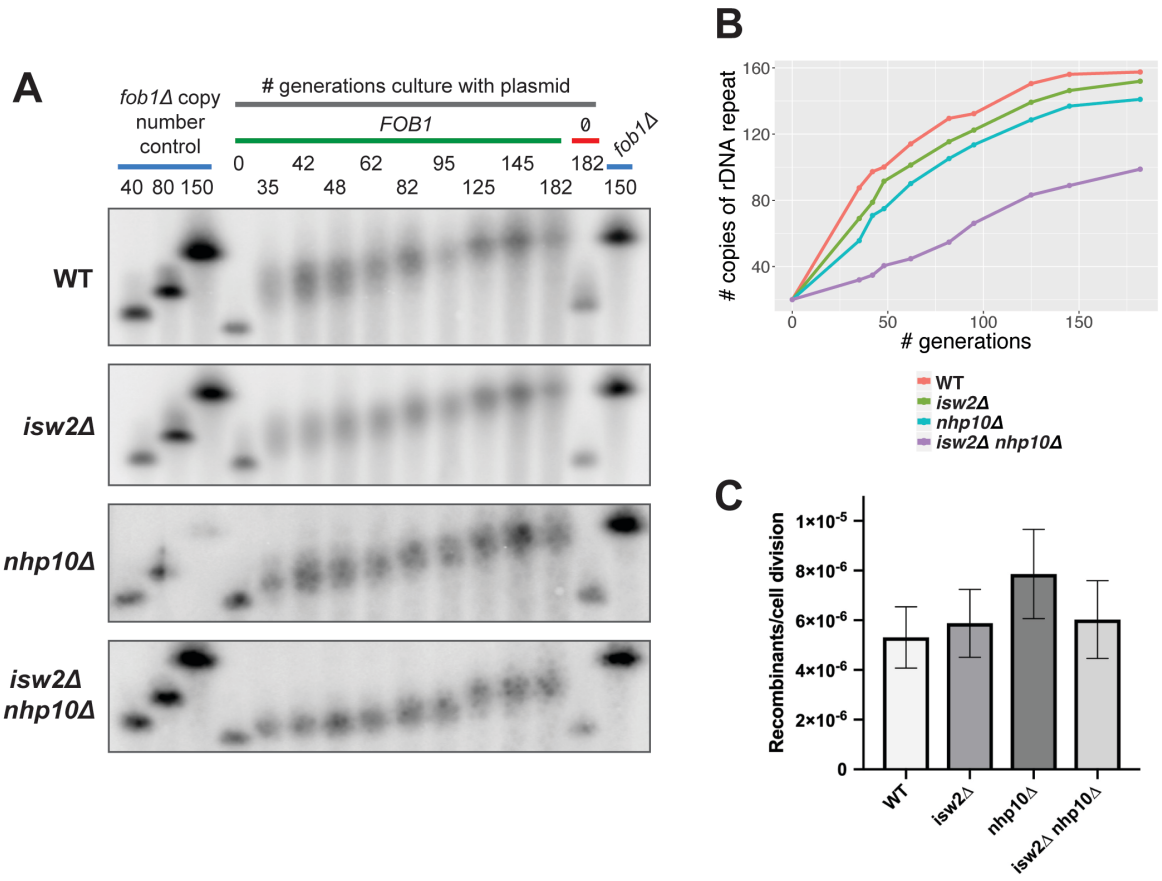

Figure 2.8: Isw2 and Ino80 affect the rate of rDNA copy number change.

(A) rDNA copy number change assay. Blue bars indicate *fob1Δ* copy number control strains that maintain the indicated number of rDNA repeats (identical 150-copy control samples run on both ends of the gel to facilitate comparison of band migration). The gray bar indicates samples grown in a time course for the indicated number of generations, in selective medium to ensure retention of either a plasmid containing *FOB1* (green bar) or the plasmid backbone pRS426 without *FOB1* (red bar). (B) Quantification of the copy number change assay. Average copy number at each time point was calculated based on migration of bands relative to controls. (C) *URA3* recombination assay. Cells containing a *URA3* allele adjacent to a *ura3-1* allele were grown under selection without uracil, then grown without selection in YPD for ~10 generations, then plated on 5-FOA plates. Number of recombination events per cell division was calculated (LURIA and DELBRUCK 1943; LEA and COULSON 1949).

Table 2.1: Chapter 2 Yeast Strains.

Strain	Genotype	Reference
W1588-4C	*MAT***a** *ade2-1 can1-100 his3-11,15 leu2-3,112 trp1-1 ura3-1*	Thomas and Rothstein 1989, Zhao *et al* 1998
YTT3320	W1588-4C; *isw2Δ::NatMX*	Au *et al* 2011
YTT6809	W1588-4C; *isw2Δ::NatMX*	this study
YTT3333	W1588-4C; *nhp10Δ::Hyg*	Au *et al* 2011
YTT2060	W1588-4C; *nhp10Δ::Hyg*	Vincent *et al* 2008
YTT3337	W1588-4C; isw2Δ::NatMX nhp10Δ::HYG	Au *et al* 2011
YTT2109	W1588-4C; *isw2Δ::NatMX nhp10Δ::HYG*	Vincent *et al* 2008
YTT1996	W1588-4C; *ISW2-K215R-3FLAG-KanMX*	Gelbart *et al* 2005
YTT1997	W1588-4C; *ISW2-K215R-3FLAG-KanMX*	Gelbart *et al* 2005
YTT3426	W1588-4C; *NHP10-3FLAG-KanMX*	Vincent *et al* 2008
YTT3427	W1588-4C; *NHP10-3FLAG-KanMX*	Vincent *et al* 2008
YTT6639	W1588-4C; *rpa49Δ::KanMX*	this study
YTT6673	W1588-4C; *isw2Δ::NatMX nhp10Δ::Hyg RPA190-2L-3FLAG::KanMX*	this study
YTT6679	W1588-4C; *RPA190-2L-3FLAG::KanMX*	this study
YTT6686	W1588-4C; *RPO31-2L-3FLAG::KanMX*	this study
YTT6693	W1588-4C; *isw2Δ::NatMX nhp10Δ::Hyg RPO31-2L-3FLAG::KanMX*	this study
YTT6915	W1588-4C; *Pol2-2L-3FLAG::KanMX*	this study
YTT6916	W1588-4C; *Pol2-2L-3FLAG::KanMX*	this study
YTT6917	W1588-4C; *isw2Δ::NatMX Pol2-2L-3FLAG::KanMX*	this study
YTT6918	W1588-4C; *isw2Δ::NatMX Pol2-2L-3FLAG::KanMX*	this study
YTT6919	W1588-4C; *nhp10Δ::Hyg Pol2-2L-3FLAG::KanMX*	this study
YTT6920	W1588-4C; *nhp10Δ::Hyg Pol2-2L-3FLAG::KanMX*	this study
YTT6921	W1588-4C; *isw2Δ::NatMX nhp10Δ::Hyg Pol2-2L-3FLAG::KanMX*	this study
YTT6922	W1588-4C; *isw2Δ::NatMX nhp10Δ::Hyg Pol2-2L-3FLAG::KanMX*	this study
YTT7009	W1588-4C; *Fob1-2L-3FLAG::KanMX*	this study
YTT7010	W1588-4C; *Fob1-2L-3FLAG::KanMX*	this study
YTT7011	W1588-4C; *isw2Δ::NatMX Fob1-2L-3FLAG::KanMX*	this study
YTT7012	W1588-4C; *isw2Δ::NatMX Fob1-2L-3FLAG::KanMX*	this study
YTT7013	W1588-4C; *nhp10Δ::Hyg Fob1-2L-3FLAG::KanMX*	this study
YTT7014	W1588-4C; *nhp10Δ::Hyg Fob1-2L-3FLAG::KanMX*	this study
YTT7015	W1588-4C; *isw2Δ::NatMX nhp10Δ::Hyg Fob1-2L-3FLAG::KanMX*	this study
YTT7016	W1588-4C; *isw2Δ::NatMX nhp10Δ::Hyg Fob1-2L-3FLAG::KanMX*	this study
YSI101	*MAT***a** *ade2-1 can1-100 his3-11,15 leu2-3,112 trp1-1 ura3-1 fob1::LEU2*	Ide *et al* 2010

YSI102	YSI101; 20 copies rDNA	Ide *et al* 2010
YSI103	YSI101; 40 copies rDNA	Ide *et al* 2010
YSI104	YSI101; 80 copies rDNA	Ide *et al* 2010
YTT6294	YSI102; isw2Δ::NatMX	this study
YTT6865	YSI102; nhp10Δ::HYG	this study
YTT6311	YSI102; isw2Δ::NatMX nhp10Δ::Hyg	this study
YTT6312	YSI102; isw2Δ::NatMX nhp10Δ::Hyg	this study
YTT3383	*MAT***a** ade2-1::pRS402 *can1-100 his3-11,15 leu2-3,112 trp1-1* ura3-1::pRS406	
YTT3385	*MAT***a** ade2-1::pRS402 *can1-100 his3-11,15 leu2-3,112 trp1-1* ura3-1::pRS406 isw2Δ::NatMX	
YTT3387	*MAT***a** ade2-1::pRS402 *can1-100 his3-11,15 leu2-3,112 trp1-1* ura3-1::pRS406 nhp10Δ::HYG	
YTT3388	*MAT***a** ade2-1::pRS402 *can1-100 his3-11,15 leu2-3,112 trp1-1* ura3-1::pRS406 isw2Δ::NatMX nhp10Δ::HYG	
YTT3469	W1588-4C; MCM4-3FLAG-KanMX	
YTT3494	W1588-4C; MCM4-3FLAG-KanMX isw2::NatMX nhp10::Hyg	

Chapter 3

A Possible Role for Isw2 and Ino80 in DNA Double Strand Break Repair Choice

Summary

DNA damage happens in the context of chromatin, and thus the response to DNA damage – the initiation of the appropriate checkpoint response, sensing of cellular conditions that influence the repair mechanism, repair of the underlying damage, attenuation of the checkpoint response, and resumption of normal growth – also happens in the context of chromatin. Regulated modification of chromatin structure around sites of DNA damage is a vital part of the cellular break response. Here, I present evidence that supports a possible role for the Isw2 and Ino80 ATP-dependent chromatin remodeling factors in regulating the balance between **h**omologous **r**ecombination (HR) and **n**on-**h**omologous **e**nd **j**oining (NHEJ) for repair of a DNA double-strand break (DSB). I find that in response to a DSB that cannot be repaired by HR, cells lacking full Isw2 and Ino80 activity fail to arrest in G2/M, fail to activate the Rad53 checkpoint kinase, and "adapt" to the DSB by mutagenic repair at rates far higher than in wild-type cells. I was unable to formally exclude the possibility that these notable phenotypes result from a persistent G1 bias in the mutant strain. Nevertheless, I propose that the data presented support the possibility of novel, parallel roles for Isw2 and Ino80 in regulating the normal balance between HR and NHEJ and that loss of full function of both factors tips the balance away from HR and towards NHEJ.

Introduction

Following replication stress, cells will initiate the S-phase checkpoint to slow or stop DNA replication, to allow for resolution of the stress before complete, accurate replication of the genome. This checkpoint response is achieved through the coordinated actions of a variety of signaling factors, kinases, and repair proteins (LABIB and DE PICCOLI 2011; SYMINGTON and GAUTIER 2011). As DNA damage happens in the context of chromatin, part of the checkpoint response to damage is mediated through modification of chromatin structure. For example, following a DSB, the ATM kinase, known as Mec1 in yeast, phosphorylates histone H2AX, facilitating the local depletion of nucleosomes and ultimately the appropriate recruitment of checkpoint and repair factors (BURMA *et al.* 2001; MORRISON *et al.* 2004; TSUKUDA *et al.* 2005; SYMINGTON and GAUTIER 2011).

The Isw2 and Ino80 ATP-dependent chromatin remodeling factors play a role in regulating the S-phase checkpoint response. Mutant yeast lacking both *ISW2*, the catalytic subunit of this remodeling factor complex, and *NHP10*, a protein unique to the Ino80 complex, have significantly delayed replication of late-replicating regions of the genome in the context of methanesulfonate (MMS) stress (VINCENT *et al.* 2008). MMS causes replication stress, and thus in WT cells, MMS treatment elicits an S-phase checkpoint response, characterized by delayed passage through S phase and activation of the Rad53 checkpoint factor, detectable as heightened levels of phosphorylated Rad53. Treatment with MMS causes a similar overall response in *isw2Δ nhp10Δ* cells, but the checkpoint activation is more intense and persists longer, with regard to both delayed progression of DNA replication and amount and persistence of phosphorylated Rad53 (AU *et al.* 2011; LEE *et al.* 2015). Genetic investigations have not identified any well-characterized DNA repair,

replication fork protection, or checkpoint pathways that Isw2 and Ino80 might participate in and whose disruption would explain the failure to attenuate the checkpoint response (LEE *et al.* 2015). In the absence of such a clear explanation, and given the physical interaction between both Isw2 and Ino80 and the single-stranded DNA binding protein RPA, it is believed that these remodeling factors contribute to attenuation of the S-phase checkpoint response either directly through RPA or through another, un-characterized mechanism (AU *et al.* 2011; LEE *et al.* 2015).

In addition to their involvement in the S-phase checkpoint response, ATP-dependent chromatin remodeling factors have demonstrated roles in the DNA damage response. The RSC complex remodels chromatin surrounding a DSB, contributing to the removal of histones in a manner that facilitates the recruitment of repair factors such as Mre11 and Yku70 (SHIM *et al.* 2007). The SWI/SNF complex is recruited to DSBs, in part by the actions of the NuA4 and Gcn5 histone acetyltransferases, where it serves a vital role in the local accumulation of phosphorylated histone H2AX (γ-H2AX), an important step in the process of break repair (PARK *et al.* 2006; BENNETT and PETERSON 2015). The Nhp10 subunit of the Ino80 complex binds the ends of DNA, where it may prevent exonucleolytic cleavage of the DNA (RAY and GROVE 2009). Ino80 increases the intra-nuclear mobility of chromatin following a DSB, which may facilitate the homology search stage of break repair, and both Ino80 and Swr1 affect the cell-cycle regulated movement of DSBs to specific subnuclear compartments (SEEBER *et al.* 2013; HORIGOME *et al.* 2014).

In the following study, I initially sought to expand on the finding that Isw2 and Ino80 contribute to the attenuation of the S-phase checkpoint response by asking whether these remodeling factors play a similar role in the G2/M checkpoint. To address this

question, I employed an established system that allows for the inducible expression of the HO endonuclease, which creates a site-specific DSB at the *MAT* locus that causes cells to arrest in G2/M (MOORE and HABER 1996). Using this approach, I was unable to draw a clear conclusion about the role played by Isw2 and Ino80 in the G2/M checkpoint, but I did find evidence that these factors have a previously un-characterized role in the DNA damage response. In the context of a persistent DSB that cannot be repaired by homologous recombination, *isw2Δ nhp10Δ* cells appear to have a dramatically shifted preference for NHEJ over HR, in contrast to the strong preference for HR over NHEJ in WT, *isw2Δ*, and *nhp10Δ* cells in response to the same situation. Though I ultimately was unable to definitively address concerns about technical limitations of the systems employed, the data presented suggest a role for Isw2 and Ino80 in dictating the mechanism of DNA double strand break repair.

Results

isw2Δ nhp10Δ cells do not arrest in G2/M or activate the Rad53 checkpoint in response to a DSB that cannot be repaired by homologous recombination

In light of the finding that Isw2 and Ino80 function in parallel to attenuate the S-phase checkpoint response, I asked whether these factors also contribute to the G2/M checkpoint response (AU *et al.* 2011; LEE *et al.* 2015). To address this question, I employed an established system to generate site-specific, inducible DSBs (MOORE and HABER 1996; LEE *et al.* 1998). This method uses a strain background in which the HO endonuclease is driven by a *GAL* promoter. When grown in galactose, such cells will express the HO endonuclease,

which creates a DSB at the mating-type *MAT* locus. In addition, the silent mating loci, *HML* and *HMR*, have been deleted, removing the endogenous homology donors used to repair the induced DSB by homologous recombination. This system has two variations. In one, a copy of the *MAT* gene that cannot be cut by HO has been integrated into Chr V, providing a homology donor for HR repair of the induced DSB that, once used for repair, prevents further cutting by HO. The other variation has no new homology donor, and so the induced DSB cannot be repaired by HR. When grown in galactose, cells of this latter background will undergo a prolonged G2/M arrest in response to the persistent, un-repaired DSB, after which most cells will go through a few rounds of cell division before the colonies become inviable, presumably due to fragmenting of the *MAT*-containing chromosome (LEE *et al.* 1998). I will refer to this latter strain background as being "HR-incompetent" due to the lack of available homology donors, not a deletion for any recombination factors such as *RAD52*.

To use this system to study Isw2 and Ino80 in the context of the G2/M checkpoint response, I generated *isw2Δ nhp10Δ* strains from the HR-incompetent strain background. In our hands, the WT strain behaved as expected in a time course experiment: After a neutral YP-glycerol preculture, cells were shifted into YP-galactose medium to induce HO expression, and by 6-8 hours after induction, cells had accumulated in G2/M [Figure 3.1A]. By 16-20 hours post-induction, the G2/M arrest appeared to relax, and by 30 hours, the cultures were growing logarithmically, the result of approximately 1% of cells having successfully "adapted". In this system, adaptation refers to the repair of the *MAT* DSB with an error-prone method, such as NHEJ, allowing the mutated HO target site to escape subsequent rounds of cutting by HO. These adapted cells will then have rates of growth and

viability, even in the presence of HO expression, on par with those in HR-competent cells (LEE *et al.* 1998). In sharp contrast, the *isw2Δ nhp10Δ* cells in this same background failed to robustly arrest in G2/M. The proportion of cells in G2/M peaked at around 12 hours post-DSB-induction, but even at this time, more than half of the population was in G1 [Figure 3.1A].

To gain further insight into the nature of the checkpoint response following the induction of HO expression in this strain, I measured phosphorylation of the kinase Rad53, a marker of checkpoint activation (SZYJKA *et al.* 2008). At the earliest time point sampled, 2 hours post-induction, the WT strain had clearly visible phosphorylated Rad53, with levels of phospho-Rad53 peaking around 6-8 hours, the same time point when G2/M arrest had been fully established, as seen by flow cytometry [Figure 3.1B]. Similarly, by 30 hours post-induction, when the population had resumed normal, logarithmic growth, all detectable Rad53 appeared to be un-phosphorylated, indicating that the Rad53-mediated checkpoint had been satisfied. In contrast to the WT and consistent with what I observed of the cell cycle response to DSB induction, the *isw2Δ nhp10Δ* cells showed no detectable phosphorylation of Rad53 at any point in the time course, indicating a lack of checkpoint activation in this strain [Figure 3.1B].

Following DSBs that cannot be repaired by homologous recombination, *isw2Δ nhp10Δ* cells have dramatically increased rates of adaptation relative to WT

Given the apparent lack of G2/M checkpoint response, I asked what might explain the lack of normal checkpoint response to this particular type of DNA damage in the *isw2Δ nhp10Δ* cells. To address this question, I looked at the growth and viability of these strains

in the context of persistent cutting by HO. To dissect individual contributions of Isw2 and Ino80, in addition to the *isw2Δ nhp10Δ* HR-incompetent strain described above, I generated a full range of *isw2Δ*, *nhp10Δ*, and *isw2Δ nhp10Δ* strains from both the HR-competent and -incompetent parents. In the HR-competent background, WT and both single mutants grow at essentially the same rates and with the same viability on glucose (in the absence of HO cutting) as in galactose (in the presence of HO cutting), while the *isw2Δ nhp10Δ* has a very mild growth defect on galactose relative to glucose [Figure 3.2A]. In the HR-incompetent background, I see significantly reduced viability in WT, *isw2Δ*, and *nhp10Δ* cells with HO expression relative to those with no HO expression, as expected. In sharp contrast, the *isw2Δ nhp10Δ* double mutant has dramatically improved viability, albeit significantly slowed growth. By 2 days after plating, all of this strain's colonies were quite small, but there were far more colonies than for WT or either single mutant. By 5 days after plating, these colonies had reached the normal size of colonies for cells grown without HO cutting, at what appeared to be comparable numbers of cells, indicating similar viability [Figure 3.2A].

We next quantified this striking difference in viability with a more quantitative colony counting assay. Briefly, cells were grown in a YP-glycerol preculture and then plated in parallel on both glucose and galactose plates. The number of colonies in each condition was counted, and survival frequency was calculated as the number of colony-forming units (CFUs) in galactose over CFUs in glucose. As expected based on the spot assay, the WT and *isw2Δ nhp10Δ* HR-competent strain had essentially identical viability with or without HO cutting. Consistent with published results, the WT HR-incompetent strain had low viability of approximately 2%, when cutting was happening (LEE *et al.* 1998) [Figure 3.2B]. The HR-

incompetent *isw2Δ nhp10Δ* strains had essentially the same viability with or without cutting, confirming the dramatic increase in viability associated with the double mutant in the HR-incompetent background.

To validate this striking phenotype, I sought to recapitulate these results in a different system that also creates an inducible, site-specific DSB break that lacks a homology donor. In this system, strains have an integrated, GAL-driven I-SceI endonuclease as well as two inverted I-SceI cleavage sites inserted into the endogenous *ADE2* gene (DENG *et al.* 2014). As with the previous experiment, I generated *isw2Δ nhp10Δ* strains in this background. In our hands, this system yielded results consistent with published data for WT cells (~1% viability), *yku70Δ* (~0.03%), and *mre11Δ* (~0.07%). Consistent with our results in the HO-based system, the *isw2Δ nhp10Δ* strain in this system had essentially 100% viability when cutting was active [Figure 3.2C]. Thus, in two distinct systems, *isw2Δ nhp10Δ* cells have dramatically improved viability in the context of persistent DSBs that cannot be repaired by homologous recombination.

HO cutting happens in *isw2Δnhp10Δ* cells, but with reduced efficiency

The results described above could be explained by HO failing to cut its target site in the double mutant, whether due to disrupted activity of the endonuclease at its target or defects in its expression. To ask whether HO cutting is indeed happening in *isw2Δ nhp10Δ* cells, I performed a Southern blot to detect the intact vs. cut HO target DNA (LEE *et al.* 1998; PAPAMICHOS-CHRONAKIS *et al.* 2006) [Figure 3.3A]. At the earliest time point sampled, 30 minutes after gal induction, I was able to detect robust cutting in WT, as over 60% of the restriction fragments containing the HO cut site were cut. The proportion of cut fragments

peaked at over 70% cut at one hour post induction. In *isw2Δ nhp10Δ* cells, I also saw clear evidence of cutting at the first time point sampled, but at nearly half the efficiency – only ~25% of the restriction fragments were cut at 30'. The maximum detectable fraction cut was less than 40%, detected at 90' post induction. In conclusion, although there is strong evidence that HO cutting is happening in the double mutant, it is not happening with identical efficiency and/or kinetics as in the WT.

All adapted *isw2Δ nhp10Δ* colonies show evidence of a mutated HO target site

The reduced efficiency of HO cutting in the double mutant led us to hypothesize that the adapted colonies in the double mutant might result from cells in which HO cutting never occurred. If such cells, and the colonies they gave rise to, were able to somehow evade HO cutting, then these cells would likely have a normal HO cut site, lacking the HO-evading mutation required for normal adaptation to a DSB that cannot be repaired by HR. To test this possibility, I sequenced the HO cut sites of fourteen WT and fifteen double mutant colonies that had been grown on galactose, and thus in principle should have adapted by mutation of the cut site through error-prone repair of the DSB. For both WT and double mutant strains, 100% of sequenced colonies grown on galactose showed a mutated HO cut site [Figure 3.4A, Table 3.2]. To strengthen our conclusion that the *isw2Δ nhp10Δ* adapters had sustained HO cutting and then mutated the cut site, I re-streaked adapter colonies of both WT and double mutant strains onto galactose. Compared to un-adapted cells, adapted WT cells had viability like what was observed on glucose, indicating a mutated HO cut site. Similarly, double mutant adapters grew considerably faster than un-adapted *isw2Δ nhp10Δ* cells on galactose. Based on these data, I concluded that all double

mutant adapter colonies arise from cells that have sustained HO cutting and mutated the HO cut site, and that therefore the striking rescue of viability in this strain did not result from failed HO expression or activity.

isw2Δ nhp10Δ cells in HR-incompetent background have persistent G1 bias

The canonical understanding of the process of adaptation to a DSB that cannot be repaired by HR is that those rare adapters abandon the fruitless attempt to repair their DSB by HR, and instead use a more error-prone repair mechanism, such as NHEJ. By mutating the HO target sequence in the course of repairing the DSB in this way, these cells gain immunity from the cycle of repeated cutting by HO, allowing for the resumption of normal growth, even in the persistent presence of HO (LEE *et al.* 1998). Thus, I hypothesized that the dramatically improved viability of *isw2Δ nhp10Δ* cells in this system resulted from a significant increase in the preference of these cells for error-prone repair of the HO-induced DSB.

We considered two primary explanations for this shift in repair mechanism preference. The first is that Isw2 and Ino80 directly contribute to the normal repair pathway choice, either by facilitating HR, by inhibiting NHEJ, or both. In this model, upon loss of normal function of both of these complexes, the cell's normal repair pathway preference would be reversed, skewed towards NHEJ and away from HR, allowing for the significantly more-frequent NHEJ-facilitated adaptation to a persistent DSB that cannot be repaired by HR. The second explanation arises from the relationship between cell cycle stage and repair mechanism preference. When trying to repair DSBs in G2/M, cells are strongly biased in favor of homologous recombination, but when trying to repair DSBs in

G1, cells block the resection that is required for HR and exhibit a preference for repair by NHEJ (AYLON *et al.* 2004; JAZAYERI *et al.* 2006; SYMINGTON and GAUTIER 2011). Unlike WT cells, *isw2Δ nhp10Δ* cells failed to arrest in G2/M following DSB induction, remaining in G1 when grown in galactose. Thus, this genotype may cause a bias towards G1 in this strain background independent of Isw2's or Ino80's direct involvement in the break response, and this G1 bias may be primarily responsible for the shift in repair preference from HR to NHEJ.

To distinguish between these possibilities, I attempted to repeat our DSB-induction time course, but beginning with arrest in G2/M. If the *isw2Δ nhp10Δ* strain truly changes the response to a DSB in a cell cycle independent manner, I would predict that even following a DSB induced in G2/M, the double mutant would still have reduced Rad53 checkpoint activation. Unfortunately, after 7 hours of culture in YP-lactate or YP-glycerol supplemented with the G2/M-arresting agent nocodazole, the WT HR-incompetent strain had reached less than 50% arrest in G2/M. The *isw2Δ nhp10Δ* strain achieved even less G2/M arrest, showing barely any effect by 7 hours [Figure 3.5]. Following overnight culture in YP-lactate with nocodazole, both strains had unhealthy DNA content and no clear G2/M arrest. After overnight culture in YP-glycerol with nocodazole, the WT had lost its G2/M arrest, and the double mutant had improved to just under half arrested. I encountered similar difficulties arresting in G2/M in the I-SceI-based strain background (data not shown). Based on these results, I was unable to distinguish between a bona fide involvement of Isw2 and Ino80 in dictating DSB repair pathway choice and an indirect effect on repair choice resulting from an unavoidable G1 bias in *isw2Δ nhp10Δ* cells.

Discussion

Here, I have shown data consistent with possible roles for the Isw2 and Ino80 ATP-dependent chromatin remodeling factors in regulating DNA double strand break repair. In response to a DSB that cannot be repaired by homologous recombination due to the absence of a suitable homology donor, *isw2Δ nhp10Δ* cells adapt to the DSB by error-prone repair at a dramatically higher rate than WT cells. This difference in repair method in the double mutant is associated with a significantly reduced G2/M arrest and essentially undetectable Rad53 checkpoint activation following DSB induction. In our DSB-inducible strains, *isw2Δ nhp10Δ* cells displayed a persistent preference for the G1 cell cycle stage. This was true in two different strain backgrounds, in a variety of growth media, both following DSB induction and following treatment with the G2/M-arresting agent nocodazole. Due to this striking cell cycle phenotype, I was unable to conclusively disprove the possibility that the observed difference in repair mechanism choice in the double mutant resulted simply from the cells being in G1, rather than from loss of pro-HR/anti-NHEJ activities of Isw2 and Ino80.

Homologous recombination is the most accurate mechanism of DNA break repair. Its accuracy relies in part on access to a homology donor to serve as a template to repair broken DNA. To maximize the likelihood of having a homology donor available, HR typically happens in the S and G2 phases of the cell cycle. So long as the break occurs in G2 or after the break site has been replicated in S phase, this "preference" reflects the availability of a replicated sister chromatid as a homology donor (IRA *et al.* 2004; HINZ *et al.* 2005; SYMINGTON and GAUTIER 2011). In the absence of a homology donor, NHEJ is able to repair DSBs, but at the cost of introducing mutations. Thus, though NHEJ can happen

throughout the cell cycle, it is predominantly used in G1, when DNA is un-replicated (KARATHANASIS and WILSON 2002; AYLON *et al.* 2004). Cell cycle factors such as cyclin-dependent kinases are crucial to this paradigm, largely through regulation of the DNA break resection machinery, as extensive resection is associated with HR, and a lack of resection with NHEJ (AYLON *et al.* 2004; HUERTAS *et al.* 2008; CHEN *et al.* 2011). Thus, cell cycle stage exerts an important influence on the mechanism of DNA damage repair, and disruption of the connection between cell cycle and repair factors alters repair mechanism. For example, mutation of residues on Sae2 involved in the protein's phosphorylation by CDKs alters the normal balance between HR and NHEJ repair (HUERTAS *et al.* 2008). Accordingly, alterations not just in the cell's ability to sense cell cycle stage, but the cell's actual cell cycle stage, could significantly affect repair pathway choice in a population of cells.

Nevertheless, the possibility remains that the G1 bias in our *isw2Δ nhp10Δ* strains is not the true explanation of our data, and that Isw2 and Ino80 do indeed influence DSB repair pathway choice. Ino80, in particular, has an established role in DNA damage repair. Following DNA double strand breaks, the ATM kinase phosphorylates H2AX around the break (BURMA *et al.* 2001). Similarly, in response to replication stress such as hydroxyurea or UV treatment, the ATR kinase phosphorylates H2AX around stalled replication forks (WARD and CHEN 2001). This phosphorylated H2AX, referred to as γ-H2AX, is bound by numerous repair factors, including Ino80 and its remodeling factor family member, Swr1, and is important for their timely enrichment at sites of damage and replication stress (PAULL *et al.* 2000; CELESTE *et al.* 2003; NAKAMURA *et al.* 2004). The Ino80 complex's Nhp10 subunit is particularly important for the complex's recognition of γ-H2AX (MORRISON *et al.*

2004). Loss of Ino80 activity causes defects in depletion of nucleosomes in the region surrounding a DSB, which is in turn necessary for the recruitment of many repair factors, including Mre11 and Yku80 (TSUKUDA *et al.* 2005; VAN ATTIKUM *et al.* 2007). Isw2 has far fewer known connections to repair, though one study found that improved replicative lifespan resulting from deletion of *ISW2* requires *RAD51*, a vital component of the HR machinery (DANG *et al.* 2014).

A body of evidence indicates that in certain situations, the Isw2 and Ino80 remodeling factors perform parallel, potentially partially redundant roles, such that there are unique phenotypes associated only with double mutants with compromised function of both complexes. This is true of the attenuation of the S-phase checkpoint and of regulation of some aspects of the ribosomal DNA locus (AU *et al.* 2011; LEE *et al.* 2015; CUTLER *et al.* 2018). I propose that, consistent with these findings, Isw2 and Ino80 may both facilitate the normal balance between HR- and NHEJ-mediated repair of DSBs. When activity of either remodeling factor is compromised individually, the other factor can compensate, preserving the normal preference for persistent homology search over NHEJ, resulting in *isw2Δ* and *nhp10Δ* single mutants behaving like WT in our experiments. Simultaneous loss of both factors, however, compromises the proper modification of break-adjacent chromatin structure. This may happen, for example, by the prevention of robust, timely resection, causing much more frequent and/or rapid abandonment of the search for a homology donor. This would in turn facilitate the repair of the DSB by NHEJ and, through the resulting mutation of the HO cut site, adaptation. An alternative explanation relies on the finding that Ino80 may directly regulate Rad53, as Ino80 subunit Ies4 interacts with and facilitates the phosphorylation of Rad53 in response to DNA damage (Kapoor 2015).

Perhaps in response to the persistent, non-HR-repairable DSB I induced, Isw2 can fulfill some of this Rad53-phosphorylating role in the absence of full Ino80 function. With loss of both factors, however, Rad53 fails to become appropriately phosphorylated, preventing a robust checkpoint response, G2/M arrest, and "correct" preference for HR over NHEJ.

Ultimately, I was unable to definitively show whether the striking phenotype associated with the *isw2Δ nhp10Δ* response to an "un-repairable" break results from a G1 bias in this strain or from novel biology. Future work could potentially address this by engineering a strain with intact Isw2 and Ino80 function but with a strong G1 bias. If such a strain also managed to show a high rate of adaptation in this system, this would support the conclusion that a strong G1 bias in the *isw2Δ nhp10Δ* strain would suffice to explain our results. If such a G1-biased strain had low rates of adaptation, on par with a WT strain, that would strengthen the claim that Isw2 and Ino80 have a novel effect on DSB repair choice. In sum, these data provide preliminary evidence of another pathway – DNA double-strand break repair choice – in which the Isw2 and Ino80 ATP-dependent chromatin remodeling factors may function in parallel.

Materials and Methods

Yeast strains and media

Strains used are listed in Table 3.1. Strains were generated using standard gene replacement protocols (GOLDSTEIN and MCCUSKER 1999). Yeast cells were grown in YP medium (2% Bacto Peptone, 1% yeast extract) supplemented with glycerol (3% final, "YP-glycerol"), glucose (2% final, "YPD"), or galactose (2% final, "YP-galactose").

DSB induction time course

Cells were grown to saturation in YP-glycerol. Cells were diluted and grown overnight until reaching OD ~0.1-0.2. Cells were filtered on a 0.45 mm nitrocellulose membrane, washed with YP-glycerol, and then released into half the original culture volume of pre-warmed YP-galactose. Cultures were grown at 30°C. At desired time points, samples were collected for cell cycle analysis by flow cytometry, protein analysis, and/or Southern blotting.

Cell cycle analysis by flow cytometry

Approximately 500 µl of cell culture was added to 1.0 ml of 100% EtOH to fix. Cells were washed in water, then re-suspended in 200 µl of 2 mg/ml RNase A in 50 mM Tris-HCl, pH 8.0 and incubated at 37°C for approximately 4 hours. Cells were spun out of RNase A and then re-suspended in 200 µl of 2 mg/ml Proteinase K in 50 mM Tris-HCl, pH 7.5 and incubated at 50°C for ~45 minutes to an hour. Cells were spun out of Proteinase K, then re-suspended in 200 µl of 50 mM Tris-HCl, pH 7.5 and stored overnight at 4°C. Samples were sonicated briefly, and then 100 µl of each sample was added to 1.0 ml of 1x SYTOX green nucleic acid stain in 50 mM Tris-HCl, pH 7.5. Samples were incubated for at least 1 hour at 4°C before running on flow cytometer. Data were analyzed with FlowJo (https://www.flowjo.com/).

Rad53 western blot analysis

Protein was prepared as described previously (LEE *et al.* 2015), using a trichloroacetic acid (TCA) prep. Samples were run on an 8% SDS-polyacrylamide gel and transferred onto

PVDF membranes. Rad53 band was detected with polyclonal goat anti-Rad53 antibody (Santa Cruz Biotech, sc-6749, clone yc-19).

Spot tests

Cells were grown to saturation overnight, and then 5x serial dilutions were plated on YPD or YP-galactose plates, as indicated.

Colony-counting viability assay

Cells were grown to saturation overnight in YP-glycerol medium. Serial dilutions of the cultures were prepared and plated onto YPD or YP-galactose plates, with dilutions chosen to ensure a countable number of colonies on each plate (targeting ~100-300 colonies per plate). Colony-forming units (CFUs) per plate were counted and then adjusted based on the dilution. The % survival was calculated as the number of CFUs on galactose plates over the CFUs on glucose.

Monitoring of HO cutting by Southern blot

Cells were washed once in water and then cell pellets snap frozen in liquid nitrogen and stored at -80°C. Cells were thawed and re-suspended in 1.0 ml of zymolyase buffer (1M sorbitol, 0.1M EDTA, 10 mM beta mercaptoethanol added fresh), then 100 µl of 12 mg/ml zymolyase 20T (prepared in same buffer) was added to each sample, then incubated at 37°C for 25' while nutating. Spheroplasts were spun down, then 2 ml Buffer G2 and 0.5 ml glass beads added. Samples were vortexed ~10 seconds, cell disruption checked on microscope, and 5 µl of 10 mg/ml stock of Proteinase K added and incubated overnight at

55°C. Samples were treated with 5 µl of 10 mg/ml stock of RNase A for 30-60 minutes at 42°C. Samples were centrifuged to spin down cell debris, and supernatant was loaded into 20/G genomic tips (Qiagen catalog # 10223) pre-equilibrated with QBT buffer (Qiagen catalog # 19054). Columns were washed 3 x 1 ml QC buffer (1.0 M NaCl; 50 mM MOPS, pH 7.0; 15% isopropanol (v/v)), then DNA eluted with 2 x 875 µl warm QF buffer (1.25 M NaCl; 50 mM Tris-Cl, pH 8.5; 15% isopropanol (v/v)). DNA was precipitated with 0.7 volumes (1.23 ml) isopropanol, and tubes inverted a few times. Samples were spun in a 4°C centrifuge at max speed. Supernatant was poured off, and pellets were washed twice in 70% EtOH, then air-dried and re-suspended in 1x TE. DNA was quantified, and 1 µg was digested with StyI restriction enzyme, then run on a 1.3% LE agarose 1x TAE gel. DNA was transferred via standard SSC transfer onto GeneScreen membranes, as described in Chapter 2 of this dissertation. Membranes were hybridized with a probe as indicated in Figure 3.3.

Sanger sequencing of HO cut site

DNA was prepared by standard phenol extraction. PCR was performed to amplify an ~500 bp fragment containing the HO cut site. BigDye PCR was performed and then samples were Sanger sequenced.

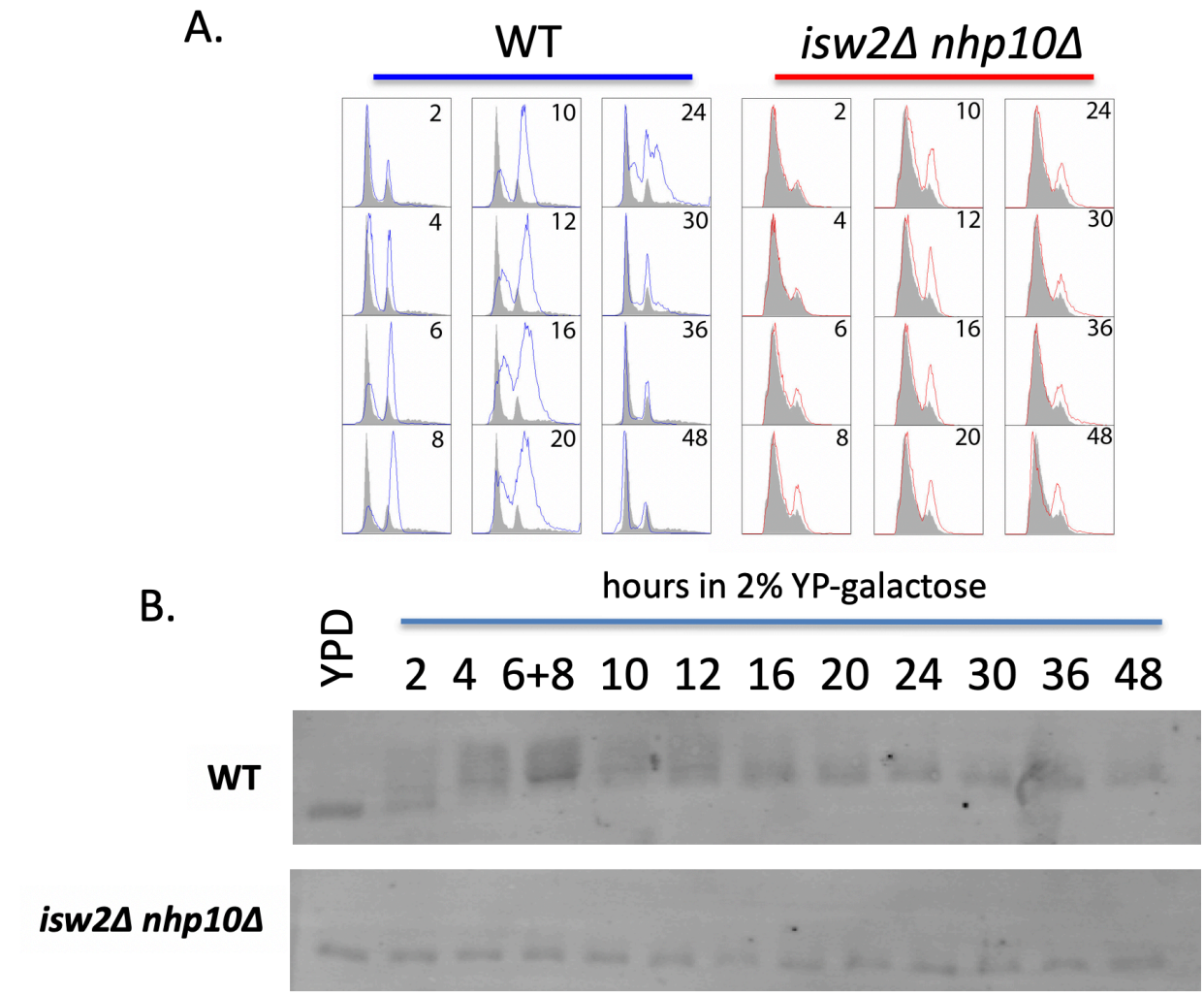

Figure 3.1: *isw2Δ nhp10Δ* cells do not arrest in G2/M or activate the Rad53 checkpoint in response to a DSB that cannot be repaired by homologous recombination.

A) Flow cytometry data showing cell cycle profiles from a DSB-induction time course in WT and *isw2Δ nhp10Δ* in the HR-incompetent background. Time in hours since DSB induction is indicated. Grey profile is for that strain's cell cycle profile in logarithmic growth in YPD. B) Rad53 western blot from the same time course described in A.

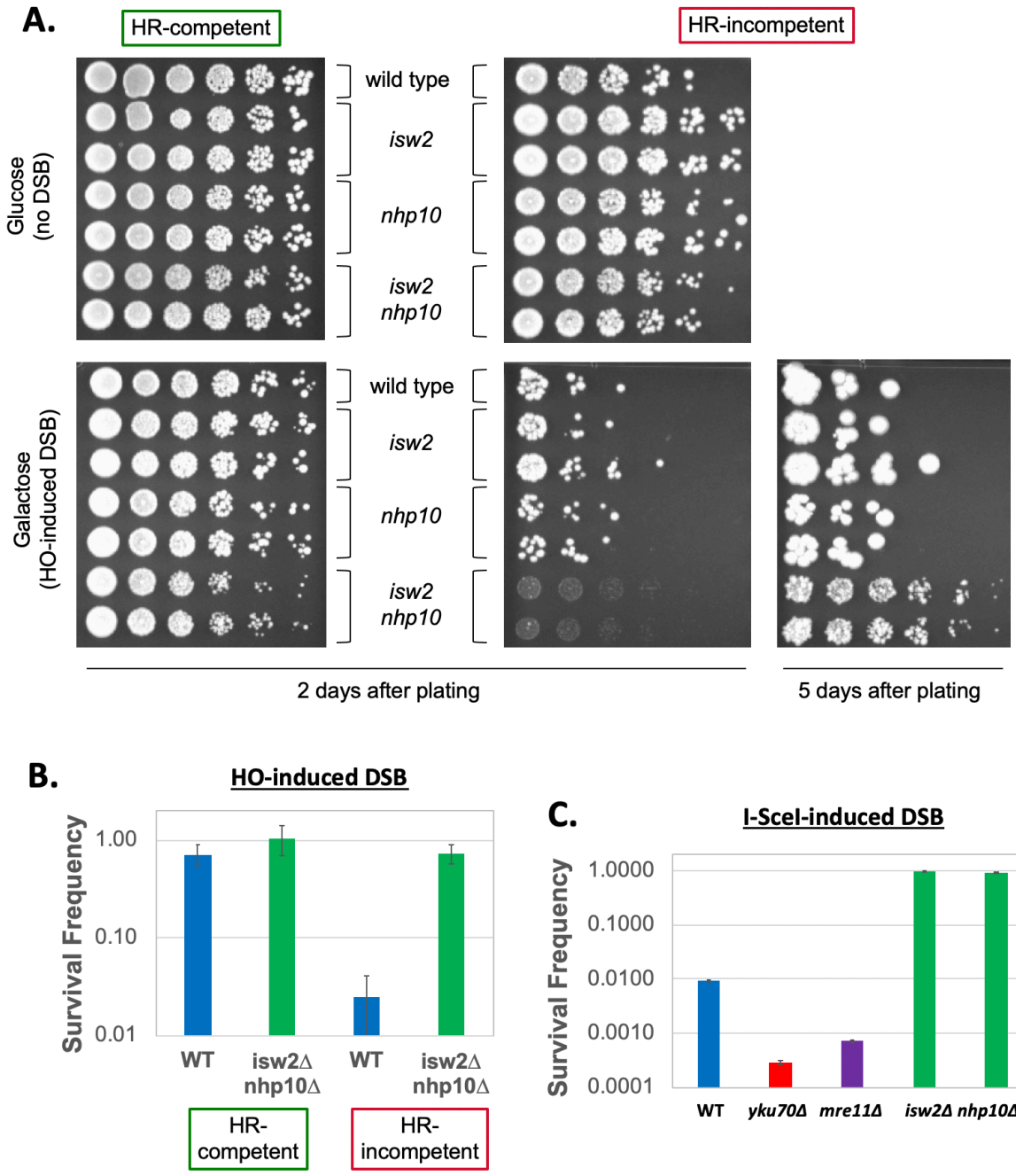

Figure 3.2: Following DSBs that cannot be repaired by homologous recombination, *isw2Δ nhp10Δ* cells have dramatically increased viability relative to WT.

A) Spot assays with five-fold dilutions of cells comparing both HR-competent and HR-incompetent WT, *isw2Δ*, *nhp10Δ*, and *isw2Δ nhp10Δ* strains. For B and C: Survival frequency = # of colony-forming units (CFUs) on galactose/glucose. Y-axis on log scale. Error bars indicate standard error of the mean. B) HO-induced DSB. n = 2 for WT and n = 3 for *isw2Δ nhp10Δ* strains. C) I-SceI induced DSB. n =2 for all strains. Two independent isolates of *isw2Δ nhp10Δ* are shown.

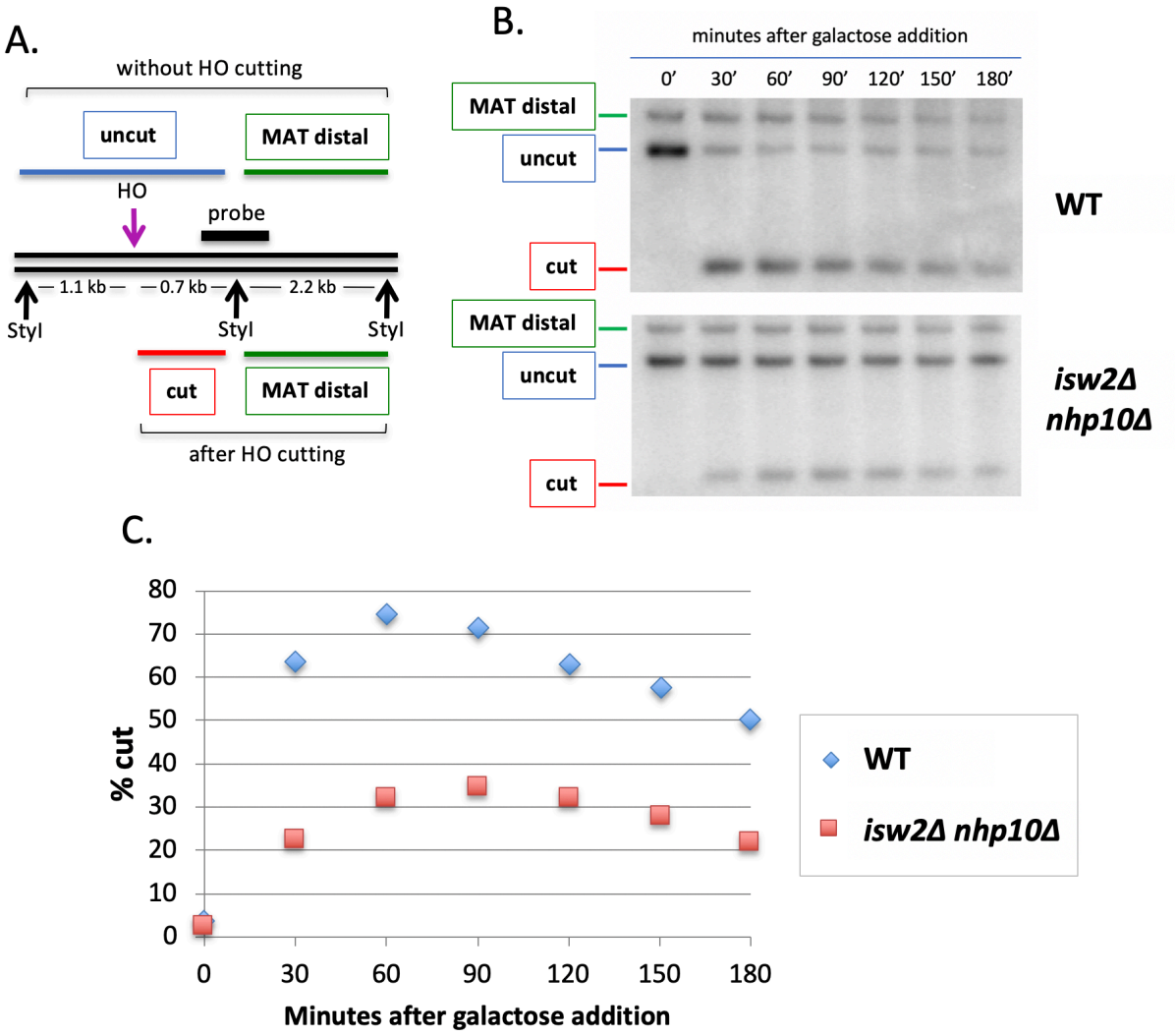

Figure 3.3: HO cutting happens in isw2Δnhp10Δ cells, but with somewhat altered efficiency and/or kinetics.

A) Diagram showing StyI cut sites flanking the HO cut site, location of Southern blot probe, and color-coded restriction fragments that resolve before and after HO cutting. B) Representative Southern blot showing 3 hour DSB induction time course in HR-incompetent WT and *isw2Δ nhp10Δ*. C) Quantification of the Southern blot in B. Band intensity was quantified, and the % cut was calculated as the amount of signal in the "cut" band divided by the total signal in the "cut" plus "uncut" bands.

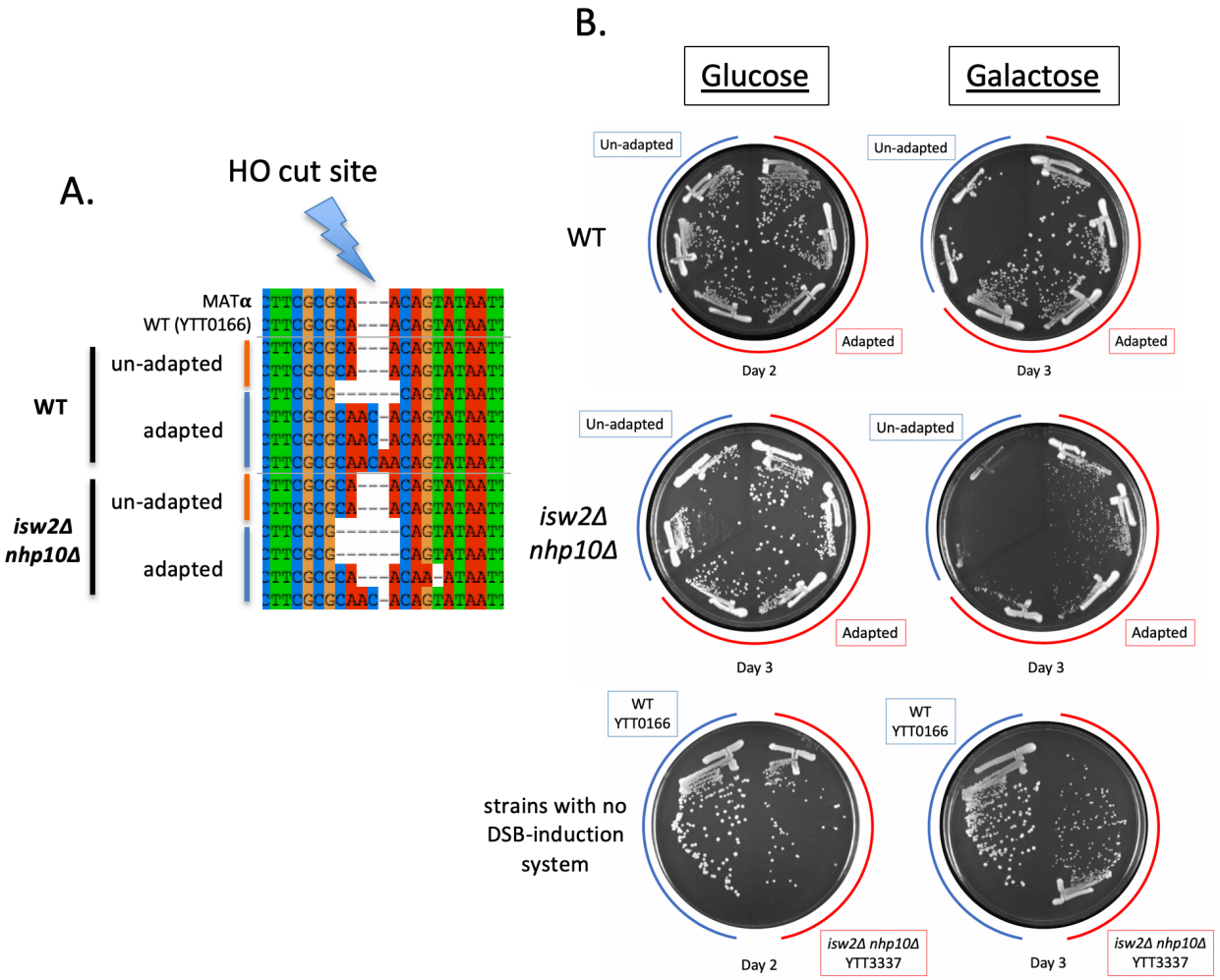

Figure 3.4: All adapted isw2 nhp10 colonies show evidence of a cut and mutated HO target site.

A) Sequence alignments centered on the HO cut site. The first 2 tracks are the SGD reference sequence for MAT**α** and the Sanger sequencing result for our standard lab WT, YTT0166. The following tracks are from the HR-incompetent WT and *isw2Δ nhp10Δ* strains, either before adaptation via growth on galactose, or after adaptation. Only 4 adapted colonies are shown per genotype; Table 3.2 contains a complete summary of sequenced colonies. B) Growth assays. The left column is glucose plates, the right column galactose plates. The top row is all HR-incompetent WT, a mix of un-adapted and adapted colonies; the middle row all HR-incompetent *isw2Δ nhp10Δ*, a mix of un-adapted and adapted colonies; and the bottom row is a mix of WT and *isw2Δ nhp10Δ* strains lacking the DSB-inducible system, showing the mild growth defect on YP-galactose in the *isw2Δ nhp10Δ* strain, independent of DSB induction or adaptation.

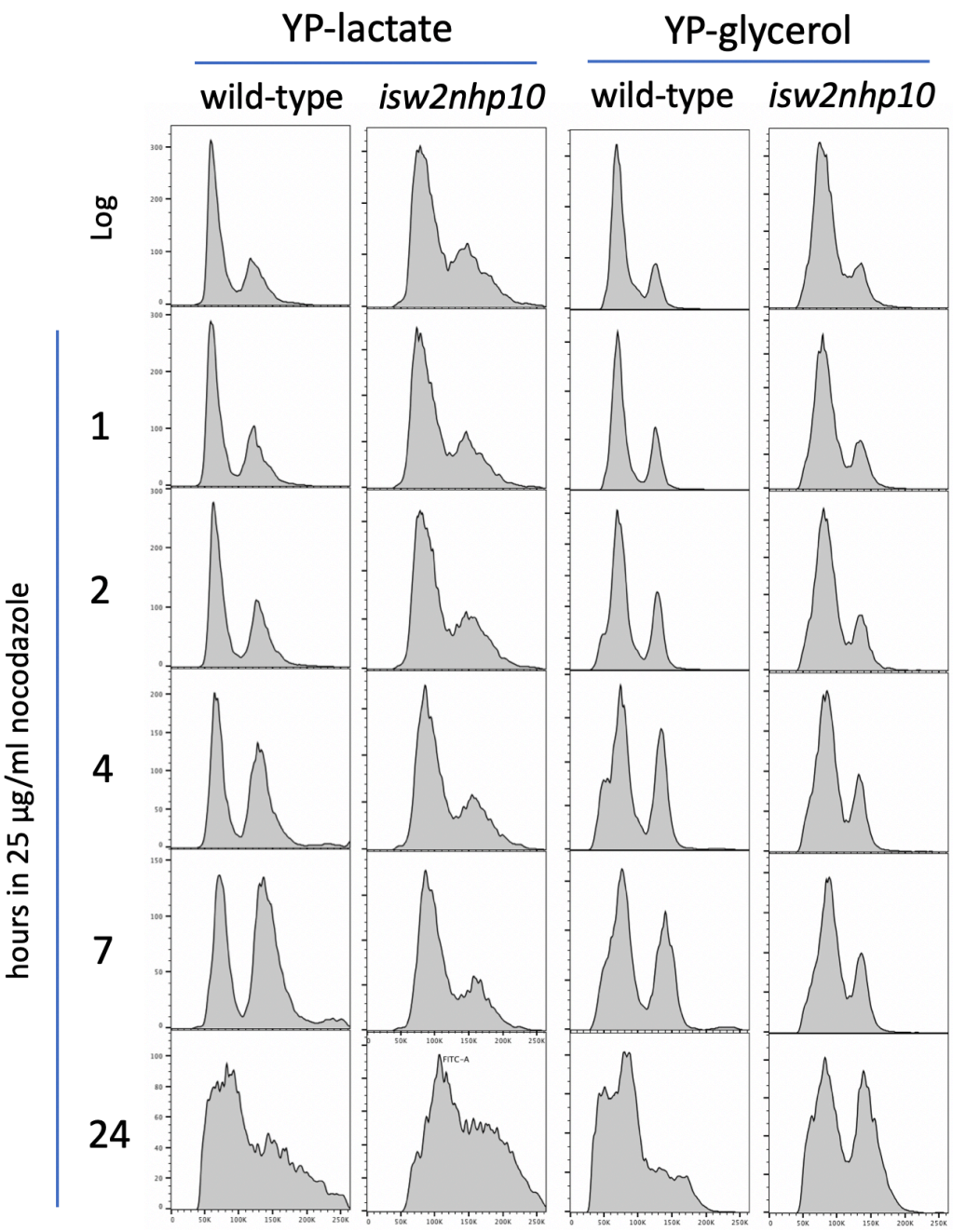

Figure 3.5: *isw2Δ nhp10Δ* cells in HR-incompetent background have persistent G1 bias.

Flow cytometry data showing cell cycle profiles, as described in Figure 1.1B. HR-incompetent WT and *isw2Δ nhp10Δ* were grown in YP-lactate or YP-glycerol, as indicated, and then nocodazole added to 25 µg/ml final concentration. Samples taken at the indicated time points.

Table 3.1: Chapter 3 yeast strains.

Strain	Genotype	Reference
YJK17	MATα ho hml::ADE1 hmr::ADE1arg5,6::Hyg::MATa-inc ade1-100 leu2,3-112 lys5 trp1::hisG ura3-52 ade3::GAL-HO	Keogh *et al* 2006
JKM179	MATα ho hml::ADE1 hmr::ADE1 ade1-100 leu2,3-112 lys5 trp1::hisG ura3-52 ade3::GAL-HO	Moore and Haber 1996
YTT6140	(YJK17 isogenic) isw2::NAT	This study
YTT6141	(YJK17 isogenic) isw2::NAT	This study
YTT6142	(YJK17 isogenic) nhp10::KanMX	This study
YTT6143	(YJK17 isogenic) nhp10::KanMX	This study
YTT6144	(YJK17 isogenic) isw2::Nat nhp10::KanMX	This study
YTT6145	(YJK17 isogenic) isw2::Nat nhp10::KanMX	This study
YTT6146	(JKM179 isogenic) isw2::NAT	This study
YTT6147	(JKM179 isogenic) isw2::NAT	This study
YTT6148	(JKM179 isogenic) nhp10::KanMX	This study
YTT6149	(JKM179 isogenic) nhp10::KanMX	This study
YTT6150	(JKM179 isogenic) isw2::Nat nhp10::KanMX	This study
YTT6151	(JKM179 isogenic) isw2::Nat nhp10::KanMX	This study
LSY2956-8D	MATα can1-100 his3-11,15 leu2-3,112 trp1-1 ura3-1 ade2-ISIR-12MH lys2::pGAL-ISceI	Deng *et al* 2014
LSY2999-6C	(LSY2956-8D isogenic) yku70::HIS3	Deng *et al* 2014
LSY3011-1D	(LSY2956-8D isogenic) mre11::KlURA3	Deng *et al* 2014
YTT6525	(LSY2956-8D isogenic) isw2::NAT nhp10::HYG	This study
YTT6526	(LSY2956-8D isogenic) isw2::NAT nhp10::HYG	This study

(KEOGH *et al.* 2006)
(MOORE and HABER 1996)
(DENG *et al.* 2014)

Table 3.2: Summary of sequenced HO cut site mutations in WT and *isw2Δ nhp10Δ* adapters.

#	Genotype	# bps gained/lost	insertion or deletion
1	WT	1	deletion
2	WT	2	deletion
3	WT	3	deletion
4	WT	3	deletion
5	WT	3	deletion
6	WT	4	deletion
7	WT	2	insertion
8	WT	2	insertion
9	WT	2	insertion
10	WT	2	insertion
11	WT	2	insertion
12	WT	2	insertion
13	WT	2	insertion
14	WT	3	insertion
1	*isw2Δnhp10Δ*	1	deletion
2	*isw2Δnhp10Δ*	1	deletion
3	*isw2Δnhp10Δ*	1	deletion
4	*isw2Δnhp10Δ*	3	deletion
5	*isw2Δnhp10Δ*	3	deletion
6	*isw2Δnhp10Δ*	3	deletion
7	*isw2Δnhp10Δ*	3	deletion
8	*isw2Δnhp10Δ*	6	deletion
9	*isw2Δnhp10Δ*	8	deletion
10	*isw2Δnhp10Δ*	15	deletion
11	*isw2Δnhp10Δ*	2	insertion
12	*isw2Δnhp10Δ*	2	insertion
13	*isw2Δnhp10Δ*	2	insertion
14	*isw2Δnhp10Δ*	3	insertion
15	*isw2Δnhp10Δ*	3	insertion

Chapter 4

Conclusions and Perspectives

The work described in this dissertation represents the continuation of a body of work that has inferred biological functions of the Isw2 and Ino80 ATP-dependent chromatin remodeling complexes from the behavior of *isw2Δ nhp10Δ* strains. This lineage of studies was initiated following the observation that many mutations and deletions of single ATP-dependent chromatin remodeling factors often produced relatively mild phenotypes, supporting the possibility that remodeling factors may perform partially overlapping or compensatory functions. To find novel functions of the Isw2 remodeling factor, a genetic screen was performed to identity genes required for robust growth in the absence of *ISW2* (VINCENT et al. 2008). This screen identified multiple subunits of the Ino80 complex – *IES2*, *IES3*, *IES5*, and *NHP10* – as having synthetic growth defects when deleted in addition to *ISW2*. Deletions of *isw2Δ* with any one of the above Ino80 subunits, as well as with a partial loss of function allele of the ATPase *INO80*, caused sensitivity to the DNA alkylating agent methyl methanesulfonate (MMS). Notably, all relevant single mutants showed similar MMS sensitivity as WT cells, highlighting the need for this combinatorial approach to reveal this phenotype. The *isw2Δ nhp10Δ* double mutant was further shown to have significantly delayed S-phase progression in the presence of MMS, a defect traced to the failed firing of late-firing origins (VINCENT *et al.* 2008).

Subsequent characterization connected this defect of late-firing origins to disrupted regulation of the S-phase checkpoint response. Upon treatment with MMS or hydroxyurea (HU), WT cells activate a robust S-phase checkpoint response, detectable by the phosphorylation of the Rad53 kinase. Checkpoint activation pauses replication progression

to allow the cell time to address the source of damage or replication stress that elicited the response (SZYJKA *et al.* 2008; LABIB and DE PICCOLI 2011). Eventually, the cell must shut down the checkpoint response to allow for the resumption of DNA replication and cell cycle progression. In *isw2Δ nhp10Δ* cells, the S-phase checkpoint is activated in response to MMS or HU treatment, but then persists much longer than in WT cells (AU *et al.* 2011). In pursuit of identifying the precise pathway through which Isw2 and Ino80 contribute to the timely attenuation of the S-phase checkpoint, numerous genetic interactions were tested, combining *isw2Δ nhp10Δ* with deletions of genes involved in checkpoint regulation, replication fork protection, and DNA damage repair. Surprisingly, none of the tested genetic interactions indicated involvement in a specific, known pathway (LEE *et al.* 2015). Though the exact mechanism remains unknown, these studies revealed novel functions of the Isw2 and Ino80 remodeling factors in regulating genome-wide replication dynamics and stress-induced checkpoint activity.

Roles for Isw2 and Ino80 at the ribosomal DNA locus

Following the studies described above, this body of work has uncovered previously un-characterized functions of these remodeling factors at the ribosomal DNA locus based on experiments in which single mutants of either Isw2 or Ino80 have little to no detectable phenotype relative to WT cells. This work identified two ways in which loss of *ISW2* and *NHP10* altered chromatin structure at the ribosomal DNA locus. In *isw2Δ nhp10Δ* cells, the proportion of actively transcribed rDNA repeats is reduced relative to in WT cells [Figure 2.2B], and multiple nucleosomes in the inter-genic spacer region of the rDNA have altered positioning, especially around the ribosomal origin of replication (rARS). In addition to

these changes in chromatin structure in *isw2Δ nhp10Δ* cells, I identified numerous functional consequences for rDNA biology. Despite the altered proportion of active rDNA repeats, I found no change in net rRNA transcription, suggesting that the transcriptional output of each active repeat is increased relative to WT. I did, however, find significantly reduced efficiency of the rARS and significantly reduced rate of rDNA copy number increase in the double mutant compared to WT.

According to one possible model to explain my collected findings, the normal function of Isw2 and Ino80 at the rDNA is to increase the proportion of actively transcribed repeats in the rDNA array. When this activity is lost, as in *isw2Δ nhp10Δ* cells, the proportion of actively transcribed repeats is reduced compared to WT, as I observe [Figure 2.2B]. This does not affect net rRNA production, as the rate of transcription per active repeat is increased. If true, this is another example of an established pattern of regulation at this locus: Although rDNA repeats tend to be either "on" or "off", the functional rate of net transcription from any one "active" repeat can be tuned to meet cellular demands, especially by modulating the density of RNA polymerase I loading (DAMMANN *et al.* 1993; FRENCH *et al.* 2003). Other work has found that rARSs are more likely to fire if they are adjacent to actively transcribed rDNA repeats (MULLER *et al.* 2000). Thus, the reduced proportion of active repeats in *isw2Δ nhp10Δ* cells would mean a reduced proportion of rARSs are adjacent to active repeats, and thus a reduced proportion of rARSs would be predicted to fire. Finally, the ARS present in the inter-genic spacer region affects the frequency of rDNA copy number increasing event, as an inefficient ARS reduces the functional rate of rDNA copy number increase, and an efficient ARS increases this rate

(GANLEY *et al.* 2009). Thus, the reduced efficiency of the rARS, driven by the reduced proportion of active repeats, could reduce the rate of rDNA copy number increase.

The data presented are also potentially consistent with Isw2 and Ino80 more directly influencing the efficiency of the ribosomal ARS. I identified subtle nucleosome positioning alterations around the rARS in *isw2Δ nhp10Δ*, and Isw2's most prominent ChIP-seq peak neatly overlaps with two of the most-affected nucleosomes, directly adjacent to the rARS (Figure 2.5). In addition, our MCM ChIP-seq data suggest the possibility that Isw2 and Ino80 may affect pre-RC formation at the rARS, as there is far less MCM signal at the rARS in the double mutant than in the WT in G1-arrested cells (figure 2.6D). Nucleosome positioning around origins can significantly influence origin efficiency (SIMPSON 1990; LIPFORD and BELL 2001). Isw2 and Ino80, which have well-characterized nucleosome sliding activities, may contribute to the optimal positioning of the rARS-flanking nucleosomes. Loss of these factors may cause slightly perturbed positioning of these nucleosomes, which may in turn prevent the robust targeting of ORC to the rARS and, subsequently, other components of replication machinery.

These MCM ChIP-seq data also suggest a possible explanation of how Isw2 and Ino80 regulate rDNA copy number change. The MCM data corroborates observations I made of short exposures of our 2D gel Southern blots of the rARS, in which I saw evidence for reduced pausing at the RFB in the double mutant compared to WT. This is also the conclusion when considering MCM ChIP-seq data in the IGS: Whether considering the proportion of MCM signal at the RFB relative to overall signal through the IGS, or the absolute amounts of signal at the RFB, pausing of the replication machinery at this locus appears less robust in *isw2Δ nhp10Δ* than in WT cells. This may explain the reduced rate of

rDNA copy number change in the double mutant, as according to one accepted model, copy number change events require a targeted DNA lesion to be introduced at replication forks paused at the RFB (KOBAYASHI and GANLEY 2005). If the replication dynamics through the rDNA in *isw2Δ nhp10Δ* cells are such that a smaller proportion of RFBs are sites of replication fork pausing, this may represent fewer opportunities for targeted DSBs that result in copy number change events.

Roles for Isw2 and Ino80 in dictating DSB repair pathway choice

In addition to studying Isw2 and Ino80 at the rDNA locus, this work also studied the roles played by these factors in responding to a DNA double-strand break that cannot be repaired by homologous recombination. In response to this situation, WT cells arrest in G2/M, robustly activate the Rad53 checkpoint kinase, and repair their DSBs with mutagenic NHEJ in approximately 1-2% of cells. This mutagenic NHEJ allows for these cells to escape from further cutting by the DSB-inducing HO endonuclease, and thus "adapt" to the persistent expression of HO. In contrast, in response to the same persistent DSB lacking a suitable homology donor, *isw2Δ nhp10Δ* cells fail to robustly arrest in G2/M, fail to activate Rad53, and adapt at dramatically higher rates [Figures 3.1, 3.2].

The strikingly increased rates of adaptation in *isw2Δ nhp10Δ* cells likely result from a significant shift away from HR and towards NHEJ repair of the induced DSB. The balance between HR and NHEJ is enacted at the sites of DNA damage in large part through the extent of resection of the free DNA ends that result from a DSB (AYLON *et al.* 2004; SYMINGTON and GAUTIER 2011; CECCALDI *et al.* 2016). Homologous recombination requires significant resection of DNA ends. Following resection, members of the *RAD52* epistasis

group – including Rad50, Rad51, Rad52, Rad54, and Rad55 – facilitate the search for a homology donor, strand invasion of the donor by the broken end, and eventually Holliday junction formation and resolution (CHAPMAN *et al.* 2012; CECCALDI *et al.* 2016). In contrast, non-homologous end joining employs Yku70 and Yk80 to promote the more-direct ligation of the free ends produced by the DSB, perhaps with loss of a few base pairs of DNA in the process, but with minimal production of single-stranded DNA (CHANG *et al.* 2017). In sum, following a DSB, extensive resection promotes repair by HR, and minimal resection promotes NHEJ.

As discussed in Chapter 3, cell cycle stage significantly influences the balance between HR and NHEJ. I cannot disprove the possibility that the proposed skewed preference for NHEJ over HR in *isw2Δ nhp10Δ* is driven principally by the striking G1 bias in this strain. However, I also did not find any clear evidence that this cell cycle bias is the only cause of this phenotype. I hypothesize that Isw2 and Ino80 may contribute to the normal amount of resection at HO-induced DSBs that cannot be repaired by HR, and that without this activity, *isw2Δ nhp10Δ* cells resect these DNA ends less, facilitating mutagenic NHEJ repair and, thus, adaptation. Ino80 is known to be recruited via γ-H2AX to DSBs, where its activity promotes the proper eviction of nucleosomes flanking the site of DNA damage (MORRISON *et al.* 2004; VAN ATTIKUM *et al.* 2004; VAN ATTIKUM *et al.* 2007). Without this reduced nucleosome occupancy, repair factors fail to be properly recruited to the break, including the Mre11 nuclease that is among the most critical factors involved in DNA resection (MORRISON *et al.* 2007; VAN ATTIKUM *et al.* 2007). Notably, some work has called into question the degree to which Ino80 is absolutely necessary for break-proximal DNA resection (TSUKUDA *et al.* 2005). Perhaps Isw2 contributes in some way to Ino80's

promotion of resection, and depending on the extent and specific nature of the DNA damage in these studies, Isw2 may be able to partially compensate for loss of full Ino80 function.

If Isw2 and Ino80 do indeed contribute to the balance between HR and NHEJ repair of DSBs, this provides another possible explanation of our finding that rDNA copy number increases more slowly in *isw2Δ nhp10Δ* cells. The canonical mechanism of copy number increase begins with the creation of a targeted DSB at a replication fork paused at the rDNA's replication fork block (RFB) (KOBAYASHI *et al.* 1998; KOBAYASHI *et al.* 2001; KOBAYASHI and GANLEY 2005; JACK *et al.* 2015), although some evidence suggests that the pausing is not necessary for recombination in this region (WARD *et al.* 2000). Depending on the transcriptional status of a nearby RNA Pol II promoter, E-pro, the DSB induced at the RFB can be repaired by homologous recombination in one of three ways: 1) an rDNA repeat is added to the rDNA array, 2) a repeat is removed from the array, or 3) there is no change in copy number (KOBAYASHI and GANLEY 2005). In addition to this *RAD52*-dependent, recombination-mediated mechanism of repair, there is also an end-repair-mediated mechanism, dependent on the replicative kinase *DUN1*, that can also mediate rDNA copy number change events, although the kinetics of copy number change may differ between these two pathways (JACK *et al.* 2015).

In the absence of full Isw2 and Ino80 function, it is possible that the recombination-mediated repair of the targeted DSB at the RFB happens less frequently. In this model, in *isw2Δ nhp10Δ* cells, a greater proportion of RFB DSBs are repaired not with HR, but with NHEJ. An overall increase in the proportion of RFB DSBs repaired by NHEJ rather than by HR could alter the kinetics of changing the rDNA copy number. This difference is likely to

be especially apparent in the context of a sustained process of increasing rDNA copy number, as in the copy number change time courses described in Chapter 2. This model is potentially testable, as NHEJ is considerably more mutagenic than HR. Thus, I would predict that following a copy number change time course such as that depicted in in Figure 2.8, WT "recovered" isolates would have unchanged DNA sequences at the RFB. In contrast, *isw2Δ nhp10Δ* "recovered" isolates, having endured some appreciable number of NHEJ – rather than HR – repair events of targeted DSBs, would show evidence of a mix of "normal" RFB sequences and mutated RFB sequences. Such sequence heterogeneity in double mutants that have endured a process of intense, sustained copy number change would support the conclusion that altered HR/NHEJ balance accounts for this phenotype.

In sum, the research summarized in this dissertation has significantly expanded our understanding of the roles of *Saccharomyces cerevisiae* Isw2 and Ino80 at the ribosomal DNA locus and suggested possible roles for these factors in regulating DSB repair pathway choice.

References

Adkins, N. L., M. Watts and P. T. Georgel, 2004 To the 30-nm chromatin fiber and beyond. Biochim Biophys Acta 1677**:** 12-23.

Agrawal, S., and A. R. D. Ganley, 2018 The conservation landscape of the human ribosomal RNA gene repeats. PLoS One 13**:** e0207531.

Allfrey, V. G., R. Faulkner and A. E. Mirsky, 1964 ACETYLATION AND METHYLATION OF HISTONES AND THEIR POSSIBLE ROLE IN THE REGULATION OF RNA SYNTHESIS. Proc Natl Acad Sci U S A 51**:** 786-794.

Au, T. J., J. Rodriguez, J. A. Vincent and T. Tsukiyama, 2011 ATP-dependent chromatin remodeling factors tune S phase checkpoint activity. Mol Cell Biol 31**:** 4454-4463.

Aylon, Y., B. Liefshitz and M. Kupiec, 2004 The CDK regulates repair of double-strand breaks by homologous recombination during the cell cycle. Embo j 23**:** 4868-4875.

Azmi, I. F., S. Watanabe, M. F. Maloney, S. Kang, J. A. Belsky *et al.*, 2017 Nucleosomes influence multiple steps during replication initiation. Elife 6.

Bachman, N., M. E. Gelbart, T. Tsukiyama and J. D. Boeke, 2005 TFIIIB subunit Bdp1p is required for periodic integration of the Ty1 retrotransposon and targeting of Isw2p to S. cerevisiae tDNAs. Genes Dev 19**:** 955-964.

Bao, Y., and X. Shen, 2007 SnapShot: chromatin remodeling complexes. Cell 129**:** 632.

Barski, A., S. Cuddapah, K. Cui, T. Y. Roh, D. E. Schones *et al.*, 2007 High-resolution profiling of histone methylations in the human genome. Cell 129**:** 823-837.

Beckouet, F., S. Labarre-Mariotte, B. Albert, Y. Imazawa, M. Werner *et al.*, 2008 Two RNA polymerase I subunits control the binding and release of Rrn3 during transcription. Mol Cell Biol 28**:** 1596-1605.

Bell, S. P., and B. Stillman, 1992 ATP-dependent recognition of eukaryotic origins of DNA replication by a multiprotein complex. Nature 357**:** 128-134.

Bennett, G., and C. L. Peterson, 2015 SWI/SNF recruitment to a DNA double-strand break by the NuA4 and Gcn5 histone acetyltransferases. DNA Repair (Amst) 30**:** 38-45.

Berger, S. L., 2002 Histone modifications in transcriptional regulation. Curr Opin Genet Dev 12**:** 142-148.

Bickmore, W. A., and B. van Steensel, 2013 Genome architecture: domain organization of interphase chromosomes. Cell 152**:** 1270-1284.

Bowman, G. D., and M. G. Poirier, 2015 Post-translational modifications of histones that influence nucleosome dynamics. Chem Rev 115**:** 2274-2295.

Breeden, L., and K. Nasmyth, 1987 Cell cycle control of the yeast HO gene: cis- and trans-acting regulators. Cell 48**:** 389-397.

Brewer, B. J., and W. L. Fangman, 1987 The localization of replication origins on ARS plasmids in S. cerevisiae. Cell 51**:** 463-471.

Brewer, B. J., and W. L. Fangman, 1988 A replication fork barrier at the 3' end of yeast ribosomal RNA genes. Cell 55**:** 637-643.

Brewer, B. J., D. Lockshon and W. L. Fangman, 1992 The arrest of replication forks in the rDNA of yeast occurs independently of transcription. Cell 71**:** 267-276.

Brownell, J. E., J. Zhou, T. Ranalli, R. Kobayashi, D. G. Edmondson *et al.*, 1996 Tetrahymena histone acetyltransferase A: a homolog to yeast Gcn5p linking histone acetylation to gene activation. Cell 84**:** 843-851.

Burma, S., B. P. Chen, M. Murphy, A. Kurimasa and D. J. Chen, 2001 ATM phosphorylates histone H2AX in response to DNA double-strand breaks. J Biol Chem 276**:** 42462-42467.

Bywater, M. J., G. Poortinga, E. Sanij, N. Hein, A. Peck *et al.*, 2012 Inhibition of RNA polymerase I as a therapeutic strategy to promote cancer-specific activation of p53. Cancer Cell 22**:** 51-65.

Cai, Y., J. Jin, T. Yao, A. J. Gottschalk, S. K. Swanson *et al.*, 2007 YY1 functions with INO80 to activate transcription. Nat Struct Mol Biol 14**:** 872-874.

Ceccaldi, R., B. Rondinelli and A. D. D'Andrea, 2016 Repair Pathway Choices and Consequences at the Double-Strand Break. Trends Cell Biol 26**:** 52-64.

Celeste, A., O. Fernandez-Capetillo, M. J. Kruhlak, D. R. Pilch, D. W. Staudt *et al.*, 2003 Histone H2AX phosphorylation is dispensable for the initial recognition of DNA breaks. Nat Cell Biol 5**:** 675-679.

Chang, H. H. Y., N. R. Pannunzio, N. Adachi and M. R. Lieber, 2017 Non-homologous DNA end joining and alternative pathways to double-strand break repair. Nat Rev Mol Cell Biol 18**:** 495-506.

Chapman, J. R., M. R. Taylor and S. J. Boulton, 2012 Playing the end game: DNA double-strand break repair pathway choice. Mol Cell 47**:** 497-510.

Chen, X., H. Niu, W. H. Chung, Z. Zhu, A. Papusha *et al.*, 2011 Cell cycle regulation of DNA double-strand break end resection by Cdk1-dependent Dna2 phosphorylation. Nat Struct Mol Biol 18**:** 1015-1019.

Clapier, C. R., and B. R. Cairns, 2009 The biology of chromatin remodeling complexes. Annu Rev Biochem 78**:** 273-304.

Clapier, C. R., J. Iwasa, B. R. Cairns and C. L. Peterson, 2017 Mechanisms of action and regulation of ATP-dependent chromatin-remodelling complexes. Nat Rev Mol Cell Biol 18**:** 407-422.

Clapier, C. R., M. M. Kasten, T. J. Parnell, R. Viswanathan, H. Szerlong *et al.*, 2016 Regulation of DNA Translocation Efficiency within the Chromatin Remodeler RSC/Sth1 Potentiates Nucleosome Sliding and Ejection. Mol Cell 62**:** 453-461.

Clerici, M., D. Mantiero, I. Guerini, G. Lucchini and M. P. Longhese, 2008 The Yku70-Yku80 complex contributes to regulate double-strand break processing and checkpoint activation during the cell cycle. EMBO Rep 9**:** 810-818.

Conconi, A., R. M. Widmer, T. Koller and J. M. Sogo, 1989 Two different chromatin structures coexist in ribosomal RNA genes throughout the cell cycle. Cell 57**:** 753-761.

Cutler, S., L. J. Lee and T. Tsukiyama, 2018 Chromatin Remodeling Factors Isw2 and Ino80 Regulate Chromatin, Replication, and Copy Number of the Saccharomyces cerevisiae Ribosomal DNA Locus. Genetics 210**:** 1543-1556.

Dammann, R., R. Lucchini, T. Koller and J. M. Sogo, 1993 Chromatin structures and transcription of rDNA in yeast Saccharomyces cerevisiae. Nucleic Acids Res 21**:** 2331-2338.

Dang, W., G. L. Sutphin, J. A. Dorsey, G. L. Otte, K. Cao *et al.*, 2014 Inactivation of yeast Isw2 chromatin remodeling enzyme mimics longevity effect of calorie restriction via induction of genotoxic stress response. Cell Metab 19**:** 952-966.

Deng, S. K., B. Gibb, M. J. de Almeida, E. C. Greene and L. S. Symington, 2014 RPA antagonizes microhomology-mediated repair of DNA double-strand breaks. Nat Struct Mol Biol 21**:** 405-412.

Dixon, J. R., S. Selvaraj, F. Yue, A. Kim, Y. Li *et al.*, 2012 Topological domains in mammalian genomes identified by analysis of chromatin interactions. Nature 485**:** 376-380.
Eaton, M. L., K. Galani, S. Kang, S. P. Bell and D. M. MacAlpine, 2010 Conserved nucleosome positioning defines replication origins. Genes Dev 24**:** 748-753.
Ebbert, R., A. Birkmann and H. J. Schuller, 1999 The product of the SNF2/SWI2 paralogue INO80 of Saccharomyces cerevisiae required for efficient expression of various yeast structural genes is part of a high-molecular-weight protein complex. Mol Microbiol 32**:** 741-751.
Elsaesser, S. J., A. D. Goldberg and C. D. Allis, 2010 New functions for an old variant: no substitute for histone H3.3. Curr Opin Genet Dev 20**:** 110-117.
Euskirchen, G. M., R. K. Auerbach, E. Davidov, T. A. Gianoulis, G. Zhong *et al.*, 2011 Diverse roles and interactions of the SWI/SNF chromatin remodeling complex revealed using global approaches. PLoS Genet 7**:** e1002008.
Fazzio, T. G., C. Kooperberg, J. P. Goldmark, C. Neal, R. Basom *et al.*, 2001 Widespread collaboration of Isw2 and Sin3-Rpd3 chromatin remodeling complexes in transcriptional repression. Mol Cell Biol 21**:** 6450-6460.
Fazzio, T. G., and T. Tsukiyama, 2003 Chromatin remodeling in vivo: evidence for a nucleosome sliding mechanism. Mol Cell 12**:** 1333-1340.
Filipescu, D., E. Szenker and G. Almouzni, 2013 Developmental roles of histone H3 variants and their chaperones. Trends Genet 29**:** 630-640.
Flanagan, J. F., and C. L. Peterson, 1999 A role for the yeast SWI/SNF complex in DNA replication. Nucleic Acids Res 27**:** 2022-2028.
Fragkos, M., O. Ganier, P. Coulombe and M. Mechali, 2015 DNA replication origin activation in space and time. Nat Rev Mol Cell Biol 16**:** 360-374.
French, S. L., Y. N. Osheim, F. Cioci, M. Nomura and A. L. Beyer, 2003 In exponentially growing Saccharomyces cerevisiae cells, rRNA synthesis is determined by the summed RNA polymerase I loading rate rather than by the number of active genes. Mol Cell Biol 23**:** 1558-1568.
Fritze, C. E., K. Verschueren, R. Strich and R. Easton Esposito, 1997 Direct evidence for SIR2 modulation of chromatin structure in yeast rDNA. Embo j 16**:** 6495-6509.
Fudenberg, G., M. Imakaev, C. Lu, A. Goloborodko, N. Abdennur *et al.*, 2016 Formation of Chromosomal Domains by Loop Extrusion. Cell Rep 15**:** 2038-2049.
Ganley, A. R., S. Ide, K. Saka and T. Kobayashi, 2009 The effect of replication initiation on gene amplification in the rDNA and its relationship to aging. Mol Cell 35**:** 683-693.
Gardner, R., C. W. Putnam and T. Weinert, 1999 RAD53, DUN1 and PDS1 define two parallel G2/M checkpoint pathways in budding yeast. Embo j 18**:** 3173-3185.
Gelbart, M. E., N. Bachman, J. Delrow, J. D. Boeke and T. Tsukiyama, 2005 Genome-wide identification of Isw2 chromatin-remodeling targets by localization of a catalytically inactive mutant. Genes Dev 19**:** 942-954.
Gkikopoulos, T., P. Schofield, V. Singh, M. Pinskaya, J. Mellor *et al.*, 2011 A role for Snf2-related nucleosome-spacing enzymes in genome-wide nucleosome organization. Science 333**:** 1758-1760.
Goldberg, A. D., L. A. Banaszynski, K. M. Noh, P. W. Lewis, S. J. Elsaesser *et al.*, 2010 Distinct factors control histone variant H3.3 localization at specific genomic regions. Cell 140**:** 678-691.

Goldmark, J. P., T. G. Fazzio, P. W. Estep, G. M. Church and T. Tsukiyama, 2000 The Isw2 chromatin remodeling complex represses early meiotic genes upon recruitment by Ume6p. Cell 103**:** 423-433.
Goldstein, A. L., and J. H. McCusker, 1999 Three new dominant drug resistance cassettes for gene disruption in Saccharomyces cerevisiae. Yeast 15**:** 1541-1553.
Grant, P. A., 2001 A tale of histone modifications. Genome Biol 2**:** Reviews0003.
Grummt, I., and C. S. Pikaard, 2003 Epigenetic silencing of RNA polymerase I transcription. Nat Rev Mol Cell Biol 4**:** 641-649.
Hamiche, A., R. Sandaltzopoulos, D. A. Gdula and C. Wu, 1999 ATP-dependent histone octamer sliding mediated by the chromatin remodeling complex NURF. Cell 97**:** 833-842.
Hinz, J. M., N. A. Yamada, E. P. Salazar, R. S. Tebbs and L. H. Thompson, 2005 Influence of double-strand-break repair pathways on radiosensitivity throughout the cell cycle in CHO cells. DNA Repair (Amst) 4**:** 782-792.
Horigome, C., Y. Oma, T. Konishi, R. Schmid, I. Marcomini *et al.*, 2014 SWR1 and INO80 chromatin remodelers contribute to DNA double-strand break perinuclear anchorage site choice. Mol Cell 55**:** 626-639.
Hsieh, T. H., A. Weiner, B. Lajoie, J. Dekker, N. Friedman *et al.*, 2015 Mapping Nucleosome Resolution Chromosome Folding in Yeast by Micro-C. Cell 162**:** 108-119.
Huertas, P., F. Cortes-Ledesma, A. A. Sartori, A. Aguilera and S. P. Jackson, 2008 CDK targets Sae2 to control DNA-end resection and homologous recombination. Nature 455**:** 689-692.
Ide, S., T. Miyazaki, H. Maki and T. Kobayashi, 2010 Abundance of ribosomal RNA gene copies maintains genome integrity. Science 327**:** 693-696.
Iida, T., and H. Araki, 2004 Noncompetitive counteractions of DNA polymerase epsilon and ISW2/yCHRAC for epigenetic inheritance of telomere position effect in Saccharomyces cerevisiae. Mol Cell Biol 24**:** 217-227.
Ira, G., A. Pellicioli, A. Balijja, X. Wang, S. Fiorani *et al.*, 2004 DNA end resection, homologous recombination and DNA damage checkpoint activation require CDK1. Nature 431**:** 1011-1017.
Ito, T., M. Bulger, M. J. Pazin, R. Kobayashi and J. T. Kadonaga, 1997 ACF, an ISWI-containing and ATP-utilizing chromatin assembly and remodeling factor. Cell 90**:** 145-155.
Jack, C. V., C. Cruz, R. M. Hull, M. A. Keller, M. Ralser *et al.*, 2015 Regulation of ribosomal DNA amplification by the TOR pathway. Proc Natl Acad Sci U S A 112**:** 9674-9679.
Jackson, J. A., and G. R. Fink, 1981 Gene conversion between duplicated genetic elements in yeast. Nature 292**:** 306-311.
Jazayeri, A., J. Falck, C. Lukas, J. Bartek, G. C. Smith *et al.*, 2006 ATM- and cell cycle-dependent regulation of ATR in response to DNA double-strand breaks. Nat Cell Biol 8**:** 37-45.
Jiang, C., and B. F. Pugh, 2009 Nucleosome positioning and gene regulation: advances through genomics. Nat Rev Genet 10**:** 161-172.
Jin, J., Y. Cai, T. Yao, A. J. Gottschalk, L. Florens *et al.*, 2005 A mammalian chromatin remodeling complex with similarities to the yeast INO80 complex. J Biol Chem 280**:** 41207-41212.
Jones, H. S., J. Kawauchi, P. Braglia, C. M. Alen, N. A. Kent *et al.*, 2007 RNA polymerase I in yeast transcribes dynamic nucleosomal rDNA. Nat Struct Mol Biol 14**:** 123-130.

Karathanasis, E., and T. E. Wilson, 2002 Enhancement of Saccharomyces cerevisiae end-joining efficiency by cell growth stage but not by impairment of recombination. Genetics 161**:** 1015-1027.
Kassabov, S. R., N. M. Henry, M. Zofall, T. Tsukiyama and B. Bartholomew, 2002 High-resolution mapping of changes in histone-DNA contacts of nucleosomes remodeled by ISW2. Mol Cell Biol 22**:** 7524-7534.
Keogh, M. C., J. A. Kim, M. Downey, J. Fillingham, D. Chowdhury *et al.*, 2006 A phosphatase complex that dephosphorylates gammaH2AX regulates DNA damage checkpoint recovery. Nature 439**:** 497-501.
Kobayashi, T., and A. R. Ganley, 2005 Recombination regulation by transcription-induced cohesin dissociation in rDNA repeats. Science 309**:** 1581-1584.
Kobayashi, T., D. J. Heck, M. Nomura and T. Horiuchi, 1998 Expansion and contraction of ribosomal DNA repeats in Saccharomyces cerevisiae: requirement of replication fork blocking (Fob1) protein and the role of RNA polymerase I. Genes Dev 12**:** 3821-3830.
Kobayashi, T., M. Nomura and T. Horiuchi, 2001 Identification of DNA cis elements essential for expansion of ribosomal DNA repeats in Saccharomyces cerevisiae. Mol Cell Biol 21**:** 136-147.
Kobor, M. S., S. Venkatasubrahmanyam, M. D. Meneghini, J. W. Gin, J. L. Jennings *et al.*, 2004 A protein complex containing the conserved Swi2/Snf2-related ATPase Swr1p deposits histone variant H2A.Z into euchromatin. PLoS Biol 2**:** E131.
Konev, A. Y., M. Tribus, S. Y. Park, V. Podhraski, C. Y. Lim *et al.*, 2007 CHD1 motor protein is required for deposition of histone variant H3.3 into chromatin in vivo. Science 317**:** 1087-1090.
Kouzarides, T., 2007 SnapShot: Histone-modifying enzymes. Cell 131**:** 822.
Kurat, C. F., J. T. P. Yeeles, H. Patel, A. Early and J. F. X. Diffley, 2017 Chromatin Controls DNA Replication Origin Selection, Lagging-Strand Synthesis, and Replication Fork Rates. Mol Cell 65**:** 117-130.
Kwan, E. X., X. S. Wang, H. M. Amemiya, B. J. Brewer and M. K. Raghuraman, 2016 rDNA Copy Number Variants Are Frequent Passenger Mutations in Saccharomyces cerevisiae Deletion Collections and de Novo Transformants. G3 (Bethesda) 6**:** 2829-2838.
Labib, K., and G. De Piccoli, 2011 Surviving chromosome replication: the many roles of the S-phase checkpoint pathway. Philos Trans R Soc Lond B Biol Sci 366**:** 3554-3561.
Lademann, C. A., J. Renkawitz, B. Pfander and S. Jentsch, 2017 The INO80 Complex Removes H2A.Z to Promote Presynaptic Filament Formation during Homologous Recombination. Cell Rep 19**:** 1294-1303.
Langst, G., E. J. Bonte, D. F. Corona and P. B. Becker, 1999 Nucleosome movement by CHRAC and ISWI without disruption or trans-displacement of the histone octamer. Cell 97**:** 843-852.
Laribee, R. N., A. Hosni-Ahmed, J. J. Workman and H. Chen, 2015 Ccr4-not regulates RNA polymerase I transcription and couples nutrient signaling to the control of ribosomal RNA biogenesis. PLoS Genet 11**:** e1005113.
Lawrence, M., S. Daujat and R. Schneider, 2016 Lateral Thinking: How Histone Modifications Regulate Gene Expression. Trends Genet 32**:** 42-56.

Lea, D. E., and C. A. Coulson, 1949 The distribution of the numbers of mutants in bacterial populations. J Genet 49**:** 264-285.
Lee, L., J. Rodriguez and T. Tsukiyama, 2015 Chromatin remodeling factors Isw2 and Ino80 regulate checkpoint activity and chromatin structure in S phase. Genetics 199**:** 1077-1091.
Lee, S. E., J. K. Moore, A. Holmes, K. Umezu, R. D. Kolodner *et al.*, 1998 Saccharomyces Ku70, mre11/rad50 and RPA proteins regulate adaptation to G2/M arrest after DNA damage. Cell 94**:** 399-409.
Li, J., G. Langst and I. Grummt, 2006 NoRC-dependent nucleosome positioning silences rRNA genes. Embo j 25**:** 5735-5741.
Lieberman-Aiden, E., N. L. van Berkum, L. Williams, M. Imakaev, T. Ragoczy *et al.*, 2009 Comprehensive mapping of long-range interactions reveals folding principles of the human genome. Science 326**:** 289-293.
Lipford, J. R., and S. P. Bell, 2001 Nucleosomes positioned by ORC facilitate the initiation of DNA replication. Mol Cell 7**:** 21-30.
Lorch, Y., J. Griesenbeck, H. Boeger, B. Maier-Davis and R. D. Kornberg, 2011 Selective removal of promoter nucleosomes by the RSC chromatin-remodeling complex. Nat Struct Mol Biol 18**:** 881-885.
Luger, K., A. W. Mader, R. K. Richmond, D. F. Sargent and T. J. Richmond, 1997 Crystal structure of the nucleosome core particle at 2.8 A resolution. Nature 389**:** 251-260.
Luria, S. E., and M. Delbruck, 1943 Mutations of Bacteria from Virus Sensitivity to Virus Resistance. Genetics 28**:** 491-511.
Majka, J., A. Niedziela-Majka and P. M. Burgers, 2006 The checkpoint clamp activates Mec1 kinase during initiation of the DNA damage checkpoint. Mol Cell 24**:** 891-901.
Mantiero, D., A. Mackenzie, A. Donaldson and P. Zegerman, 2011 Limiting replication initiation factors execute the temporal programme of origin firing in budding yeast. Embo j 30**:** 4805-4814.
Marahrens, Y., and B. Stillman, 1992 A yeast chromosomal origin of DNA replication defined by multiple functional elements. Science 255**:** 817-823.
Marshall, W. F., 2002 Order and disorder in the nucleus. Curr Biol 12**:** R185-192.
Martinez-Campa, C., P. Politis, J. L. Moreau, N. Kent, J. Goodall *et al.*, 2004 Precise nucleosome positioning and the TATA box dictate requirements for the histone H4 tail and the bromodomain factor Bdf1. Mol Cell 15**:** 69-81.
Mavrich, T. N., I. P. Ioshikhes, B. J. Venters, C. Jiang, L. P. Tomsho *et al.*, 2008 A barrier nucleosome model for statistical positioning of nucleosomes throughout the yeast genome. Genome Res 18**:** 1073-1083.
McKinley, K. L., and I. M. Cheeseman, 2016 The molecular basis for centromere identity and function. Nat Rev Mol Cell Biol 17**:** 16-29.
Melo, J. A., J. Cohen and D. P. Toczyski, 2001 Two checkpoint complexes are independently recruited to sites of DNA damage in vivo. Genes Dev 15**:** 2809-2821.
Merz, K., M. Hondele, H. Goetze, K. Gmelch, U. Stoeckl *et al.*, 2008 Actively transcribed rRNA genes in S. cerevisiae are organized in a specialized chromatin associated with the high-mobility group protein Hmo1 and are largely devoid of histone molecules. Genes Dev 22**:** 1190-1204.
Mirny, L. A., 2011 The fractal globule as a model of chromatin architecture in the cell. Chromosome Res 19**:** 37-51.

Mito, Y., J. G. Henikoff and S. Henikoff, 2005 Genome-scale profiling of histone H3.3 replacement patterns. Nat Genet 37**:** 1090-1097.
Mizuguchi, G., X. Shen, J. Landry, W. H. Wu, S. Sen *et al.*, 2004 ATP-driven exchange of histone H2AZ variant catalyzed by SWR1 chromatin remodeling complex. Science 303**:** 343-348.
Moore, J. K., and J. E. Haber, 1996 Cell cycle and genetic requirements of two pathways of nonhomologous end-joining repair of double-strand breaks in Saccharomyces cerevisiae. Mol Cell Biol 16**:** 2164-2173.
Moreira, J. M., and S. Holmberg, 1999 Transcriptional repression of the yeast CHA1 gene requires the chromatin-remodeling complex RSC. Embo j 18**:** 2836-2844.
Morrison, A. J., J. Highland, N. J. Krogan, A. Arbel-Eden, J. F. Greenblatt *et al.*, 2004 INO80 and gamma-H2AX interaction links ATP-dependent chromatin remodeling to DNA damage repair. Cell 119**:** 767-775.
Morrison, A. J., J. A. Kim, M. D. Person, J. Highland, J. Xiao *et al.*, 2007 Mec1/Tel1 phosphorylation of the INO80 chromatin remodeling complex influences DNA damage checkpoint responses. Cell 130**:** 499-511.
Muller, M., R. Lucchini and J. M. Sogo, 2000 Replication of yeast rDNA initiates downstream of transcriptionally active genes. Mol Cell 5**:** 767-777.
Murawska, M., and A. Brehm, 2011 CHD chromatin remodelers and the transcription cycle. Transcription 2**:** 244-253.
Nakamura, T. M., L. L. Du, C. Redon and P. Russell, 2004 Histone H2A phosphorylation controls Crb2 recruitment at DNA breaks, maintains checkpoint arrest, and influences DNA repair in fission yeast. Mol Cell Biol 24**:** 6215-6230.
Neigeborn, L., and M. Carlson, 1984 Genes affecting the regulation of SUC2 gene expression by glucose repression in Saccharomyces cerevisiae. Genetics 108**:** 845-858.
Olins, A. L., and D. E. Olins, 1974 Spheroid chromatin units (v bodies). Science 183**:** 330-332.
Ou, H. D., S. Phan, T. J. Deerinck, A. Thor, M. H. Ellisman *et al.*, 2017 ChromEMT: Visualizing 3D chromatin structure and compaction in interphase and mitotic cells. Science 357.
Papamichos-Chronakis, M., J. E. Krebs and C. L. Peterson, 2006 Interplay between Ino80 and Swr1 chromatin remodeling enzymes regulates cell cycle checkpoint adaptation in response to DNA damage. Genes Dev 20**:** 2437-2449.
Papamichos-Chronakis, M., and C. L. Peterson, 2008 The Ino80 chromatin-remodeling enzyme regulates replisome function and stability. Nat Struct Mol Biol 15**:** 338-345.
Papamichos-Chronakis, M., S. Watanabe, O. J. Rando and C. L. Peterson, 2011 Global regulation of H2A.Z localization by the INO80 chromatin-remodeling enzyme is essential for genome integrity. Cell 144**:** 200-213.
Park, J. H., E. J. Park, H. S. Lee, S. J. Kim, S. K. Hur *et al.*, 2006 Mammalian SWI/SNF complexes facilitate DNA double-strand break repair by promoting gamma-H2AX induction. Embo j 25**:** 3986-3997.
Pasero, P., A. Bensimon and E. Schwob, 2002 Single-molecule analysis reveals clustering and epigenetic regulation of replication origins at the yeast rDNA locus. Genes Dev 16**:** 2479-2484.
Paull, T. T., E. P. Rogakou, V. Yamazaki, C. U. Kirchgessner, M. Gellert *et al.*, 2000 A critical role for histone H2AX in recruitment of repair factors to nuclear foci after DNA damage. Curr Biol 10**:** 886-895.

Peterson, C. L., and I. Herskowitz, 1992 Characterization of the yeast SWI1, SWI2, and SWI3 genes, which encode a global activator of transcription. Cell 68**:** 573-583.
Raisner, R. M., P. D. Hartley, M. D. Meneghini, M. Z. Bao, C. L. Liu *et al.*, 2005 Histone variant H2A.Z marks the 5' ends of both active and inactive genes in euchromatin. Cell 123**:** 233-248.
Ranjan, A., F. Wang, G. Mizuguchi, D. Wei, Y. Huang *et al.*, 2015 H2A histone-fold and DNA elements in nucleosome activate SWR1-mediated H2A.Z replacement in budding yeast. Elife 4**:** e06845.
Ray, S., and A. Grove, 2009 The yeast high mobility group protein HMO2, a subunit of the chromatin-remodeling complex INO80, binds DNA ends. Nucleic Acids Res 37**:** 6389-6399.
Reinke, H., and W. Horz, 2003 Histones are first hyperacetylated and then lose contact with the activated PHO5 promoter. Mol Cell 11**:** 1599-1607.
Rodriguez, J., J. N. McKnight and T. Tsukiyama, 2014 Genome-Wide Analysis of Nucleosome Positions, Occupancy, and Accessibility in Yeast: Nucleosome Mapping, High-Resolution Histone ChIP, and NCAM. Curr Protoc Mol Biol 108**:** 21.28.21-16.
Rydberg, B., W. R. Holley, I. S. Mian and A. Chatterjee, 1998 Chromatin conformation in living cells: support for a zig-zag model of the 30 nm chromatin fiber. J Mol Biol 284**:** 71-84.
Saha, A., J. Wittmeyer and B. R. Cairns, 2002 Chromatin remodeling by RSC involves ATP-dependent DNA translocation. Genes Dev 16**:** 2120-2134.
Salim, D., W. D. Bradford, A. Freeland, G. Cady, J. Wang *et al.*, 2017 DNA replication stress restricts ribosomal DNA copy number. PLoS Genet 13**:** e1007006.
Sanborn, A. L., S. S. Rao, S. C. Huang, N. C. Durand, M. H. Huntley *et al.*, 2015 Chromatin extrusion explains key features of loop and domain formation in wild-type and engineered genomes. Proc Natl Acad Sci U S A 112**:** E6456-6465.
Sanchez, J. C., E. X. Kwan, T. J. Pohl, H. M. Amemiya, M. K. Raghuraman *et al.*, 2017 Defective replication initiation results in locus specific chromosome breakage and a ribosomal RNA deficiency in yeast. PLoS Genet 13**:** e1007041.
Sandmeier, J. J., S. French, Y. Osheim, W. L. Cheung, C. M. Gallo *et al.*, 2002 RPD3 is required for the inactivation of yeast ribosomal DNA genes in stationary phase. Embo j 21**:** 4959-4968.
Sanij, E., G. Poortinga, K. Sharkey, S. Hung, T. P. Holloway *et al.*, 2008 UBF levels determine the number of active ribosomal RNA genes in mammals. J Cell Biol 183**:** 1259-1274.
Santoro, R., J. Li and I. Grummt, 2002 The nucleolar remodeling complex NoRC mediates heterochromatin formation and silencing of ribosomal gene transcription. Nat Genet 32**:** 393-396.
Schneider, D. A., 2012 RNA polymerase I activity is regulated at multiple steps in the transcription cycle: recent insights into factors that influence transcription elongation. Gene 493**:** 176-184.
Schoeftner, S., and M. A. Blasco, 2009 A 'higher order' of telomere regulation: telomere heterochromatin and telomeric RNAs. Embo j 28**:** 2323-2336.
Schubeler, D., D. M. MacAlpine, D. Scalzo, C. Wirbelauer, C. Kooperberg *et al.*, 2004 The histone modification pattern of active genes revealed through genome-wide chromatin analysis of a higher eukaryote. Genes Dev 18**:** 1263-1271.

Seeber, A., V. Dion and S. M. Gasser, 2013 Checkpoint kinases and the INO80 nucleosome remodeling complex enhance global chromatin mobility in response to DNA damage. Genes Dev 27**:** 1999-2008.
Sexton, T., E. Yaffe, E. Kenigsberg, F. Bantignies, B. Leblanc *et al.*, 2012 Three-dimensional folding and functional organization principles of the Drosophila genome. Cell 148**:** 458-472.
Shen, X., G. Mizuguchi, A. Hamiche and C. Wu, 2000 A chromatin remodelling complex involved in transcription and DNA processing. Nature 406**:** 541-544.
Shim, E. Y., S. J. Hong, J. H. Oum, Y. Yanez, Y. Zhang *et al.*, 2007 RSC mobilizes nucleosomes to improve accessibility of repair machinery to the damaged chromatin. Mol Cell Biol 27**:** 1602-1613.
Shimada, K., Y. Oma, T. Schleker, K. Kugou, K. Ohta *et al.*, 2008 Ino80 chromatin remodeling complex promotes recovery of stalled replication forks. Curr Biol 18**:** 566-575.
Simpson, R. T., 1990 Nucleosome positioning can affect the function of a cis-acting DNA element in vivo. Nature 343**:** 387-389.
Smith, J. S., and J. D. Boeke, 1997 An unusual form of transcriptional silencing in yeast ribosomal DNA. Genes Dev 11**:** 241-254.
Stern, M., R. Jensen and I. Herskowitz, 1984 Five SWI genes are required for expression of the HO gene in yeast. J Mol Biol 178**:** 853-868.
Strahl, B. D., and C. D. Allis, 2000 The language of covalent histone modifications. Nature 403**:** 41-45.
Strohner, R., A. Nemeth, P. Jansa, U. Hofmann-Rohrer, R. Santoro *et al.*, 2001 NoRC--a novel member of mammalian ISWI-containing chromatin remodeling machines. Embo j 20**:** 4892-4900.
Struhl, K., and E. Segal, 2013 Determinants of nucleosome positioning. Nat Struct Mol Biol 20**:** 267-273.
Sun, Z., J. Hsiao, D. S. Fay and D. F. Stern, 1998 Rad53 FHA domain associated with phosphorylated Rad9 in the DNA damage checkpoint. Science 281**:** 272-274.
Swygert, S. G., S. Kim, X. Wu, T. Fu, T. H. Hsieh *et al.*, 2019 Condensin-Dependent Chromatin Compaction Represses Transcription Globally during Quiescence. Mol Cell 73**:** 533-546.e534.
Symington, L. S., and J. Gautier, 2011 Double-strand break end resection and repair pathway choice. Annu Rev Genet 45**:** 247-271.
Szyjka, S. J., J. G. Aparicio, C. J. Viggiani, S. Knott, W. Xu *et al.*, 2008 Rad53 regulates replication fork restart after DNA damage in Saccharomyces cerevisiae. Genes Dev 22**:** 1906-1920.
Talbert, P. B., and S. Henikoff, 2017 Histone variants on the move: substrates for chromatin dynamics. Nat Rev Mol Cell Biol 18**:** 115-126.
Thomas, B. J., and R. Rothstein, 1989 The genetic control of direct-repeat recombination in Saccharomyces: the effect of rad52 and rad1 on mitotic recombination at GAL10, a transcriptionally regulated gene. Genetics 123**:** 725-738.
Tosi, A., C. Haas, F. Herzog, A. Gilmozzi, O. Berninghausen *et al.*, 2013 Structure and subunit topology of the INO80 chromatin remodeler and its nucleosome complex. Cell 154**:** 1207-1219.

Tran, H. G., D. J. Steger, V. R. Iyer and A. D. Johnson, 2000 The chromo domain protein chd1p from budding yeast is an ATP-dependent chromatin-modifying factor. Embo j 19**:** 2323-2331.
Tsukiyama, T., P. B. Becker and C. Wu, 1994 ATP-dependent nucleosome disruption at a heat-shock promoter mediated by binding of GAGA transcription factor. Nature 367**:** 525-532.
Tsukiyama, T., J. Palmer, C. C. Landel, J. Shiloach and C. Wu, 1999 Characterization of the imitation switch subfamily of ATP-dependent chromatin-remodeling factors in Saccharomyces cerevisiae. Genes Dev 13**:** 686-697.
Tsukiyama, T., and C. Wu, 1995 Purification and properties of an ATP-dependent nucleosome remodeling factor. Cell 83**:** 1011-1020.
Tsukuda, T., A. B. Fleming, J. A. Nickoloff and M. A. Osley, 2005 Chromatin remodelling at a DNA double-strand break site in Saccharomyces cerevisiae. Nature 438**:** 379-383.
Udugama, M., A. Sabri and B. Bartholomew, 2011 The INO80 ATP-dependent chromatin remodeling complex is a nucleosome spacing factor. Mol Cell Biol 31**:** 662-673.
van Attikum, H., O. Fritsch and S. M. Gasser, 2007 Distinct roles for SWR1 and INO80 chromatin remodeling complexes at chromosomal double-strand breaks. Embo j 26**:** 4113-4125.
van Attikum, H., O. Fritsch, B. Hohn and S. M. Gasser, 2004 Recruitment of the INO80 complex by H2A phosphorylation links ATP-dependent chromatin remodeling with DNA double-strand break repair. Cell 119**:** 777-788.
Varga-Weisz, P. D., M. Wilm, E. Bonte, K. Dumas, M. Mann *et al.*, 1997 Chromatin-remodelling factor CHRAC contains the ATPases ISWI and topoisomerase II. Nature 388**:** 598-602.
Venkatesh, S., and J. L. Workman, 2015 Histone exchange, chromatin structure and the regulation of transcription. Nat Rev Mol Cell Biol 16**:** 178-189.
Vincent, J. A., T. J. Kwong and T. Tsukiyama, 2008 ATP-dependent chromatin remodeling shapes the DNA replication landscape. Nat Struct Mol Biol 15**:** 477-484.
Walmsley, R. M., L. H. Johnston, D. H. Williamson and S. G. Oliver, 1984 Replicon size of yeast ribosomal DNA. Mol Gen Genet 195**:** 260-266.
Ward, I. M., and J. Chen, 2001 Histone H2AX is phosphorylated in an ATR-dependent manner in response to replicational stress. J Biol Chem 276**:** 47759-47762.
Ward, T. R., M. L. Hoang, R. Prusty, C. K. Lau, R. L. Keil *et al.*, 2000 Ribosomal DNA replication fork barrier and HOT1 recombination hot spot: shared sequences but independent activities. Mol Cell Biol 20**:** 4948-4957.
Warner, J. R., 1999 The economics of ribosome biosynthesis in yeast. Trends Biochem Sci 24**:** 437-440.
Weiner, A., A. Hughes, M. Yassour, O. J. Rando and N. Friedman, 2010 High-resolution nucleosome mapping reveals transcription-dependent promoter packaging. Genome Res 20**:** 90-100.
Weintraub, H., and M. Groudine, 1976 Chromosomal subunits in active genes have an altered conformation. Science 193**:** 848-856.
Whitehouse, I., A. Flaus, B. R. Cairns, M. F. White, J. L. Workman *et al.*, 1999 Nucleosome mobilization catalysed by the yeast SWI/SNF complex. Nature 400**:** 784-787.
Whitehouse, I., O. J. Rando, J. Delrow and T. Tsukiyama, 2007 Chromatin remodelling at promoters suppresses antisense transcription. Nature 450**:** 1031-1035.

Whitehouse, I., C. Stockdale, A. Flaus, M. D. Szczelkun and T. Owen-Hughes, 2003 Evidence for DNA translocation by the ISWI chromatin-remodeling enzyme. Mol Cell Biol 23**:** 1935-1945.
Whitehouse, I., and T. Tsukiyama, 2006 Antagonistic forces that position nucleosomes in vivo. Nat Struct Mol Biol 13**:** 633-640.
Winston, F., and M. Carlson, 1992 Yeast SNF/SWI transcriptional activators and the SPT/SIN chromatin connection. Trends Genet 8**:** 387-391.
Woodcock, C. L., and R. P. Ghosh, 2010 Chromatin higher-order structure and dynamics. Cold Spring Harb Perspect Biol 2**:** a000596.
Woolford, J. L., Jr., and S. J. Baserga, 2013 Ribosome biogenesis in the yeast Saccharomyces cerevisiae. Genetics 195**:** 643-681.
Yadon, A. N., B. N. Singh, M. Hampsey and T. Tsukiyama, 2013 DNA looping facilitates targeting of a chromatin remodeling enzyme. Mol Cell 50**:** 93-103.
Yang, J. G., T. S. Madrid, E. Sevastopoulos and G. J. Narlikar, 2006 The chromatin-remodeling enzyme ACF is an ATP-dependent DNA length sensor that regulates nucleosome spacing. Nat Struct Mol Biol 13**:** 1078-1083.
Yoshida, K., J. Bacal, D. Desmarais, I. Padioleau, O. Tsaponina *et al.*, 2014 The histone deacetylases sir2 and rpd3 act on ribosomal DNA to control the replication program in budding yeast. Mol Cell 54**:** 691-697.
Yuan, G. C., Y. J. Liu, M. F. Dion, M. D. Slack, L. F. Wu *et al.*, 2005 Genome-scale identification of nucleosome positions in S. cerevisiae. Science 309**:** 626-630.
Zhang, H., D. N. Roberts and B. R. Cairns, 2005 Genome-wide dynamics of Htz1, a histone H2A variant that poises repressed/basal promoters for activation through histone loss. Cell 123**:** 219-231.
Zhang, Y., S. J. Anderson, S. L. French, M. L. Sikes, O. V. Viktorovskaya *et al.*, 2013 The SWI/SNF chromatin remodeling complex influences transcription by RNA polymerase I in Saccharomyces cerevisiae. PLoS One 8**:** e56793.
Zhao, X., E. G. Muller and R. Rothstein, 1998 A suppressor of two essential checkpoint genes identifies a novel protein that negatively affects dNTP pools. Mol Cell 2**:** 329-340.
Zhou, C. Y., S. L. Johnson, L. J. Lee, A. D. Longhurst, S. L. Beckwith *et al.*, 2018 The Yeast INO80 Complex Operates as a Tunable DNA Length-Sensitive Switch to Regulate Nucleosome Sliding. Mol Cell 69**:** 677-688.e679.
Zhou, Y., R. Santoro and I. Grummt, 2002 The chromatin remodeling complex NoRC targets HDAC1 to the ribosomal gene promoter and represses RNA polymerase I transcription. Embo j 21**:** 4632-4640.
Zou, L., 2013 Four pillars of the S-phase checkpoint. Genes Dev 27**:** 227-233.
Zou, L., and S. J. Elledge, 2003 Sensing DNA damage through ATRIP recognition of RPA-ssDNA complexes. Science 300**:** 1542-1548.

Vita

Education: Ph.D., Molecular & Cellular Biology, May 2019
Fred Hutch Cancer Research Center & University of Washington
Seattle, Washington, USA
Thesis advisor: Toshio Tsukiyama, D.V.M., Ph.D.

Bachelor of Arts *cum laude*, May 2009
Amherst College, Amherst, MA
Advisor: Caroline Goutte, Ph.D.

Publications: Soghoian, D. Z., H. Jessen, M. Flanders, K. Sierra-Davidson, **S. Cutler**, T. Pertel, S. Ranasinghe, M. Lindqvist, I. Davis, K. Lane, J. Rychert, E. S. Rosenberg, A. Piechocka-Trocha, A. L. Brass, J. M. Brenchley, B. D. Walker & H. Streeck (2012) HIV-specific cytolytic CD4 T cell responses during acute HIV infection predict disease outcome. Sci Transl Med, 4, 123ra25.

Ranasinghe, S., M. Flanders, **S. Cutler**, D. Z. Soghoian, M. Ghebremichael, I. Davis, M. Lindqvist, F. Pereyra, B. D. Walker, D. Heckerman & H. Streeck (2012) HIV-specific CD4 T cell responses to different viral proteins have discordant associations with viral load and clinical outcome. J Virol, 86, 277-83.

Lindqvist, M., J. van Lunzen, D. Z. Soghoian, B. D. Kuhl, S. Ranasinghe, G. Kranias, M. D. Flanders, **S. Cutler**, N. Yudanin, M. I. Muller, I. Davis, D. Farber, P. Hartjen, F. Haag, G. Alter, J. Schulze zur Wiesch & H. Streeck (2012) Expansion of HIV-specific T follicular helper cells in chronic HIV infection. J Clin Invest, 122, 3271-80.

Ranasinghe, S., **S. Cutler**, I. Davis, R. Lu, D. Z. Soghoian, Y. Qi, J. Sidney, G. Kranias, M. D. Flanders, M. Lindqvist, B. Kuhl, G. Alter, S. G. Deeks, B. D. Walker, X. Gao, A. Sette, M. Carrington & H. Streeck. (2013) Association of HLA-DRB1-restricted CD4(+) T cell responses with HIV immune control. Nat Med, 19, 930-3.

Cutler, S., L. J. Lee & T. Tsukiyama. (2018) Chromatin Remodeling Factors Isw2 and Ino80 Regulate Chromatin, Replication, and Copy Number of the Saccharomyces cerevisiae Ribosomal DNA Locus. Genetics, 210, 1543-1556.

Chong, S.Y., **S. Cutler**, J.J. Lin, S. Biggins, T. Tsukiyama, Y.C. Lo & C.F. Kao. H3K4 methylation at active genes mitigates transcription-replication conflicts during replication stress. In preparation.